KTH Architecture and the Built Environment

ROCK DAMAGE CAUSED BY UNDERGROUND EXCAVATION AND METEORITE IMPACTS

Ann Bäckström

September 2008

TRITA-LWR PhD Thesis 1044
ISSN 1650-8602
ISRN KTH/LWR/PHD 1044-SE
ISBN 978-91-7415-035-3

Doctoral Thesis
KTH-Engineering Geology and Geophysics Group
Department of Land and Water Resources Engineering
Royal Institute of Technology (KTH)
SE-100 44 STOCKHOLM, Sweden

SUMMARY

The characterisation of fractures is of primary importance for several engineering applications concerning rock masses. Representing the fracturing process in rocks on the meter scale, plus the interaction of fractures on the centimetre to decimetre scale, is crucial for accuracy of prediction in rock engineering design given that the rock mass is a discontinuum, rather than a continuum. Moreover, it is important for rock engineering design to be able to validate numerical simulations, i.e. to check that they adequately represent the rock reality. Hence, the interactions of fractures on the microscopic scale (mm-cm scale) have been investigated, as well as the possibility to characterise the fractured rock mass at the mesoscopic scale (dm-m scale). Finally, the possibility of remotely identifying the fracture frequency has been investigated by using geophysical methods, particularly electric resistivity measurements, as applied to two examples of rock masses fractured by meteorite impact. The investigation work has been conducted on crystalline, mainly granitic rock, fractured both by natural and artificial processes.

The work at the micro- and meso-scale was conducted within the framework of the international project for DEmonstration of COupled models and their VALidation against EXperiments (DECOVALEX), between 2004 and 2007. The emphasis of the studies within this project was on the Thermo-Hydro-Mechanical and Chemical aspects (DECOVALEX-THMC) by means of coupled modelling extended to include chemical effects and applications to the Excavation Damaged Zone (EDZ) around excavations in crystalline rock. Aspects of the microscopic fracturing in laboratory experiments, where the chemical effect on mechanical properties of an ultra-brittle granite are included, are investigated as a step in the understanding of the fracturing processes. The effect of the salinity was identified on several portions of the resulting stress-strain curve from a uniaxial compressive test. In the samples used in this study, a set of pre-testing natural microfractures was found. They were oriented parallel to the maximum current principal stress in the rock mass, which seems to be their probable cause. The influence of the pre-existing fractures on further induced fractures is discussed and the influence of pre-existing fractures on the development of the EDZ around blasted tunnels in crystalline rock is investigated from characterisations of a tunnel wall at the Äspö Hard Rock Laboratory (HRL) in Sweden.

By using the laser scanning technique, different features of the EDZ are characterized by studying the difference between the theoretical model of the tunnel and the blasted tunnel as measured *'in-situ'*. This enables the evaluation of the efficiency of the tunnel blasting technique and appears to be a promising method for the documentation of tunnels in 3-D. By combining information on:

i) the overbreak and underbreak;
ii) the orientation and visibility of blasting drillholes; and
iii) the natural and blasting fractures in three dimensions,

a much deeper analysis of the rock mass for site characterization in relation to the blasting technique can be achieved based on the new method of data acquisition.

In contrast to engineering-induced rock fracturing, where one of the goals may be to minimize rock damage, meteorite impacts cause abundant fracturing in the surrounding bedrock. This type

of fracturing is intense and occurs throughout a large volume of the bedrock (> 100 km^3). This large volume of rock manifests impact structures that can be candidates for potential heat-exchange sources for extraction of geothermal energy. In order to investigate the extent and radial changes of impact-induced fracturing, the fracture frequency and the electric resistivity of outcrops of crystalline basement rocks at the Lockne impact structure and the suggested Björkö impact structure (Sweden) have been studied. Based on the collected data, the effect of fracturing on the electric properties of the rock is estimated and correlated with the fracture frequency. A negative linear correlation between the logarithm of fracture frequency and the logarithm of electric resistivity was found. This can be used as a tool for detecting fractures at large depth and, for identifying the extent of fractured structures, or for prospecting for structures suitable for geothermal energy retrieval.

Thus, the work reported in this thesis enables a more accurate modelling of rock fractures, both for the modelling supporting rock engineering design and for interpretation of meteorite impact phenomena. Additionally, further development of two characterization tools has been implemented:

- firstly, the development of the assessment method for the damage around tunnels from their overall fracture geometry;
- secondly, the estimation of fracturing from measurements of the electric resistivity of highly fractured rock volumes, such as those found in connection with impact structures.

PREFACE

This Doctoral Thesis consists of an overview of the research work on characterization of rock mass fracturing that was published in the papers collected in the Appendices and listed below:

Paper I. Bäckström, A., Cosgrove, J. W., and Hudson, J. A. 2008. Interpretation of the development of induced cracks within a pre-cracked rock microstructure and the similarities with the geometry of larger-scale geological fractures. *Submitted to the Journal of Structural Geology.*

Paper II. Bäckström, A., Lanaro, F., Christiansson, R., 2006. Coupled chemical-mechanical behaviour: the influence of salinity on the uniaxial compressive strength of the Smålands granite, Sweden. *Proc. of the 2nd International Conference on Coupled T-H-M-C Processes in Geo-Systems: Fundamentals, Modeling, Experiments and Applications, Geo-Proc 2006*, 437-443.

Paper III Bäckström, A., Antikainen, J., Backers T., Feng, X., Jing, L., Kobayashi, A., Koyama, T., Pan, P., Rinne, M., Shen, B., Hudson, J. A., 2008. Numerical modelling of uniaxial compressive failure of granite with and without saline porewater. *International Journal of Rock Mechanics and Mining Sciences, 45(7), 1126-1142.*

Paper IV Bäckström, A., Feng, Q., Lanaro, F. & Christiansson, R. 2006. Evaluation of the Excavation Damage Zone (EDZ) by using 3-D laser scanning technique. *Proc. of the 4th Asian Rock Mechanics Symposium, eds Leung CF Y and Zhou YX, World Scientific, 2006*.

Paper V Bäckström, A., Feng, Q., Lanaro, F., 2008. Excavation Damage Zone (EDZ) at the TASQ tunnel (Äspö, Sweden) – Quantification of blasting effects on the geological settings by 3D-laser-scanning. *Submitted to Engineering Geology.*

Paper VI Bäckström, A. 2004. A study of impact fracturing and electric resistivity related to the Lockne impact structure, Sweden. Peer-reviewed and published, eds Koeberl, C. and Henkel, H., *Impact Tectonics: Proceedings of the 8th Workshop of the ESF Program IMPACT. Springer-Verlag. 2004.*

The following papers are related to the research described here but are not appended in this Doctoral Thesis.

- Bäckström, A., Feng, Q., Lanaro, F. (2008) Improvement of fracture mapping efficiency by means of 3D laser scanning. Proceedings of the 42nd U.S. Rock Mechanics Symposium, San Francisco, 29 June – 2 July 2008.

- Bäckström, A. and Lanaro, F. (2008) Synopsis of the genesis of microcracks in brittle rock. Proceedings of the 33rd International Geological Congress (IGC), Oslo, 6-14 August 2008.

- Rutqvist, J., Bäckström, A., Chijimatsu, M., Feng, X.-T., Huang, X.-H., Hudson, J. A., Jing, L., Kobayashi, A., Koyama, T., Lee, H.-S., Pan, P.-Z., Rinne, M., Shen, B., and Sonnenthal, E. (2008) Comparison of different approaches for modeling of coupled THMC processes in the EDZ of geological nuclear waste repositories. Proceedings of GeoProc2008, Lille, 1-5 June 2008.

- Hudson, J. A., Bäckström A, Rutqvist J., Jing L., Backers T., Chijimatsu M., Feng X.-T., Kobayashi A., Koyama T., Lee H.-S., Pan P.-Z., Rinne M., Shen B. (2008) Final Report of DECOVALEX-THMC Task B. EDZ Guidance Document - characterising and modelling the excavation damaged zone (EDZ) in crystalline rock in the context of radioactive waste disposal. Swedish Nuclear Inspectorate (SKI) Report. 68 p.

- Rutqvist J., Bäckström A., Jing L., Hudson J., Feng X.-T., Pan P.-Z., Rinne M., Shen B., Lee H.-S., Backers T., Koyama T., Kobayashi A., Chijimatsu M. (2008) DECOVALEX-THMC Task B, Phase 3: A benchmark simulation study of coupled THMC processes in the excavation disturbed zone associated with geological nuclear waste repositories. Swedish Nuclear Inspectorate (SKI) Report. 51 p.

- Bäckström A. (2008) Äspö Hard Rock Laboratory - DECOVALEX - Validation of the ultrasonic borehole investigation in the TASQ tunnel. Internal Progress Report. Swedish Nuclear Fuel and Waste Management Company (SKB), 84 p.

- Hudson J. A. and Jing, L. (Bäckström, A. co-author of chapter 2) (2006) DECOVALEX-THMC, Task B. Understanding and characterizing the excavation disturbed zone (EDZ), phase II. Progress report 2006. Swedish Nuclear Inspectorate (SKI), 104 p.

- Bäckström, A., Henkel, H. and Katuzi, M.-R. (2006) Gravity model of the Lockne Impact Crater. The 27th Nordic Geological Winter Meeting - Abstract volume. Bulletin of the Geological Society of Finland, Special Issue 1, 2006, 20 p.

- Jacobsson, L. and Bäckström, A. (2005) Uniaxial compression tests of intact rock specimens at dry condition and at saturation by three different liquids: distilled, saline and formation water- DECOVALEX-Äspö Hard Rock Laboratory. Internal Progress Report (IPR-05-33). Swedish Nuclear Fuel and Waste Management Company (SKB), 100 p.

- Bäckström, A., Grünfeld, K., Johansson, M. (2004) Fracture mapping of rock outcrops from the Björkö structure. Björkö Energy program, Report to Swedish Energy Agency, 34 p.

- Bäckström, A., and Henkel, H. (2003) Geology and rock physical properties in the Björkö (Mälaren) area. Department of Land and Water Resources Engineering, Royal Institute of Technology, Stockholm. Report to Swedish Energy Agency.

ACKNOWLEDGEMENTS

The research work presented in this thesis was conducted partly at the Division of Engineering Geology and Geophysics, Department of Land and Water Resources Engineering, Royal Institute of Technology (KTH), Stockholm, Sweden, and partly at the company Berg Bygg Konsult AB (BBK), Solna, Sweden. More people than it is possible to properly mention here have supported me in various ways. If you feel that you are one of them, then these thanks are for you: I would like to express my outmost gratitude for your help and support.

First of all, I am deeply grateful to my supervisors, Docent. Herbert Henkel (Björkö geothermal energy project) and Prof. Robert Zimmerman, Prof. Em. John A Hudson and Dr. Flavio Lanaro (DECOVALEX-THMC project). Your academic guidance, advice and suggestions, but most of all, your positive and encouraging attitude towards my work has been a key component for maintaining my interest at all times. For the chance of seeing his brilliant mind at work during our collaboration on Paper I, I thank Prof. John Cosgrove. I also would like to express my gratitude to the president of BBK, Kennert Röshoff, for his continuous support and encouragement for my research work. To all my colleagues at BBK, and at the division of Engineering Geology and Geophysics at KTH, both former and current, I would like to express my utmost gratitude for your encouragement and help.

This thesis was made possible by the generosity of the Swedish Nuclear Fuel and Waste Management Co (SKB) and The Swedish Energy Agency. The work was conducted in two phases: 1) the Björkö geothermal energy project, for the period of 2001-2004; 2) the International Project DECOVALEX-THMC, for the period of 2004-2007. I would like to express my sincerest gratitude to Rolf Christiansson of SKB for his arrangement of the financial support and his sincere attitude towards my research. I would also like to take the opportunity to thank all the colleagues in these projects for the comments, fruitful discussion and co-operation during the workshops.

I am grateful to my colleagues, Dr. Quanhong Feng and Mrs. Guojuan Wang, who have performed the in-situ laser scanning of the TASQ tunnel at Äspö Hard Rock Laboratory (ÄHRL), and a large part of the post processing of the laser scanning data. I would also like to thank Dr. Lars Jacobsson, at SP laboratory in Borås, for lending me his assistance and expertise during the laboratory tests. For their help during the work in the TASQ tunnel, I would like to thank the people at Äspö HRL, and especially Dr. Carl-Johan Hardenby and Dr. Christer Andersson. I am grateful to Dr. Kristof Schuster at Bundesanstalt für Geowissenschaften und Rohstoffe (BGR) in Hannover, for his expertise and advice during and after the ultrasonic measurements at the TASQ tunnel. For their inventiveness and humour, crucial for successful field campaigns, I wish to thank Ulrika Lindberg, Malin Johansson and Pauline Eggebratt.

To two persons who have changed the course of my life I would like to extend my profound gratitude: Mrs. Berit Albers who, with her interest for nature, opened my eyes to the wonderful world of Öland, when I was five; and Prof. Em. Maurits Lindström who introduced me to the subject of meteorite impacts at Stockholm University. For showing me that there are people out there with whom you can have wonderful discussions on the topic of meteorite impacts, I am grateful to Teemu Öhman, Evelin Versh and all of the students in the ESIR group.

I am deeply grateful to my father for his unreserved support for my interest. I would also like to thank the rest of my family and my friends, for their tolerance.

Finally I owe my dearest thanks to my Henrik, for his love, patience and unwavering support.

CONTENTS

NOTATION

Notation	Name	Unit
A	Fracture surface energy	J
C_0	Cohesive strength	MPa
c	The half-length of a Griffith crack	m
c_B	Longitudinal wave velocity of a pressure wave	m/s
c_L	Velocity of a longitudinal wave	m/s
d_a	Apparent depth	km
D	Crater diameter	km
E	Young's modulus	GPa
F	Fracture frequency	m^2/m^3
K	Tensile strength	MPa
K_0	Bulk modulus	GPa
L	Mean trace length	m
p	Fluid pressure	MPa
s	Side length in the sampling area	m
S_1	Total major principal stress	MPa
S_3	Total least principal stress	MPa
UCS	Uniaxial compressive strength	MPa
t_L	Thickness of upper layer	m
x	Distance	m
y	Ratio depending on spacing and trace length	
Y	Yield stress	%
ε_a	Axial strain	%

Notation	Name	Unit
ε_r	Radial strain	%
ε_{vol}	Volumetric strain	%
ε_{vol}^{cr}	Crack volumetric strain	%
ε_{vol}^{e}	Elastic volumetric strain	%
ϕ	Friction angle	°
ρ_0	Uncompressed density	kg/m^3
λ	Trace length of fractures	m
μ	Shear modulus	GPa
θ	Angle of the normal of the shear fracture to the axis of the major principal stress	°
σ_1	Major principal stress	MPa
σ_3	Minor principal stress	MPa
σ_a	Axial stress	MPa
σ_{ci}	Crack initiation stress	MPa
σ_{HEL}	Stress at Hugoniot's Elastic Limit	MPa
σ_L	Longitudinal stress	MPa
σ_N	Normal stress	MPa
σ_t	Tensile stress	MPa
τ	Shear stress	MPa
ν	Poisson's ratio	-

ABSTRACT

The intent of this thesis is to contribute to the understanding of the origin of fractures in rock. The man-made fracturing from engineering activities in crystalline rock as well as the fracturing induced by the natural process of meteorite impacts is studied by means of various characterization methods. In contrast to engineering induced rock fracturing, where the goal usually is to minimize rock damage, meteorite impacts cause abundant fracturing in the surrounding bedrock. In a rock mass the interactions of fractures on the microscopic scale (mm-cm scale) influence fractures on the mesoscopic scale (dm-m scale) as well as the interaction of the mesocopic fractures influencing fractures on the macroscopic scale (m-km scale). Thus, among several methods used on different scales, two characterization tools have been developed further. This investigation ranges from the investigation of micro-fracturing in ultra-brittle rock on laboratory scale to the remote sensing of fractures in large scale structures, such as meteorite impacts. On the microscopic scale, the role of fractures pre-existing to the laboratory testing is observed to affect the development of new fractures. On the mesoscopic scale, the evaluation of the geometric information from 3D-laser scanning has been further developed for the characterisation of fractures from tunnelling and to evaluate the efficiency of the tunnel blasting technique in crystalline rock. By combining information on: i) the overbreak and underbreak; ii) the orientation and visibility of blasting drillholes and; iii) the natural and blasting fractures in three dimensions; a analysis of the rock mass can be made. This analysis of the rock mass is much deeper than usually obtained in rock engineering for site characterization in relation to the blasting technique can be obtained based on the new data acquisition. Finally, the estimation of fracturing in and around two meteorite impact structures has been used to reach a deeper understanding of the relation between fracture, their water content and the electric properties of the rock mass. A correlation between electric resistivity and fracture frequency in highly fractured crystalline rock has been developed and applied to potential impact crater structures. The results presented in this thesis enables more accurate modelling of rock fractures, both supporting rock engineering design and interpretation of meteorite impact phenomena.

Keywords: Excavation Damage Zone (EDZ); Fracture analysis; Pre-existing fractures; Class II behaviour; 3D laser scanning; Impact fracturing

INTRODUCTION AND CONTENTS OF THE THESIS

Introduction

The topic of rock damage is immense, and has been studied through most of human history. The importance of understanding it has been crucial in the history of most of the great civilizations on Earth. This has been mainly to steer clear of dangers involved in the use of rock as a building material, e.g. when building roads, water-control (aqueducts and dams), great walls, caves, tunnels, tombs and underground storage facilities for different goods. It should be noted that the word 'damage' in this thesis has been used as a short hand for 'enhanced fracturing'. The word is not necessarily intended to denote any subjective connotations of the rock becoming inferior. Generally, rock damage does indicate a worse material for civil engineering but not necessarily for mining methods where, for example in block caving, a more fractured rock may be a better rock in terms of the ease of mining. Knowledge of rock behaviour and rock damage has been built from experience of stone masons and people working in the extraction of the material in quarries and mines (Hagerman 1943). This progressed into empirical studies of the material in controlled laboratory experiments (Ulusay and Hudson 2007), as well as the study of geological materials and traces of their forming processes and interactions in nature (Price and Cosgrove 1990, Twiss and Moores 1992, Park 1997).

Currently, the building of conceptual models and numerical simulations of the behaviour of rock with fractures is rapidly developing (*i.e.* Jing 2003). The diverse uses of rock masses for: i) exploiting of hydrocarbon, groundwater or geothermal reservoirs; ii) placing underground storage for nuclear waste; ii) locating transportation facilities; iii) extracting construction materials; imposes large demands on the prediction of performance of the rock material. Irrespective of the scale of an observed phenomenon, the performance of the rock mass is critically affected by the presence of fractures, often termed discontinuities (Priest 1993). This is especially important for crystalline rocks as the intact rock strength is high and permeability to fluid flow is practically negligible. Thus, most of the interactions and transport occur in the discontinuities (Starzec 2001).

Objectives and structure of the thesis

In two projects, the international DECOVALEX program (DEmonstration of COupled models and their VALidation against EXperiments) (Hudson and Jing 2007) and the Björkö geothermal energy project (Henkel 2002), I had the opportunity to investigate fractures due to different causes, at different scales using several different detection methods.

Starting from a deeper understanding of the characterization of fractures in meteorite impact structures and ending with the Excavation Damaged Zone (EDZ) through investigation on several different scales, this study has been conducted with the aim of improving fracture characterization methods from field scale to laboratory scale. This has resulted into the identification of pre-existing fractures in specimens of Ävrö granite from the Äspö Hard Rock Laboratory (HRL) and discussion on their origin, via further developments of the 3D laser-scanning method at tunnel scale. This method has been developed into a characterization method for the damage produced during tunnel blasting. Furthermore, an improvement in the comprehension of the correlation between fracture frequency and electric resistivity has been achieved to be used as a tool for detecting fractures at large depth during prospecting of suitable structures for geothermal energy retrieval.

The target of the DECOVALEX-THMC (Thermal-Hydro-Mechanical-Chemical) Project has been to live up to the the comment by Wawersik (2000) in which he states that "Successful validations of numerical codes mandate a close collaboration between experimentalists and analysts drawing from the full gamut of observations, measurements, and mathematical results". During this investigation, several characterization methods have been used. We have strived to optimize the parameter acquisition from an *'in-situ'* case study to be used for numerical modelling of coupled THMC-processes in the EDZ. During these investigations, laboratory scale experiments of the mechanical behaviour of granite specimens were conducted. These produced the input and the validation cases for the simulations by four different numerical modelling tools, such as: the elasto-plastic/elasto-viscoplastic model (EPCA), the damage expansion model, the FRACOD code and the particle flow code (PFC).

The development of the fractures in these specimens before and after testing was studied by means of vacuum impregnation of the specimens with epoxy resin containing fluorescent dye. Fracture analysis was then performed on the pictures of the specimens.

Furthermore, the information at tunnel scale was analysed and strategies for the characterisation of the EDZ and characterization methods suitable for use during the construction of a deep repository were developed. In the case of the meteorite structures, the induced rock fractures were also studied using fracture mapping together with remote geophysical investigatons.

Remote investigations of the fractures of two meteorite impact structures using electric resistivity is also presented in this thesis. One of the structures is suggested to be an impact structure. In these investigations, the main aim has been to identify the fracture frequency of strongly fractured crystalline rock and its effect on the electric resistivity. The

impact craters investigated in this study are large structures and the energy released in the impact causes fractures on all scales to form. The energy in the central part of the remaining structure has caused a fracture network with high fragmentation within the structure, whereas the attenuation of the impact energy outwards from the impact decreases the development of the fracture network caused by the impact. This decrease has been used to identify the limit of the crater structure in the Lockne impact crater, and to investigate the volume of strongly fractured rock in the suggested Björkö impact crater (Fig. 1).

The structure of this thesis is presented in Fig. 2. This thesis opens with an introduction about fractures characterized on different scales;

i) Micro-scale, where an analysis of the interaction between microcracks in the Ävrö granite is presented (Paper I). The results from the mechanical tests where the complete process of microstructural breakdown during the uniaxial compressive failure of intact crystalline rock is discussed (Paper II) together with the use of this type of laboratory test to evaluate the capability and validity of four different numerical models (Paper III).

ii) Meso-scale, where the possibilities of using the 3D laser-scanning method as a validation method of the blasting performance (Paper IV and Paper V) and,

iii) Macro-scale, where the results from the investigation of the two structures; the Lockne meteorite impact crater, and the suggested Björkö meteorite impact crater from which an improvement of the correlation between fracture frequency and electric resistivity was performed. The extent of the Lockne crater is discussed in paper IV as well as the correlation of the electric resistivity to the fracture frequency, whereas data added from the Björkö structure are presented in the text.

In the discussion and conclusions, the major results from the research are discussed, followed by the manuscript of the papers.

Rock damage and its measurement

When rock is subjected to significant changes of stress so that inelastic behaviour occurs, it can experience permanent damage in the form of brittle and/or plastic deformations. Brittle deformations will result in damage manifested by the initiation of fractures and propagation of initiated and pre-existing fractures. The geometry and location of the fractures will depend on the magnitude and orientation of the applied stress components and the experienced stress-path. There are several processes that induce stresses in the rock mass, both natural, such as deformation resulting from orogenic processes, deformation resulting from anorogenic processes and "shrinkage" caused by cooling or desiccation (*i.e.* Price and Cosgrove 1990, Twiss and Moores 1992, Park 1997), and the extreme case of meteorite impacts (Melosh 1989, French 1998), as well as anthropogenic influences due to civil, mining and petroleum engineering activities (Hudson and Harrison 1997).

To perform any analysis of the formation of these discontinuities, the characterization of the rock mass and the creation of a geological

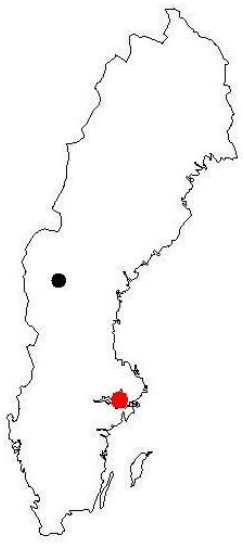

Fig. 1. Sweden with the location of the Lockne impact crater (black circle), and the location of the Björkö structure (red circle).

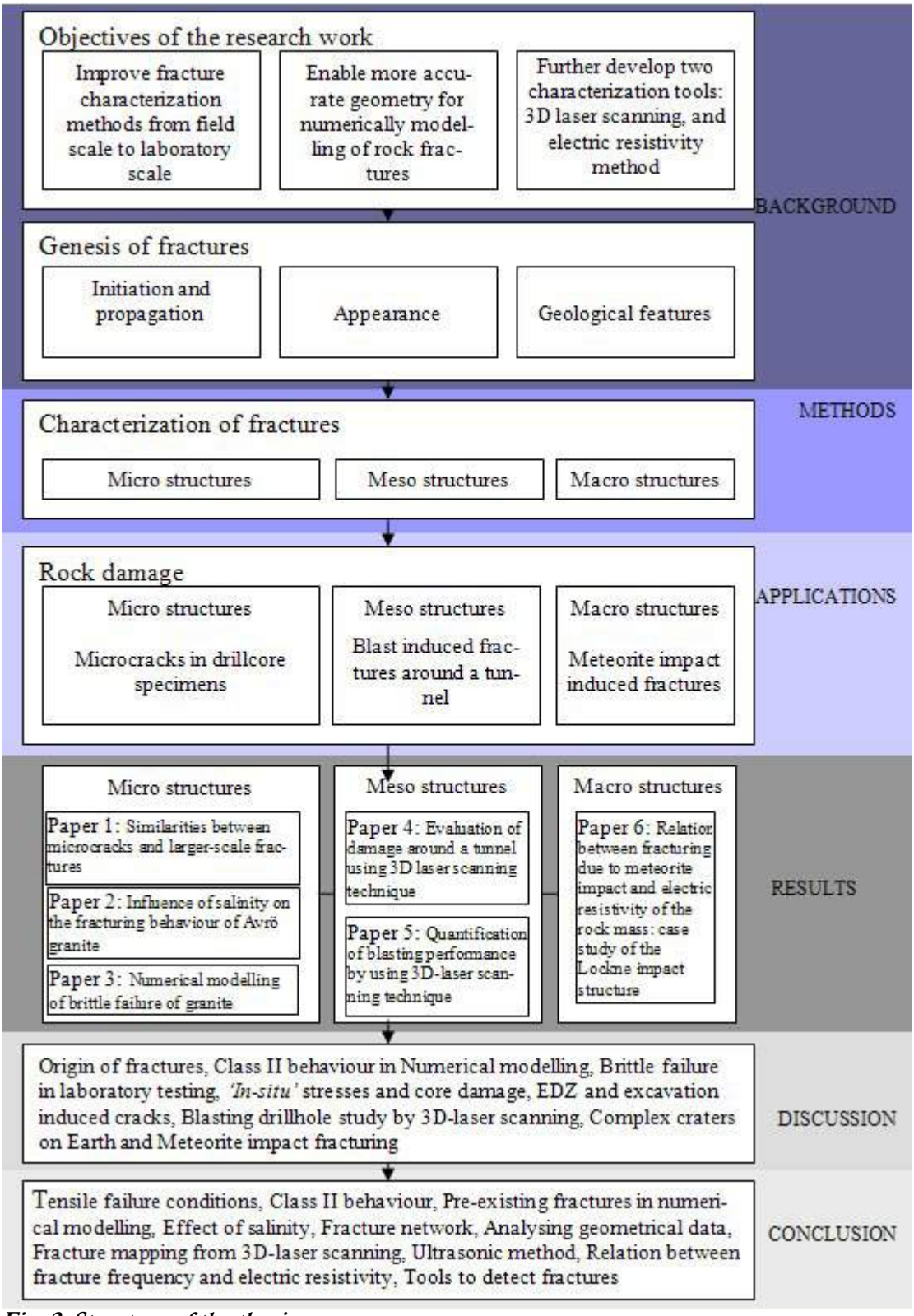

Fig. 2. Structure of the thesis.

database upon which the definition of rock types, structural discontinuities and material properties is based, is crucial (Hoek 2007). Even the most sophisticated analysis can become a meaningless exercise if the geological information upon which it is based is inadequate or inaccurate. Depending on the case studied, an optimization of the parameter acquisition from the *'in-situ'* case study is needed. When the observation scale decreases, the distinction between the properties of various discontinuities such as size,

orientation, shape, *etc.*, becomes more difficult. This exerts large demands on the mapping method.

The most direct mapping method is geological observation where several properties of the fracture can be observed, described and/or quantified, such as orientation, visible length, surface roughness, *etc.* For this type of observations to be feasible, the fracture needs to be located in an accessible outcrop or tunnel wall and to be large enough to be observable. This is not always the case, especially for small-scale fractures. Alternative methods for observing these small-scale fractures are neeeded, such as: i) observation of thin sections of a sample of the rock (Fujii *et al.* 2007); ii) observations of polished sections (Kranz 1883); iii) vacuum impregnation of the specimens with epoxy resin containing fluorescent dye and photografical or microscopy observations (Åkesson *et al.* 2004, Nara *et al.* 2006); iv) observations with scanning electron microscopy (Kranz 1983) or; v) confocal laser scanning microscopy (CLSM), which is a combination of laser-scanning and fluorescent dye (Liu *et al.* 2006). In recent years, development of computer aided image-analysis programs has greatly facilitated microstructural characterization through analysis of digital images obtained from thin sections (Nasseri and Mohanty 2008).

Microfractures are a vital key in the understanding of the rock's history as they may be used to infer the paleo and current local stress regimes. There are apparent morphological and mechanical similarities between microcracks and joints and faults. Knowledge about microcrack populations is a necessary input to studies that model the micromechanics of fracture and fault formation (Kranz, 1983). In several studies, it has been shown that pre-existing fracture sets have a stronger influence on fracture propagation in the rock mass than the mineral shape and distribution in the intact rock in the same rock mass (see *e.g.*, Nara *et al.* 2006, Nara and Kaneko 2006, Nasseri and Mohanty 2008). Thus, further investigations of microcracks and their role in fracture mechanics when accounting for the deformational behavior of the rock mass are needed (Walton 1958). To be able to account for the complexity of the rock mass in numerical simulations of rock mass, the knowledge of the microscopic heterogeneities in the material at the scale of laboratory tests must be increased (Wawersik 2000).

Apart from procedures such as grouting or support, it is not possible to alter the rock mass features, but timely knowledge can facilitate the understanding of the rock structure and the effect of the perturbation imposed on the geological structure of the rock mass via blasting which is an inherently destructive process and inflicts damage to the surrounding rock (Singh and Xavier 2005). One of the possible methods of excavation considered in the design of an underground radioactive waste repository (SKB 2004) is blasting. When blasting a tunnel, a zone of damaged rock will be produced around the tunnel periphery. This zone is called the Excavation Damaged Zone (EDZ), and could act as a conductive structure for water flow along the tunnel and hence facilitate radionuclide migration away from the repository (Bäckblom *et al.* 1997). The EDZ has been investigated extensively in recent years (e.g. Bäckblom and Martin 1999, Cai *et al.* 2001, Bossart *et al.* 2002, Chandler 2004, Tsang *et al.* 2005).

Several methods for evaluating the damage from the surface geometry of the tunnel exist, such as: manual measurements, standard surveying, laser surveying with reflectors, photographic sectioning and light sectioning methods. Their feasibility is mainly limited by their being either subjective, manually intensive, time-consuming or often providing detailed information only for a select number of points instead of the entire scene (Warneke *et al.* 2007). The time constrains during the tunnelling production cycle when blasting demands that the characterization of the damage is attained through a method with minimal time consumption. This criterion must be met while still obtaining sufficient information for the evaluation of the damage. This requires the development of a measurement and analysis method where the time for the mapping/surveying is short, the method is accurate and precise, the proce-

dure is simple to use and has a possibility to function under a large range of conditions (Maerz *et al.* 1996).

Direct geological observations and measurements in the field that are generally feasible on outcrops. Apart from them, tunnel walls or cuts into the rock and laboratory measurement of small-scale fractures are alternative methods of detecting fractures inside the rock mass (King *et al.* 2006). In the investigation of the extent of large structures, such as meteoritic impact structures, the fracture frequency within the rock mass is of interest. As fractures change the physical properties of the rock, several geophysical methods have been developed to detect their presence inside the rock mass.

Geophysical methods are all subjected to interpretation of anomalies in the geophysical records (Lowrie 1997). Alternative geophysical methods are available for applications at different scales or to be employed as a combination of adequate methods in each individual case to taking advantage of the mutually constrained information they provide.

Geophysical techniques focus on detecting different physical properties such as seismic velocity (P- and S- wave velocity), resistivity, magnetic field and gravity changes. The seismic methods provide an indirect measure of material properties that can identify the extent of damage. For example, seismic velocity is a function of the elastic properties and the density of the rock mass. The presence of inelastic elements, such as fractures, causes variations in seismic velocity and the direction of the propagation wave, making this method suitable for identification of such disturbances in the rock (Emsley et al., 1997). Electro-magnetic methods, on the other hand, are used to identify electrically conductive structures in the rock, and are quite suitable for detecting fractures. This is because fractures conduct water, and as water is bipolar, it is electrically conductive. Thus, the water content has a significant effect on the electric resistivity of the rock mass (Carmichael, 1989). The amount of electrically conductive minerals and the electric conductivity of salts dissolved in the fluid can also influence the resistivity, thus limiting this method to situations where these properties are known.

Granite is commonly a mixture of non-conductive minerals, which gives granite a high resistivity, generally larger than 10 000 Ωm. This leaves the water and it's content to be the conductive feature in granitic rock masses. It is known from studies using Slingram and VLF electromagnetic techniques to map fracture zones and for ore prospection in crystalline shield areas that the electric resistivity in fractured rock can have rather low values (Eriksson 1980, Henkel 1988). Studies have also been made in connection with site selection for radioactive waste disposal (Eriksson *et al.* 1997, Thunehed *et al.* 2004, Mattsson *et al.* 2005, Thunehed and Triumf 2005, Thunehed and Triumf 2006). Typical low values are around 2000 Ωm in fractured rocks. Even lower values down to 30 Ωm are found for fault gouge (Henkel 1988). However, for this method to be useful in high fracture frequency situations where the structure is out of reach, the quantitative assessment of fracture frequency using electric resistivity needs to be improved.

Though time it has been found that there is no point in collecting data for data sake; the understanding of the underlying phenomenon is what renders the information useful. Before one can characterise fractures in an efficient way the definition and formation of fractures are crucial, thus this is discussed in the following sections.

GENESIS OF FRACTURES

Fractures are one type of discontinuity described by Priest (1993) as "the mechanical breaks of negligible tensile strength in a rock". The term 'discontinuity' does not provide any information concerning age, geometry or mode of origin; this also applies to the term 'fracture'. From characteristics measured on fractures, these parameters, such as: orientation, size, aperture and surface, can be derived. The age of the fracture is often identified from the relation of the fracture to other indications of age in the rock mass, such as: other fractures, folds, faults, intrusions, fillings and various sedimentary struc-

tures. According to many authorities in structural geology, fracture development is generally related to three main geological processes:

- deformation resulting from orogenic processes,
- deformation resulting from anorogenic processes (processes not in connection to an orogentic process)
- "shrinkage" caused by cooling or desiccation (i.e. Price and Cosgrove 1990, Twiss and Moores 1992, Park 1997).

The formation of fractures from meteoritic impacts on the Earths surface cannot be subdivided into these groups. It is a process of extraterrestrial origin and will thus occur outside of this division. It is only in recent days that meteorite impacts have been recognized as an important process for reforming the Earth's surface (Melosh, 1989).

In this thesis research, fractures from meteorite impacts and blasting of tunnels are investigated. These two special situations, natural and anthropogenic, are both related to the Earth surface and the formation processes have short time frame in the geological framework and are superposed on earlier sedimentary and/or tectonic structures.

Fracture initiation and propagation

The fracturing process is characterised by a certain velocity of propagation. Different fracturing processes are characterised by different propagation velocity, however, fracturing in rock is always initiated at the microscale. Microcracking is highly dependent on the mineralogy, fabric and microstructures of a given rock type. Microcracks preferably grow from initial flaws in the rock with a favourable angle to the stress state. These initial flaws can be weaknesses in the matrix due to thermal contraction during cooling, cleavage planes in minerals (such as feldspars and mica) and mineral boundaries (such as between quartz grains) (Fig. 3). Flaws can be found in magmatic rocks that have not experienced any secondary metamorphic influence. As nature is complex, it is likely that the rock type encountered has had a long and

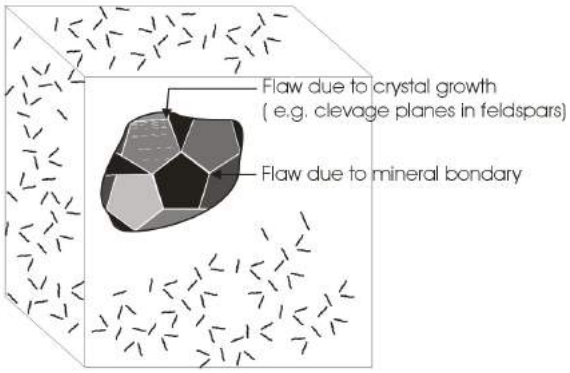

Fig. 3. Schematic representation of pre-existing flaws in the mineral matrix, sources of fracture initiation.

literally stressful journey to the present situation, thus, other influences such as tectonic stresses during deformation causing foliation, partial mineral solution, stress relaxation during uplift and associated release of overburden stress must be considered for understanding the presence of flaws and defect in the rock fabric (Kowallis and Wang, 1983). The influence of the formation process on fracture development is strong in the rock group of sedimentary rocks, where bedding planes, gradation during sedimentation, ripple marks, truncated cross bedding, bioturbation, desiccation cracks, pillow lava, flame structures, sole marks, slump structures (Price and Cosgrove 1990) and many more other processes influence the microcrack distribution and possible propagation.

Several attempts have been made to describe fracture initiation and propagation. The Griffith's theory is one of the simpler and elegant developed descriptions (Jaeger *et al.* 2007). In short, it describes the onset of fracture propagation of one crack in a system under equilibrium where the energy change of the system is due to the release of elastic strain energy that is supplied as surface energy of the crack and as potential energy of the rock body, which represents the external applied load. Griffith described how the energy would rearrange in the system rock-fracture when the fracture grows from its half-length to a longer half-length, while the load is maintained constant (Fig. 4a). The crack can only extend if the strain energy released by the crack propagation is at least large enough

to supply the surface energy required to form the new surface area of the crack faces. The Griffith's theory implies that small cracks require larger stresses to continue to grow than larger cracks. The tensile stress at the crack tip must be large enough to break the atomic bonds of the rock matrix at the crack tip and can be described as:

$$\sigma_t = \sqrt{\frac{2AE}{\pi c}} \qquad (1)$$

where the A is the surface energy of an elliptical flaw with major axis length 2c. By experiments on glass, Griffith showed by using reasonable values for the physical constants in Eq. (1) that the tensile strength of specimens of glass approximates the theoretical atomic bond strength of glass. Griffith also considered two-dimensional elliptical flaws with random orientation in biaxial compression and in his analysis he assumed that the elliptical flaws were so spaced that they did not directly interfere with each other. Then he could show that that the stress at the fracture tip would be tensile even under applied compressive stress, and the local tensile stresses would be a maximum when:

$$\cos 2\theta = \frac{\sigma_1 - \sigma_3}{2(\sigma_1 + \sigma_3)} \qquad (2)$$

where θ is the angle the flaw makes with the axis of maximum principal stress (Fig. 4b). He also identified that the local tensile stresses at the fracture tip would reach the critical stress for the extension of the fractures when:

$$(\sigma_1 - \sigma_3)^2 + 8K(\sigma_1 + \sigma_3) = 0 \qquad (3)$$

where K is the tensile strength and provided that $\sigma_1 \neq \sigma_3$ and $(3\sigma_1 + \sigma_3) > 0$. The rock mass can experience that the fluid pressure (p) in the pores of the rock is larger than the total least principal stress (S_3), even though it is compressive, so that the minor principal stress (σ_3) becomes tensile. This can cause tensile failure if:

$$(S_3 - p) > K \qquad (4a)$$

or if:

$$(S_1 - S_3) < 4K \qquad (4b)$$

Eq. 4b is in fact the criterion used in the method for inferring the *'in-situ'* stresses in the rock mass by means of hydraulic fracturing (Ask 2004).

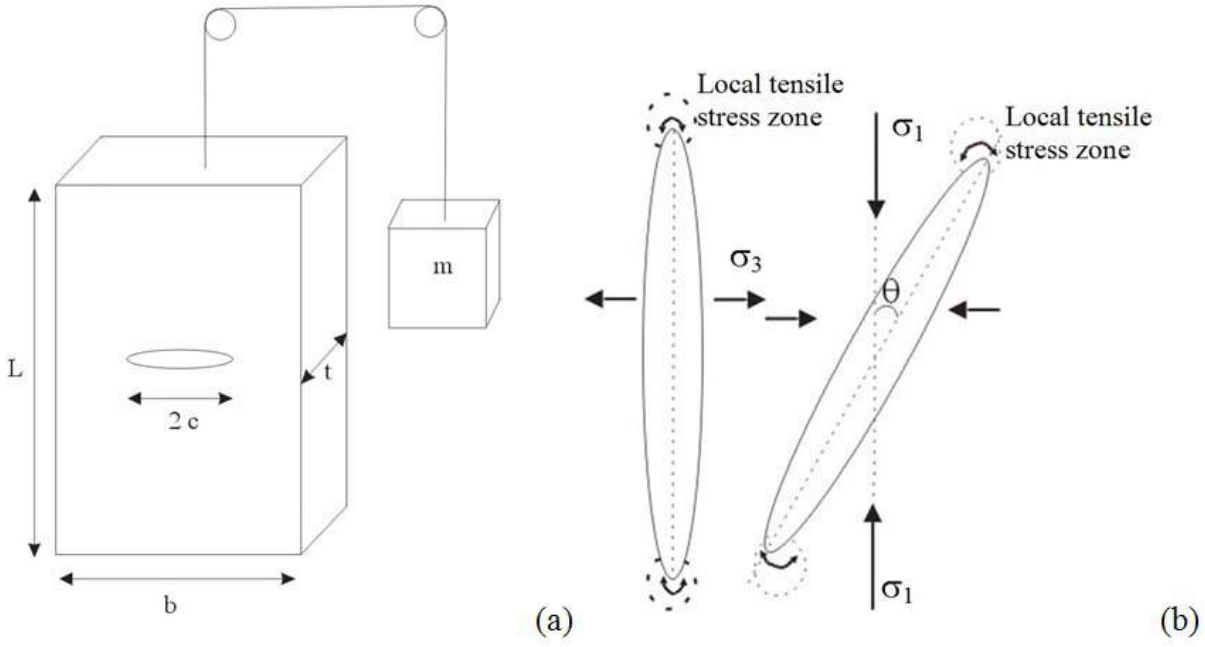

Fig. 4. (a) Sketch of a fracture extending under constant applied load according to the derivation of the Griffith criterion (after Jaeger et al. 2007). (b) Sketch of the stress concentration near the end of elliptical flaws under different stress conditions and orientations to the major principal stress (after Price and Cosgrove 1990).

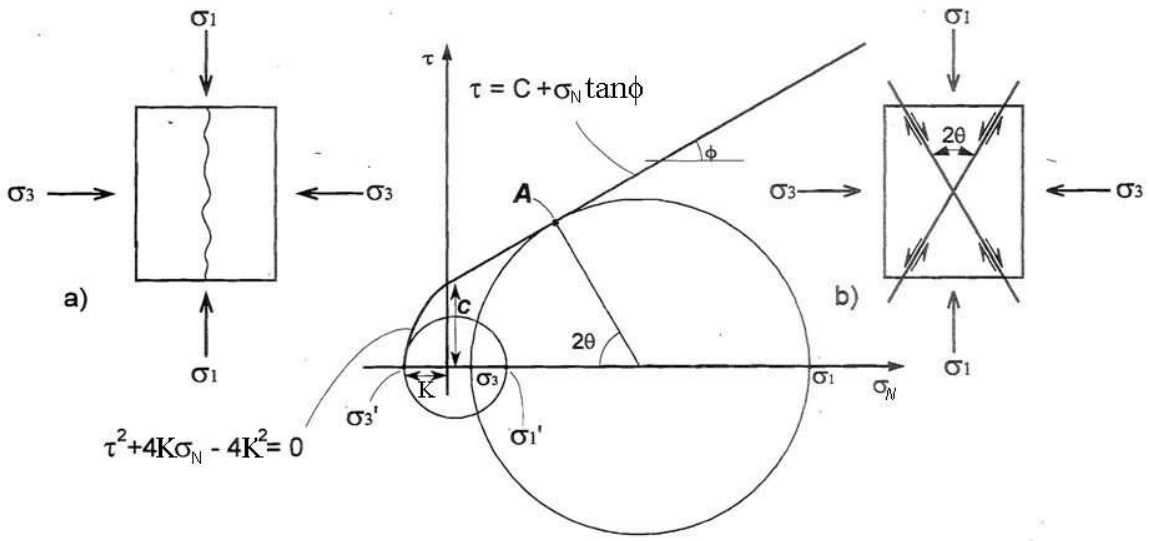

Fig. 5. Combined Griffith and Navier-Columb's failure envelope (after Price & Cosgrove 1990).

Fracture appearance

The relation for fractures experiencing tensile extension is non-linear as presented in Eq. (3) and it can be expressed in the Mohr's space by describing the relation between the maximum shear stress τ and the normal stress σ_N acting on a fracture at failure as presented by Murell (1958):

$$\tau^2 + 4K\sigma_N - 4K^2 = 0 \qquad (5)$$

were τ is the shear stress and σ_N is the normal stress. The fractures forming in extension are, as the word suggests, open, but they will close when the normal stress reach a certain value, after which the fracture propagates with the two surfaces touching, more or less.

So far, pure tensile or Mode I fracturing has been described. However, there is another basic type of fracturing found in brittle rock - shear or Mode II fracturing. Shearing fracturing is best described by the failure of a rock sample along one or two shear planes and it occurs in compression. The condition for initiation of this type of failure can be described in a 2D Mohr's stress space, as an envelope developed from stress circles on a Navier-Columb failure criterion. This criterion is described by means of the normal stress and two parameters, the cohesive strength of the material (C_0) and the angle of internal friction (ϕ) (also called friction angle) (Fig. 5) as:

$$\tau = C_0 + \sigma_N \tan\phi \qquad (6)$$

The uniaxial compressive strength of a rock with this linear failure criterion can therefore be related to the cohesive strength and friction angle. At failure, two sets of fractures can be produced. In compression, these fractures describe an acute angle to the direction of major stress. By measuring the angle that the normal of the failure plane makes to the direction of the major principal stress θ, the

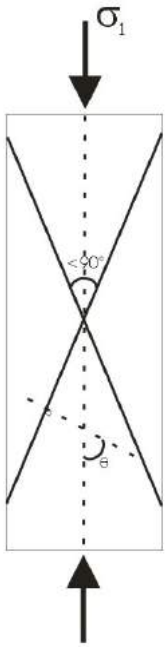

Fig. 6. Conjugate shear fractures in a compression test (after Priest 1993).

optimal shear conditions are described by:

$$\pm\theta = (45° - \phi/2) \quad (7a)$$

or

$$2\theta = 90° - \phi \quad (7b)$$

The principal stresses during the formation of conjugate shear fractures can be back-calculated using mechanical properties from laboratory tests of the material when the angle θ is known (Fig. 6).

The tensile and shear fractures are the two types of fractures generally used to describe fracture initiation and propagation. Unfortunately nature is not clear cut, thus hybrid fractures where shear has occurred although the fracture is open can of course be found during characterization of fractures in the field (Price and Cosgrove 1990). A shear fracture that in a later stage can experience extension and open will be quite similar to the hybrid fractures.

Geological features of fractures

The characterization of fractures and their interrelation can be used to reconstruct the history of the rock mass - this is a major part of the science of structural geology. Several properties can be used for identifying the age relation between different generations of fractures, the stress and hydrological situation at failure, the situation from mineralization to re-crystallisation, heating and cooling of the rock, etc. In this section, some of the properties of fractures in brittle rocks are presented such as orientation, size, aperture and surface.

Orientation

The orientation of the fractures in 3D space is one of the most crucial aspects of the fracture. The spatial relation between fractures yields information about their age relation. Examples of these are the effect of one failure event on the other, such as displacement of older fractures at the event of formation of new fractures, the abuttal of new fractures to old due to the old fractures effect on the local stress state, conjugated shear fractures formed during the same failure event with a systematic orientation relation, *etc.*

In Fig. 7, a sketch of a rock wall with several generations of fractures is illustrated. The most conspicuous feature is the fractures denoted with Shear II that cause dislocation of the pre-existing fractures. The fact that there are pre-existing fractures in the rock mass, denotes that this is not the earliest event. The fractures formed first are the ones displaced by the shear II fracture and are denoted with Shear I. The inter-relation between the pre-existing sets of Shear I fracture identifies

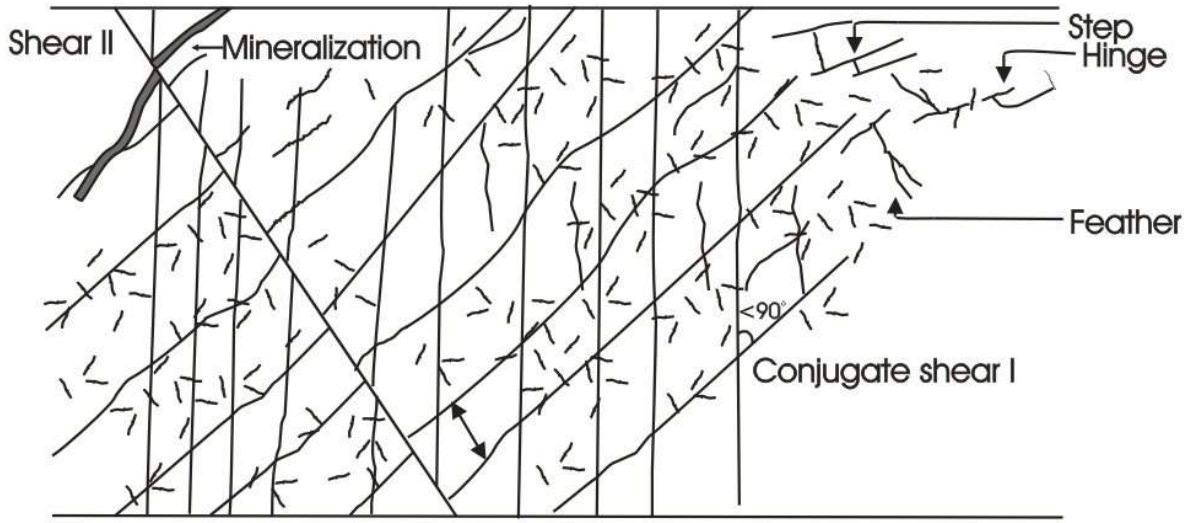

Fig. 7. Sketch of age relation between fractures. Three formation events can be found in this scene: the formation of the Shear I fractures, where the distance between fractures is represented by the arrow; one extensional phase where the mineralization took place; and the formation of the Shear II fracture. Three examples of different terminations of fractures can be seen in the upper right corner.

them as conjugate shear fractures. Their geometry can be used to calculate the principal stresses and their orientation at the time of formation.

The fracture filled with minerals has probably experienced extension and mineralization after the formation of the conjugate Shear I fractures. In fact, the mineralized fracture crosses one of the conjugate shear fractures and the mineralization is not affected by shear. Mineralization is affected by the Shear II fracture and thus it predates it. To summarize, there are three formation events in this scene: the first and third are from shear events while the second has experienced an extension.

Size

Fractures range from micro-fractures, hardly visible to the naked eye, to km long faults, seen as long walleyes in the landscape. The measurement of the persistence of individual fractures is dependent on the exposure of the fracture. During geological mapping in tunnels the size of the tunnel opening is limiting, whereas in drill cores the persistence of fractures larger than the diameter of the borehole cannot be measured at all. The properties of the fractures vary such as: persistence, or length; surface roughness or morphology of the fracture; and aperture. The interrelation between the different fracture properties vary depending on the. For a large fracture the roughness of the surface have a smaller influence on the mechanical properties compared to a small fracture (Fardin 2003). But these large fractures can have a waviness which may play a role in the behaviour of the fracture (Lanaro 2001). Hydraulic, mechanic and hydro-mechanic testing of fractures in the laboratory are often done on small scale samples. These samples generally have a stronger resistance to deterioration and propagation than larger scale fractures. Their interrelation must be regulated with scaling rules (Price and Cosgrove 1990, Lanaro 2001, Fardin 2003).

Aperture

The distance between the two rock walls on either side of the fracture is generally called the width of the fracture. The width varies, depending of the roughness of the two rock wall surfaces. Different minerals can be crystallised on the fracture surface (Fig. 8), which implies that width might be equal or larger than aperture. The 'mechanical aperture' of a fracture is used to describe the arithmetic mean distance between the rough walls of a fracture (Renshaw 1995, Lanaro 2001) and will coincide with the width of the fracture for a fracture without mineralization on the fracture surfaces. In an open fracture with a surface mineralization, the mechanical aper-

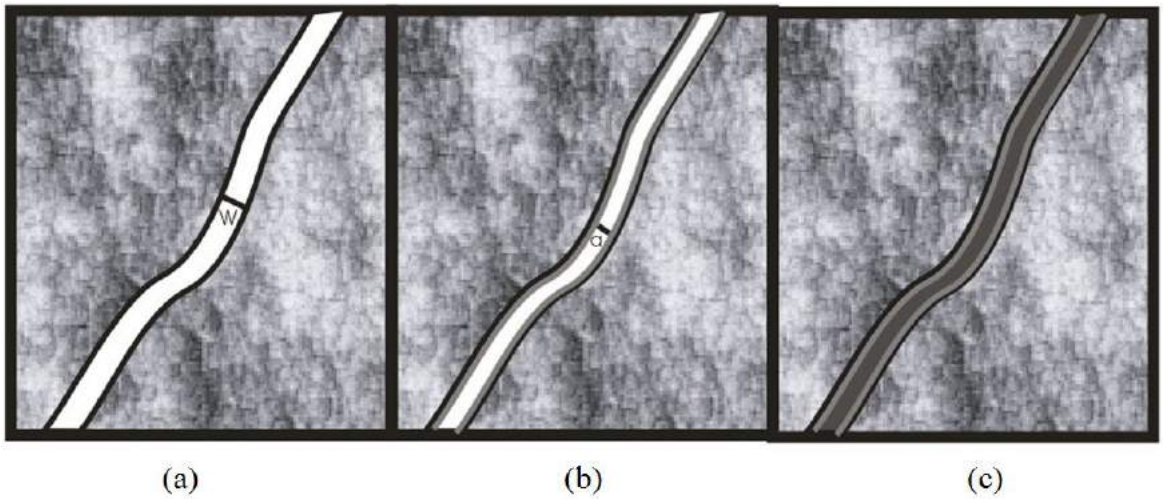

Fig. 8. Sketch of fracture width and aperture. (a) open fracture without surface mineralization, where the width coincide with the mechanical aperture and is measured as the distance between the two fracture walls; (b) open fracture with mineralization, where the mechanical aperture and the hydraulic aperture are smaller than the width; (c) Sealed fracture, where the mineralization has stopped all hydraulic connectivity in the fracture The mechanical aperture is also zero and the mineralization affects the cohesive strength of the fracture.

ture is measured from the surface of the mineralization.

Fractures are also pathways for fluid circulation. Therefore, an equivalent 'hydraulic aperture' is used to estimate the flow through a single fracture plane. The flow is sensitive to the distribution of fracture aperture (Steele et al 2006). For high flow rates and large apertures, the assumption that the hydraulic aperture and the mechanical aperture are equal is adequate but, for tight fractures with low flow, this assumption is not applicable. In fact, the roughness of the fracture surface causes preferential paths and through leading to tortuosity effects. The contact areas must also be taken into account. Various analytical and numerical solutions for different conditions have been studied and reported in the literature (e.g. Zimmerman and Bodvarsson 1996, Koyama 2007).

Surface

The roughness of the fracture surface has been identified as one of the most important fracture features that influence the mechanical behaviour and fluid flow of the fracture (Lanaro 2001). Depending on the scale, the roughness of a fracture can be variable. Thus, knowledge of scaling properties is useful. The kind of origin and the history of the fracture will affect the roughness. The roughness of the fractures affects the deformability of the fracture, as a fracture with a large roughness will not slide as easily as a smooth fracture. Fractures that have experienced shear dislocation of the two surfaces can be polished by the frictional movements creating smooth surfaces, called 'slickensides' (Roberts 1989), or scratches and irregularities on the opposite surfaces such as striation in the direction of movement. Mineralization growing in voids of fractures experiencing shear will also display a striated growth pattern related to the stresses acting on the fracture surface. Fracture surfaces where slickensides have been developed will be likely to be more prone to activation. Shearing of fractures can also alter the preferential flow-paths through the fracture because the riding up of the asperities can cause channels to occur perpendicular to the shearing direction (Koyama 2007).

CHARACTERIZATION OF FRACTURES

In the previous paragraphs we have encountered several characteristics of fractures. They can be measured by using several methods

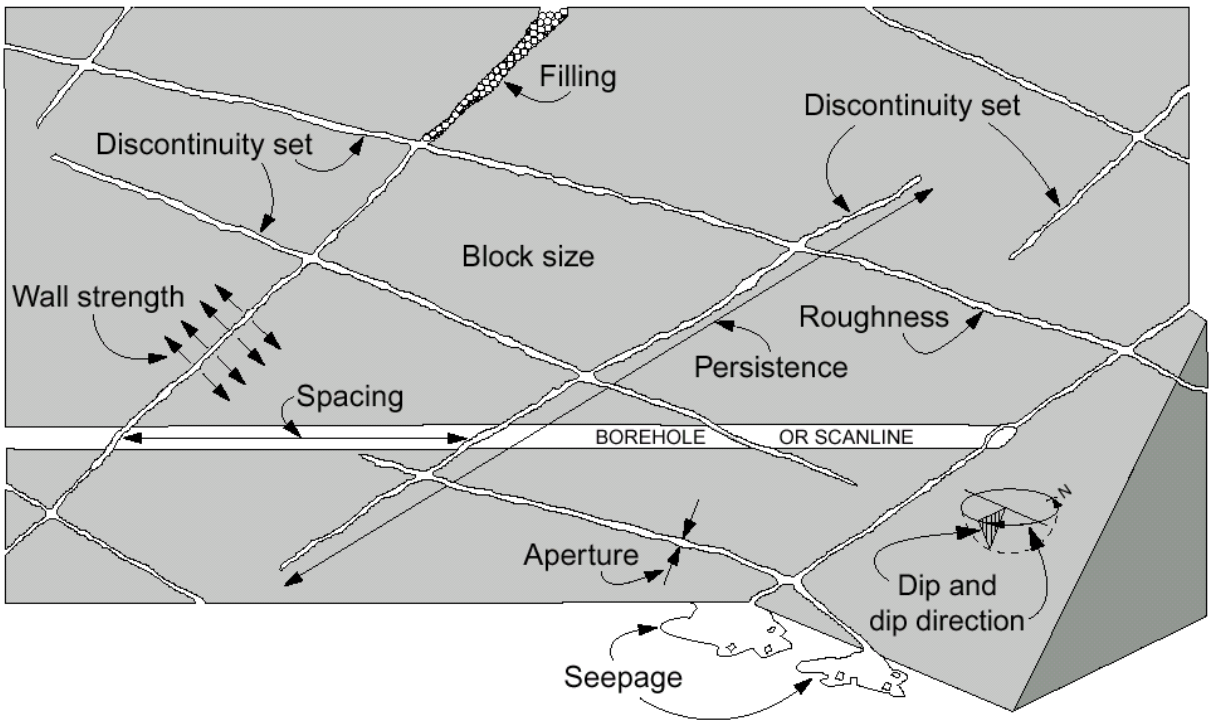

Fig. 9. Fracture characteristics on outcrop scale (Harrison and Hudson, 2000).

for characterizing fractures. As stated earlier, the direct ocular observation is the most used method in geological investigations where a sketch of the position of the fractures is made together with the recording of the orientation, size, frequency, infill materials, surface characteristics, water conductivity and other relevant information for the specific case. This method gives a more or less accurate overview of the fracture properties depending on the person performing the geological mapping. Several of the features that generally can be measured on the outcrop are presented in Fig. 9. This method does not need large cumbersome instruments but the results are sketches, lists or diagrams with information which need further analysis to yield qualitative or quantitative models of the situation.

This information can be further enhanced using different geophysical methods to measure several physical properties. These methods can be applied *'in-situ'* as far-field or near-field methods, on boreholes, or in laboratory on drillcores or specimens. Each case has specific results related to the measured physical properties and a property database needs to be accumulated and correlated to identify geological structures before the response from remote information is analysed. Examples of *'in-situ'* methods for the far-field large structures are:

- measurements of gravity, where rock material with high density influences the gravity field,
- magnetic measurements, where the magnetic properties of a rock structure deviate compared to the surrounding rock,
- electric resistivity where the electric conductivity of a rock structure deviates from the surrounding rock.

The elastic properties of the rock allows for variation in the rock's density to be identified using seismic methods. The method of electric resistivity is further discussed in section 0 where it is presented in the context of its use for identifying different characteristics of meteorite impact craters.

For a more detailed investigation of the behaviour and failure mechanisms of a rock mass, the investigation of fractures in sound rock at microscale must be conducted. To be able to measure the characteristics of these fractures, rock specimens need to be retrieved, prepared and observed by using:

i) thin sections of the rock sample (*e.g.* Fujii et al. 2007);

ii) observations from polished sections (*e.g.* Kranz, 1883);

iii) vacuum impregnation of the specimens with epoxy resin containing fluorescent dye (Åkesson *et al.* 2004, Nara *et al.* 2006);

iv) scanning electron microscopic observations (*e.g.* Kranz 1983);

v) confocal laser scanning microscopy (CLSM), which is a combination of laser-scanning and flourecent dye (Liu *et al.* 2006). These observations are used for improving the simulation tools used to model the failure behaviour of rocks (Boulon *et al.* 2002, Al-Shayea 2005).

Microstructural fracture propagation depends on the mineralogy, fabric, cleavage and microstructures of the rock type. Generally, in granite, there are three orthogonally oriented preferential directions called the rift plane, the grain plane and the hardway plane (Nara *et al.* 2006).

The characterization of the fractures in a specific case is limited by the amount of detail that can be reached. The level of detail depends on what methods are used and how well they are mutually constraining.

Microstructural investigations of the Ävrö Granite

The failure behaviour during a uniaxial compressive test on the laboratory scale was investigated to optimize the parameter acquisition to be used for numerical modelling of coupled Thermal-Hydro-Mechanical-Chemical (THMC) processes. During these investigations, the influence of the hydrological environment on the mechanical behaviour of specimens of Ävrö granite was studied. A further analysis of the fracture development

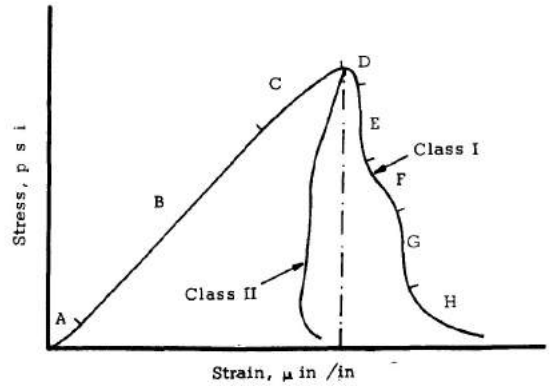

Fig. 10. A Class I complete stress-strain curve monotonically increases in strain; a Class II complete stress-strain curve does not monotonically increase in strain (after Wawersik and Fairhurst 1970).

in these specimens was conducted using the method of vacuum impregnation of the specimens with epoxy resin containing fluorescent dye and then performing a fracture analysis on the specimens. This type of granite has an extreme brittle behaviour during this type of test, called Class II behaviour, thus this behaviour needed to be studied further before any further simulations of the failure behaviour of the EDZ could be conducted. Class II behaviour is identified by an axial strain that does not monotonically increase after the peak stress (Fig. 10) (Wawersik and Fairhurst, 1970). The results from these small scale simulations of the experiments were used as a basis for the behaviour of the rock matrix in the further simulation of the EDZ around the tunnel which was conducted on a larger scale. The study presented here is the information that could be gained from the laboratory experiments and the consequent analysis of the fracture network in the specimens.

A series of laboratory tests was performed to obtain the complete stress-strain curves and to address the chemical and time dependent influences on the mechanical strength of a crystalline intact rock. The tests were all conducted on Pre-Cambrian Ävrö granite from the Äspö Hard Rock Laboratory (ÄHRL) in Sweden. From the modal analysis made on five of the specimens, they are mainly composed of feldspar, quartz and mica in the following percentages: 66 %, 25 % and 6 %, respectively (Jansson *et al.* 2007).

To prevent any bias of the results due to structural differences between the specimens, the specimens were taken in a "cyclic order" from two cores of diameter 51 mm drilled horizontally 3 m apart from each other at the 450 m level of Äspö HRL, Sweden (Fig. 11).

The specimens were prepared for the uniaxial compressive test according to the ISRM standard (Fairhurst and Hudson 1999) with exception of the water saturation.

The twenty specimens were divided into four groups with five specimens in each group. The first group was composed of specimens that had been dried and the rest of the samples were saturated with fluids having different salinities. Group 2 specimens were saturated with distilled water, according to the ISRM Suggested Method (Fairhurst and Hudson 1999); whereas, the specimens in the two last groups were saturated with waters having a salinity of 0.68 % (denoted 'formation water') and 10 % (denoted 'saline water'), respectively. Most of the specimens were saturated for 90 days, but two of the specimens saturated with distilled water and three of the specimens saturated with formation water had a saturation time of only 40 days.

During the uniaxial compression test, the parameters axial stress (σ_a), axial strain (both local and total ε_a) and the radial strain (ε_r) were recorded. The uniaxial compressive strength (σ_c) was obtained as the highest axial stress for the individual specimens. From the laboratory records, the Young's modulus (E) of each specimen was calculated from the slope of the stress-strain curve between 40-60% of the UCS and the Poisson's ratio (ν) as the slope of the radial strain-axial strain

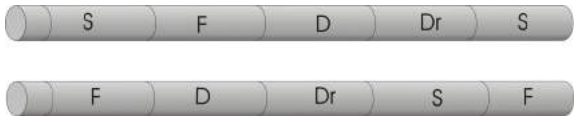

Fig. 11. Example of cyclic sampling of the cores where the (S) is the specimens subject to saline environment, (F) formation water, (D) distilled water and (Dr) are dry conditions.

curve between 40-60% of the uniaxial compressive strength.

The crack initiation stress (σ_{ci}) is determined using the method suggested in Martin and Chandler (1994). The crack initiation stress is obtained from the deviation from the elastic response of the specimen as the axial cracking starts in the pre-peak region of the stress-strain curve. The crack initiation stress is obtained from the crack volumetric strain curve.

Table 1. Mechanical properties of the specimens as tested for different chemical conditions (after 90 days immersion) (Paper II).

Specimen group		Young's modulus (E) [GPa]	Crack initiation stress (σ_{ci}) [MPa]	UCS [MPa]	+ve slope of the Class II post failure locus [GPa]
Dry	Min.	70.4	140	273.9	87
	Mean	71.6	157	302.3	95
	Max.	72.7	179	335.8	111
Distilled	Min.	67.5	132	249.4	85
	Mean	68.5	142	270.5	101
	Max.	69.4	151	287.4	111
Formation	Min.	66.1	126	232.8	84
	Mean	66.6	133	248.5	97
	Max.	67.2	140	264.2	115
Saline	Min.	65.1	115	220.4	82
	Mean	66.8	130	249.4	141
	Max.	67.8	143	277.0	209

By subtracting the elastic volumetric strain from the total volumetric strain measured from the specimens the crack volumetric strain is obtained. The total volumetric strain of the specimens subject to UCS tests is calculated as:

$$\varepsilon_{vol} = \varepsilon_a + 2\varepsilon_r \qquad (8)$$

where ε_{vol} is the total volumetric strain, the ε_a is the axial strain and the ε_r is the radial strain measured during the test. Thus the crack volumetric strain ε_{vol}^{cr} is calculated by:

$$\varepsilon_{vol}^{cr} = \varepsilon_{vol} - \frac{1-2\nu}{E}\sigma_a \qquad (9)$$

In Martin and Chandler (1994), the elastic volumetric strain is expressed as:

$$\varepsilon_{vol}^{e} = \frac{1-2\nu}{E}(\sigma_1 - \sigma_3) \qquad (10)$$

where ε_{vol}^{e} is the elastic volumetric strain, σ_1 is the major principal stress, and σ_3 is the minor principal stress. The minor principal stress in uniaxial compression stress tests is 0, and so σ_a in Eq. (9) equals σ_1.

After retrieving the crack volumetric strain curve, an adjustment to scale is made so that the maximum value of the curve is set to 0. The crack initiation stress is visually obtained as the first non-zero point of the fitted crack volumetric curve (Eloranta and Hakala 1999).

The general trend is that the slopes of the failure loci for several of the samples subjected to saline water have a higher positive slope than those for the specimens from the other groups (Table 1). My experiments also suggest that there is an effect of salinity on the post-failure behaviour of brittle rocks. With high saline water, the specimens act more in a more ductile manner than those with low salinity water.

A change in the mechanical properties could be seen in the physical testing performed with different hydro-chemical conditions for the specimens of the crystalline rock type: Ävrö granite (Fig. 12). There is an effect of water salinity on the mechanical properties of specimens of crystalline rocks. In this study, the effect of weak saline water on Young's modulus and the compressive strength increased with the immersion time (Paper II). The data are unfortunately rather limited and no definite conclusions on the distinction between chemical effects and heterogeneity in the rock material could be made.

Fifteen of the specimens that were subjected to the uniaxial compression test were used in a subsequent fracture analysis. One reference specimen was left undeformed and was impregnated with epoxy containing fluorescent dye to identify the microcracks in the specimens. Two fracture sets were identified: a pre-existing set that can be seen in all the specimens and an induced set from the uniaxial compression test. The pre-existing frac-

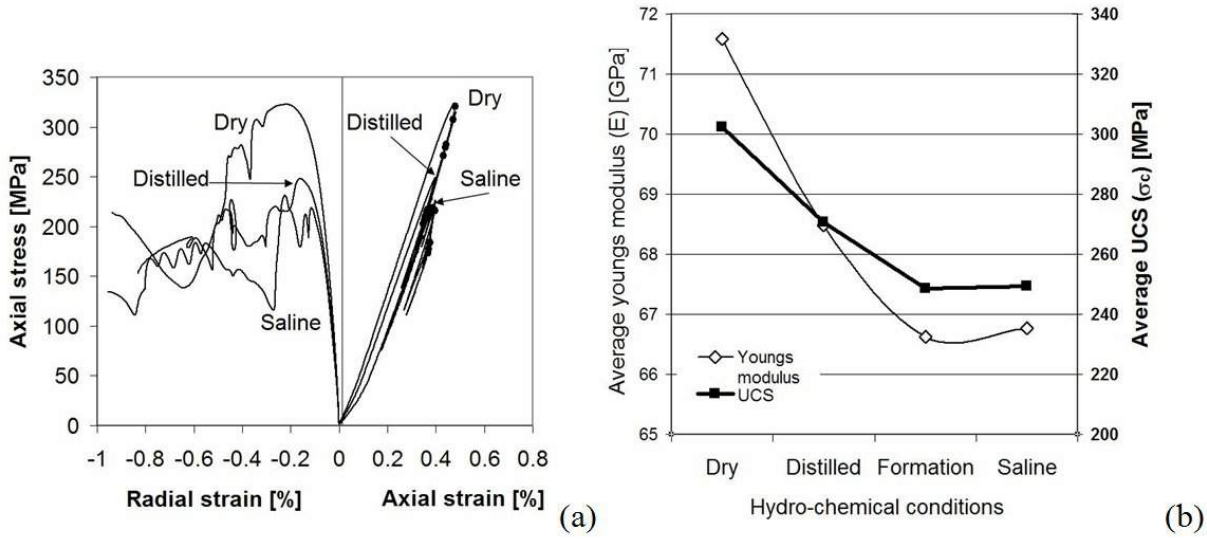

Fig. 12. (a) Stress-strain curves for three specimens subjected to the conditions: dry, saturated with distilled and saline water after 90 days immersion; (b) mean Young's modulus and UCS for the same samples (the Young's modulus values are hollow diamonds with the axis shown on the left and the UCS values are the filled squares with the axis shown on the right) (Paper III).

tures set could be clearly identified in the reference specimen and the specimens after uniaxial compression (Fig. 13).

For the pre-existing fracture set, the microfractures are small (about 2-5 mm in length), and individual microfractures have a consistent orientation throughout the entire sample. They are found in the light minerals (feldspars and quartz) and their distribution is homogeneous. The stress experienced by the core was not strong enough to propagate the microfractures through the more ductile minerals such as the micas. Consequently, the size of the pre-existing microfractures depends on the grain size.

The analysis of the microcracks revealed that a pre-existing fracture set with an orientation close to perpendicular to the specimen axis was present in all the samples. These pre-existing fractures are probably produced by the current principal stresses in the rock mass.

The micro fractures are sub-vertical with strike and dip angle of 110/70-90° and 290/70-90° according to the Swedish National Grid RT90. This orientation is about 10° apart from the orientation of the major principal stress and is therefore almost perpendicular to plane of the minor and intermediate principal stresses. From the comparison between the orientation of the pre-existing fractures and the stress-field in the rock mass, it is likely that they were either produced tectonically or at the time of extraction by drilling. According to the available stress measurements, the difference between magnitude of the major and minor principal stress is about 20 MPa. This value is in the same order of magnitude as the tensile strength of the Ävrö granite that was measured in laboratory experiments to be about 13±1.5MPa (SKB, 2006). This implies that the level of stress before or during drilling might have reached the tensile strength of the rock causing the microcracks.

On the pre-existing microcracks, a second set of microcracks was superimposed by loading the sample in a uniaxial compression during which strong Class II behaviour was identified (Fig. 12). Observations of the resulting microstructure provided information on crack development and crack interaction as also reported in Paper I. As for the pre-existing fractures, also the experimentally induced fractures show a tendency to propagate in the more brittle minerals. These fractures are parallel with the applied compressive stress and are much more developed than the pre-existing fractures. The key role of the pre-existing fractures is that of inhibiting the propagation of the test-induced fractures. In the specimens several instances of

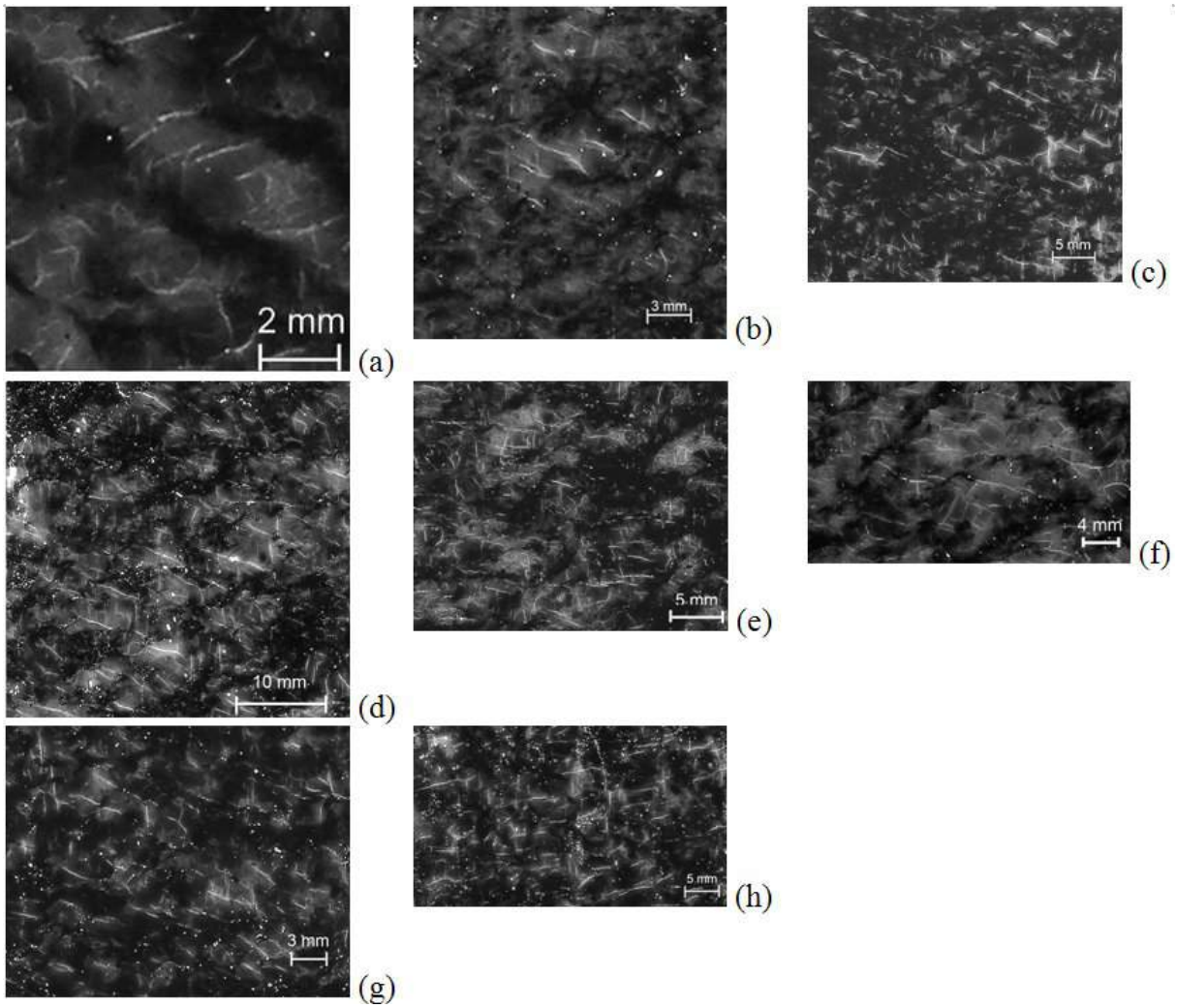

Fig. 13. (a)-(h) Examples of pre-existing fractures intergranular: (a) specimen no. 17; (b) specimen no. 4; (c) specimen no. 19; (d) specimen no. 25; (e)-(f) specimen no. 18; (g) specimen no. 19 and; (h) specimen no. 29.

the test initiated fractures abutting to the pre-existing fractures were found.

The pre-existing fractures were oriented at a large angle to the specimen axis, *i.e.* in an orientation at which they were unlikely to be reactivated during uniaxial compressive testing. In the specimens, there are examples of the effect of the difference in elastic properties between grains on the fracture propagation of both the pre-existing and experimentally induced microfractures. However, there is a larger effect of the pre-existing fracture set on the propagation of the experimentally induced fractures. This is supported by the finding of Nasseri and Mohanty (2008). During standard tensile tests (Mode I) on three different granites, they found that the average microfracture length and orientation had a larger effect on the fracture toughness than the grain size and orientation, which were similar for all samples. As in Nara *et al.* (2006), they found that fractures propagating at right angle with respect to the major set of weakness planes yielded the highest fracture toughness value. These fractures were also characterized by increased roughness, segmentation and higher deflection angles. The contrary was observed when fractures were propagating parallel to the dominant weakness planes.

In the experiments, the rock fails under uniaxial loading but numerous tensile (Mode I) microfractures are generated. These fractures can then link together to form embryonic macroscopic shear failure planes as it can be seen in Fig. 14. The change from Mode I behaviour to Mode II is due to the increase of

the differential stress to a value greater than four times (σ_1-σ_3 > 4K) the tensile strength of the rock, *K* (Fig. 5). This change from one mode of failure to another is often associated with a gradual transition from a set of aligned but randomly distributed extensional fractures (Fig. 14a to c) to a set of aligned extensional fractures arranged in a conjugate set of *en echelon* arrays (Fig. 14d to f).

In conclusion, the effects of the microstruc-

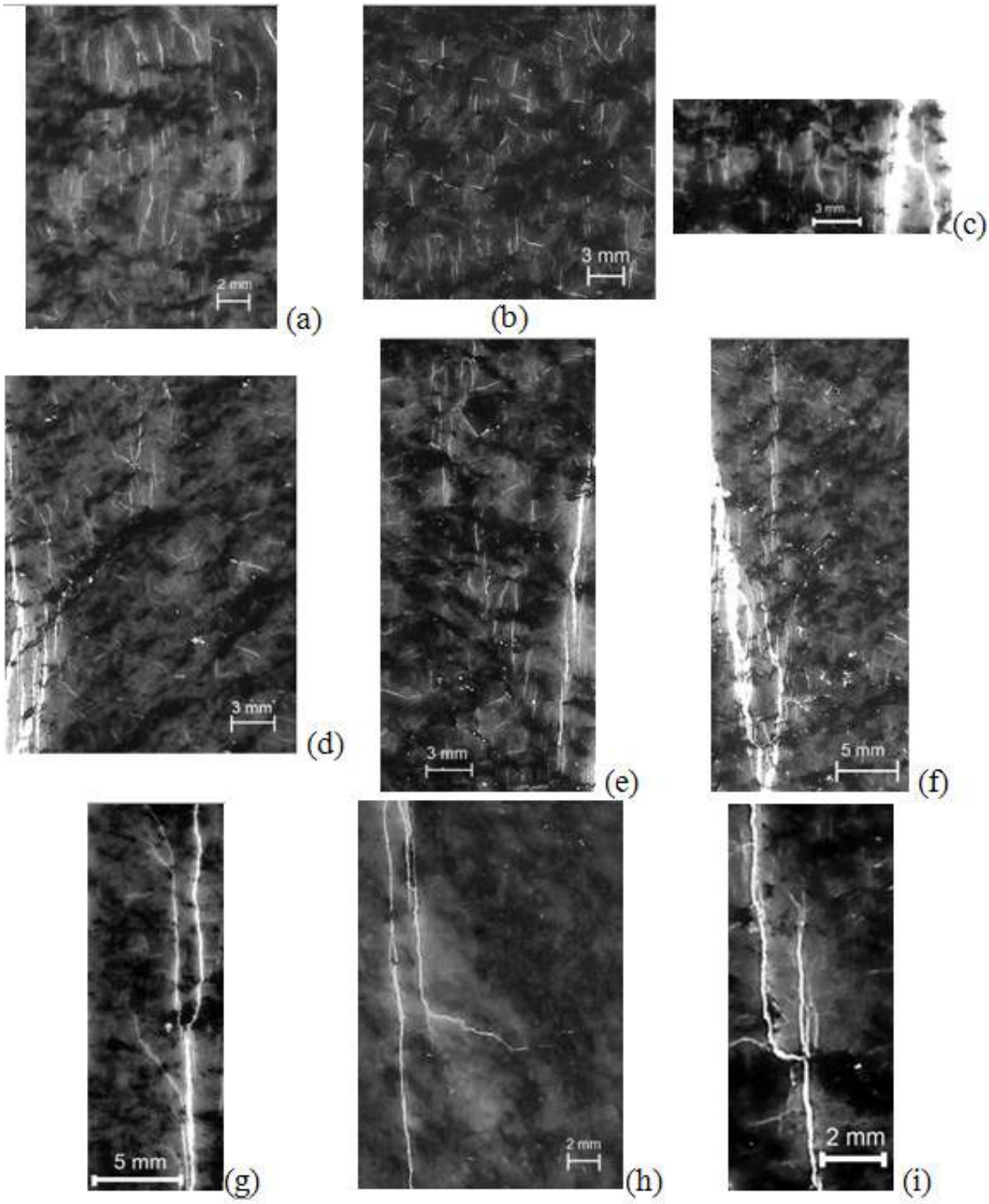

Fig. 14. (a)-(c) Examples of loading-induced fractures: (a) specimen no. 24; (b) specimen no. 31; (c) specimen no. 19; (d)-(f) En echelon extensional fractures with increasing coalescence into a shear fracture; (d) specimen no. 6; (e) specimen no. 17; (f) specimen no. 4; (g)-(i) different termination of fractures; (g)-(h) specimen no. 9; (i) specimen no. 26.

tural properties (microfractures) on fracture propagation seem to control the experimentally induced failure and have more influence than other properties, such as the mineral shape and distribution. When numerical modelling of these experiments is carried out, it is then important to take into account these observations on pre-existent microcracking.

Mesostructural investigation of the Excavation Damage Zone (EDZ)

Rock subjected to significant or violent stress changes experiences inelastic deformations that can either be brittle or plastic. When creating an opening in a rock mass, the removal of rock will inevitably change the stress situation in the rock mass surrounding the opening. In crystalline rocks, this change can cause brittle deformation, and hence damage, as manifested by the initiation of fractures and propagation of pre-existing and initiated fractures. The geometry of the fractures will depend on the magnitude and orientation of the applied stress components and on the experienced stress-path. The opening will cause displacements in the surrounding rock, due to unloading of the unsupported surfaces of the excavation where the normal and shear stresses are zero. This force the principal stresses to rotate and change magnitude to accommodate this. By creating a empty volume, also the fluid pressure is also reduced to zero (or atmospheric pressure) inducing any fluid in the surrounding rock mass to flow into the opening (*e.g.* Hudson *et al.* 2008). Zuidema (2003) stated that "the EDZ cannot be avoided but measures can be taken to minimize its effects. An appropriate layout of the underground openings and use of adequate mining techniques can certainly mitigate the effects". This introduces the second significant factor on the development of fractures in the EDZ that is the excavation method. Besides these two factors governing the EDZ, also the geological structure of the rock mass determines the type of fracturing that develops in the EDZ.

To summarize, the development of EDZ depends on several aspects, the most significant among which are:

i) geological conditions;
ii) stress field and;
iii) blasting performance.

The latter is the only aspect we can modify. Thus, the question is: Can we control the blasting performance to such an extent that we can reduce EDZ and increase the stability and safety of the tunnel?

Four large investigations of the EDZ have been performed in Sweden. Three of these projects have been hosted by the Äspö Hard Rock Laboratory (HRL). The Äspö HRL was established at the end of the eighties as a full scale laboratory for developing and testing equipment and methods for characterization the rock mass for constructing and operating a deep repository for spent nuclear fuel. Previous to the Äspö HRL, a large scale project, the Stripa Project (*e.g.* Pusch 1989, Olsson 1992, Börgesson *et al.* 1992), was performed at the Stripa Mine in the years 1980-1992 where the two main objectives were: i) to develop techniques to characterize potential repository sites in granite and; ii) examine engineered barrier materials and designs that could enhance the long-term safety of the repository.

The three projects performed at the Äspö HRL relevant to this thesis research are:

i) Blasting damage investigation in access ramp section 0/526-0/565 m (Christiansson and Hamberg 1991, Olsson 1991, Ouchtelony *et al.* 1991, Kornfält *et al.* 1991, Nilsson 1991, Pusch and Stanfors 1992);
ii) Zone of Excavation Disturbance Experiment (ZEDEX) (Emsley *et al.* 1997);
iii) Investigations in the TASQ Tunnel that is divided here into two parts: a) Experience of blasting (Olsson *et al.* 2004) and; b) DECOVALEX THMC.

During the DECOVALEX THMC Project, investigations of the EDZ were made in the TASQ Tunnel. The Tunnel Äspö Site designation Q (TASQ) is located at a depth of 450 m at the Äspö Hard Rock Laboratory (HRL), Oskarshamn, Sweden. The excavation technique used was blasting. Care was taken to limit the EDZ. The excavation of

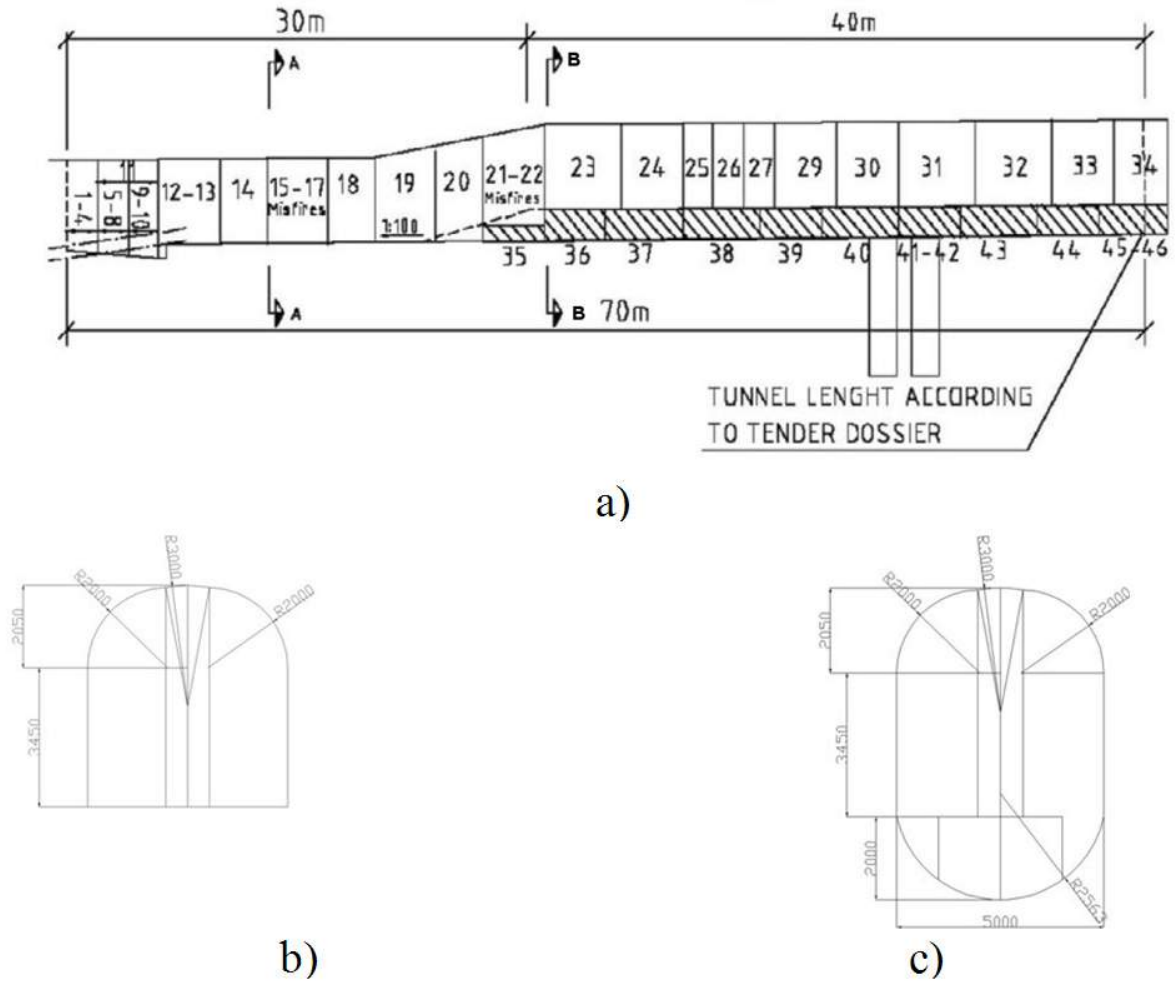

Fig. 15. a) The design of the tunnel from the side showing the blasting rounds; A and B denominates the different cross sections shown in b) and c). b) the horse-shoe shaped cross section used in the first part of the tunnel (about 30 m); c) the oval cross section used in the following 40 m excavated with heading and bench.

the 80 m long TASQ Tunnel was divided in two steps: the first step was carried out by ordinary tunnelling with full face excavation and, after approximately 30 m from the start section, the second step was excavated by top heading and bench blasting (Fig. 15) (Olsson *et al.* 2004).

In this tunnel, detailed investigations of the EDZ were made by means of:

i) cut-out sections in the wall from which detailed fractures mapping was obtained (Fig. 16a);

ii) 3D laser scanning of the wall surfaces of the tunnel (Fig. 16b) and;

iii) ultrasonic investigations in eight boreholes drilled in the same cross section of the tunnel in the vicinity of the cut-out (Fig. 16c).

The cut-out was mapped together with an adjacent part of the wall to build a geological model of the fracture pattern (Fig. 18). When mapping in tunnels, different types of fractures are identified depending on the genesis of the fractures. The 'blast induced fractures' are fractures originating from a blasting drillhole in the tunnel walls. On the other hand, 'induced fractures' are fractures without infilling material that are produced by the excavation but do not originate from the drillholes themselves. These fractures are probably caused by the high stresses, the stress release due to the blasting process or by the redistribution of stresses due to the excavation of the tunnel (Olsson *et al.* 2004).

A fracture network model was set up to simulate the development of a fracturing in the rock mass surrounding a tunnel. The ge-

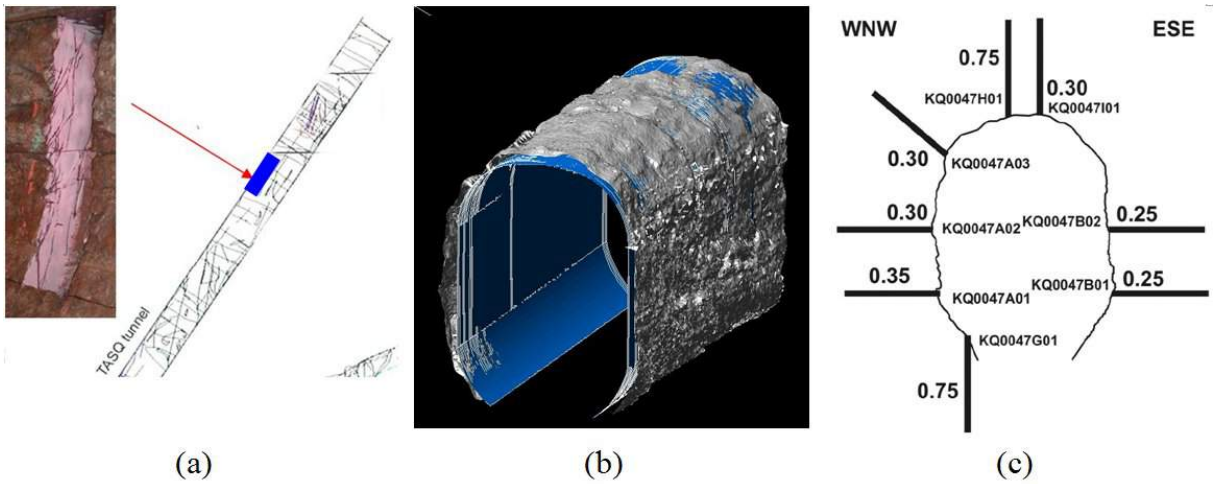

Fig. 16. a) The cut-out in the WNW tunnel wall with a depth and width of about 0.5 m and a height of about 2 m. b) a 3D model of the geometry of the blasted tunnel in grey and the designed tunnel in blue. c) drillholes for the ultra-sonic seismic measurements in a cross section close to the cut-out.

ometry was assumed to be semi-circular, which was required for the application of the different modelling tools, and not elliptical as the true shape of the tunnel (Fig. 15c). In combination with rock mechanics data from the Äspö HRL, the fracture network in Fig. 18 was used to simulate the initial state in five numerical models for modelling the time-dependent behaviour of the rock mass over 100 000 years (Rutqvist *et al.* 2008).

The blasting damage of the TASQ tunnel was analysed by evaluating several parameters obtained from the geometry of the tunnel measured by a 3D laser-scanning method.

The geometrical data on the "as-built" tunnel are evaluated with respect to blasting induced damage. Detailed geometric data were used to provide basic audit data for comparing the "as-designed" tunnel with the "as-built" tunnel. The volume of excavation extending outside and inside the tunnel perimeter as-designed, *i.e.,* the overbreak and underbreak, respectively, were evaluated (Fig. 17). Furthermore, the geometry of the drillholes was combined with the information on the tunnel contour and natural fractures to evaluate the causes of overbreak (Fig. 19).

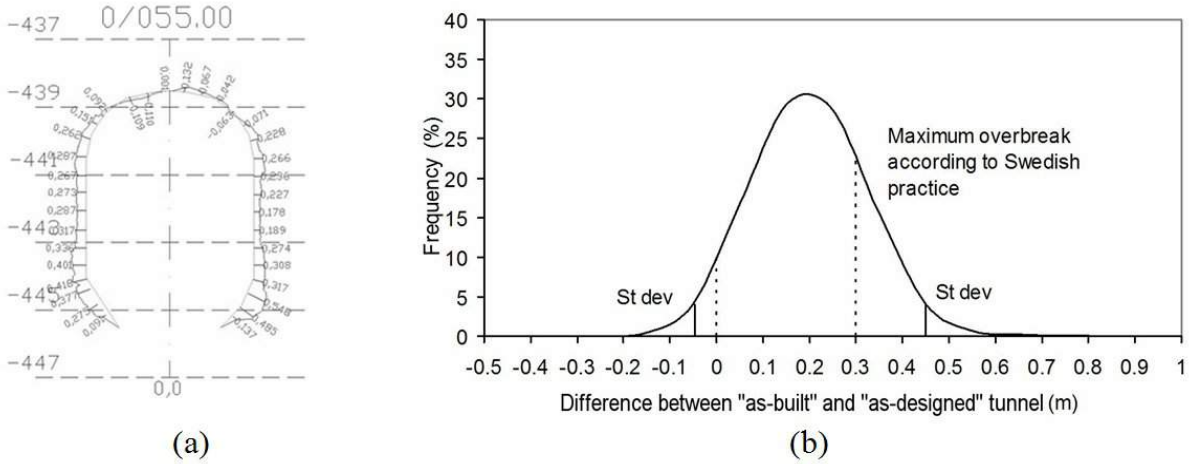

Fig. 17. (a) One of the profiles of the tunnel where the distance between the "as-built" and "as-designed" tunnel is evaluated. (b) The frequency distribution of the difference between "as-built" and "as-designed" profiles from the 3D laser scanning (point-distance 1 to 3 mm). About 65 335 values are considered. The overbreak larger than 0.3 m is about 20%.

In Sweden, generally the standard for acceptable overbreak in tunnels is set to 0.3 m. For the examined tunnel, the performance of the blasting had previously been evaluated to strictly conforming to the design. However, there had not been any attempt to quantifying this conformity. In this study, we have shown that there is about 20% of overbreak in the section investigated along about 11m of tunnel. Additionally, we have identified two large areas of overbreak in the walls that could be explained by the geological conditions and blasting performance.

A semi-automatic fracture mapping for obtaining the fracture plane geometry, its extent and orientation, was performed with the information from the 3D laser scanning. The semi-automatic mapping was then compared with the fracture mapping from a geological survey of the same area of the tunnel. The digital mapping and manual mapping identified the same fracture sets (a NNE and a WNW fracture set) and the average orientation of the fracture sets obtained by the two techniques almost coincides (Fig. 20).

It was concluded that one has to compromise between time and level of detail of the scanning result. Especially in tunnel excavation, this optimisation is crucial for safety and cost effectiveness. The 3D laser scanning method can also be used as a complementary method to traditional geological mapping because it produces a large amount of highly accurate geometrical data in a short time. For the most profitable use, this method should be applied in all tunnelling operations since the laser scanning can be performed at the same time as the geological mapping. The limited time spent at the tunnel face also reduces the risk of injuries associated with falling blocks and allows a prompt installation of the ground support (Warneke *et al.,* 2007).

This method gives an opportunity to tailor-make drill-and-blast operation programs based on the geology and tunnel design. It can also be used to discover deficiencies and adjust the blasting operation to achieve a more accurate cross section of the tunnel. This will reduce the need for unnecessary rock reinforcement and hazards to personnel.

Several geophysical methods can be used to characterize the fractures on the tunnel wall, as presented at the start of section 0. It is well known that ultrasonic measurements supply information of the sonic wave velocity, which can be used to quantify the elastic properties of the rock mass. Several investigations have been made where the detection of fractured rock has been proven using this method (Zimmerman and King 1985, Carlson and Young 1993, Autio 1997, Hirahara *et al.* 1999, Borm *et al.* 2003, Cardarelli *et al.* 2003, Klose *et al.* 2007).

In the investigation at the TASQ Tunnel, the

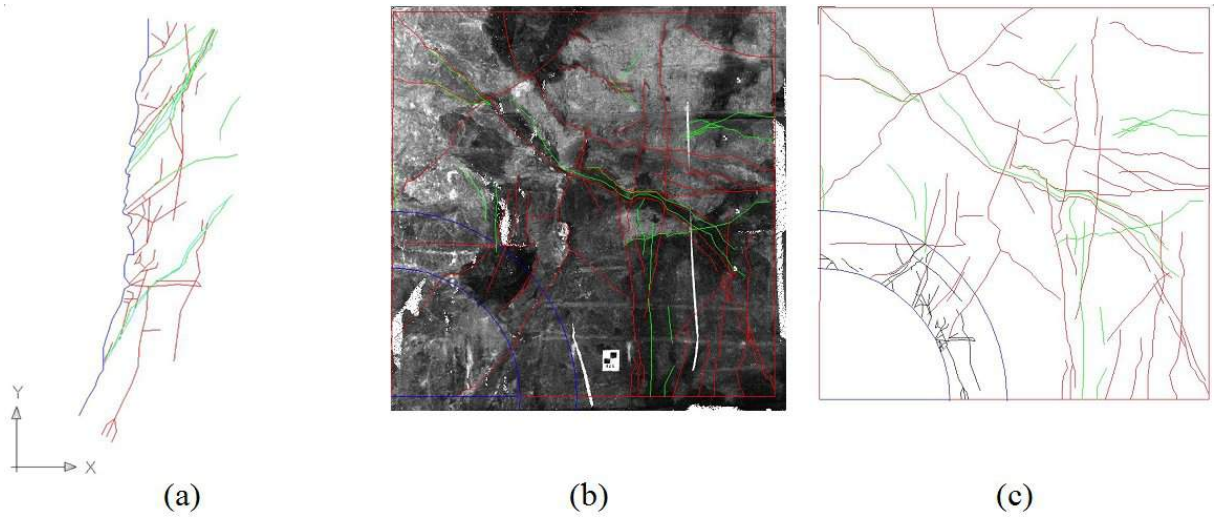

Fig. 18. a) Fracture network in the cut-out on the WNW tunnel wall. Red fractures are open fractures, green fractures are closed and the light blue fractures are natural. b) Orthophoto generated from the laser scanning for the part of the wall juxtaposed to the cut-out. c) Combined fracture network used in the simulation by Rutqvist et al. (2008).

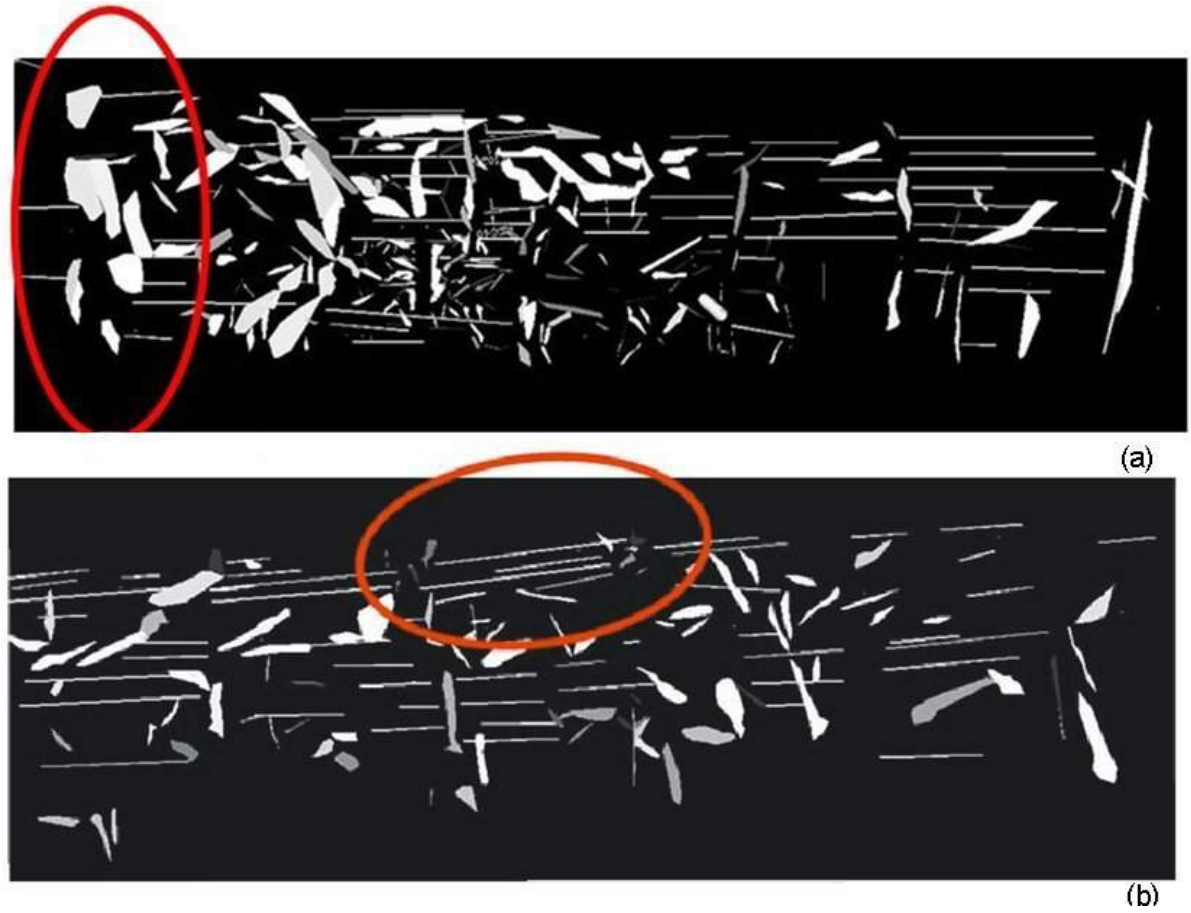

Fig. 19. 2D image of the fractures and drillhole model of the TASQ Tunnel. (a) Left side of the TASQ Tunnel (the floor is in the lower part and the tunnel face is on the right). (b) Right side of the TASQ tunnel (the floor is in the upper part and the tunnel face is on the right).

ultrasonic wave velocity method was applied. An attempt to correlate the effect of the stress, blasting and the geological prerequisites for the development of the EDZ has been made through measurements of ultrasonic wave velocities in holes drilled on the tunnel wall. Measurements were conducted in eight boreholes, each 3 m long. The results have been correlated to the geology (from the core investigation) and the detection of large fractures was confirmed. According to Schuster (2007), the quality of the obtained measurement data was high. Seismic P- and S_V-wave onsets could be determined and different parameters were derived from the data, including seismic P- and S_V-wave velocities. Besides the travel time information, absolute and relative amplitude information were also determined from all datasets. The absolute and relative amplitude information was mainly obtained for the estimation of the degree and extent of the EDZ but also to obtain information about dynamic elastic parameters such as *'in-situ'* pseudo elastic parameters. The Young's modulus and Poisson's ratio, for example, are of interest for geo-mechanical modelling and comparison with parameters derived from core measurements in the laboratory.

The result obtained when comparing the measurement of the ultra sonic wave velocity and the mapping of fractures from the drill-cores is reported in (Bäckström 2008) together with a further analysis of the rotational measurements to estimate the usefulness of the ultrasonic method in the context of characterizing the rock mass surrounding the tunnel. The results show that the ultrasonic method can detect and predict the location of open fractures crossing the borehole in crystalline rocks (Table 2). Fractures are distinguished as more abrupt changes in the ultrasonic wave propagation (indicated as certain in the seismic investigation). The changes in rock type have been identified as less distinct

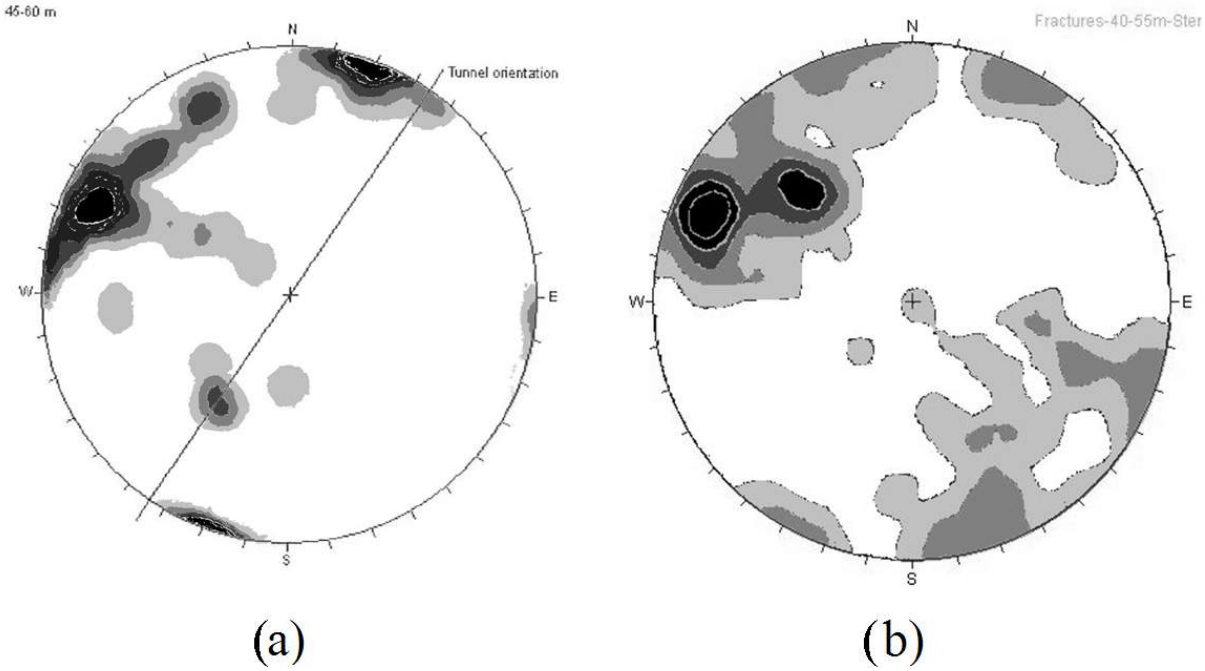

Fig. 20. Equal angle pole plot of the fractures: (a) manually mapped fractures with a truncation of 1 m; (b) Semi-automatic mapping based on the information from the 3D laser scanning with a truncation of 0.5 m. The contours represent steps of 1-1.5% frequency.

changes in the ultrasonic wave propagation (indicated as uncertain in the seismic investigation).

Macrostructural investigation of fractures caused by meteorite impact

In structures as large as impact craters, some parts are not accessible from the surface. This forces the investigator to rely on remote methods such as geophysical methods. As already stated in the introduction and section 0, fractures change the physical properties of the rock, consequently, several geophysical methods have been developed to detect the presence of fractures in the rock mass.

Two macrostructures were investigated in this study: the suggested Björkö meteorite impact structure (Flodén *et al.* 1993; Bäckström and Henkel 2003) and the Lockne meteorite impact structure (Wickman 1988; Lindström and Sturkell 1992), both located in Sweden. The aim of these investigations has been to identify the fracture frequency in crystalline rock and its effect on the electric resistivity. The investigated meteoritic craters are large structures and the energy released by the impact causes fractures to form on all scales. The energy in the central part of the structure has caused a highly fragmented fracture network, whereas the attenuation of the impact energy outwards from the impact centre decreases the development of the fracturing. This decrease has been used to identify the size of the Lockne impact structure.

Both of the meteorite impact structures investigated are located in Sweden. The Lockne crater is located in the county Jämtland at 63°00'N, 14°50'E according the Swedish National Grid. The largest city in the vicinity is Östersund, located north of the structure. The presence of shocked quartz in the deposits of this crater has proven its origin as the result of a meteoritic impact (Lindström and Sturkell 1992, Therriault and Lindström 1995). The other structure is a suggested impact structure located close to the eastern coast of Sweden in the county Södermanland, 59°20'N, 17°50'E, according the Swedish National Grid. The largest city in the vicinity is Stockholm, the capital of Sweden, located about 15 km east of the structure. These two were selected for this study because of the occurrence of outcrops. Both of them are formed in crystalline basement, although the Lockne meteorite impacted in an about 80 m thick sedimentary deposit, the impact was large enough to form a crater in the crystalline basement.

Table 2. Identified fractures or other structural features that can be distinguished in the seismic interval velocity data, the drillcores and the Borehole Image Processing System (BIPS) loggings (Bäckström, 2008).

Drillhole name	Suggested section with fractures from seismic (m)	Fractures indication in the drillcore and in the BIPS loggings (m)
KQ0047A01	0.20-0.25	0.248 -open in the core and visible in BIPS
KQ0047A01	0.7-0.75	0.743 -open fracture in the drillcore and visible in BIPS
KQ0047A02	0.55-0.6	0.592 -open in the core and visible in BIPS
	0.7-0.8	0.734 -open in the core and visible in BIPS (actually two fractures exist in this section)
	1.2-1.25	1.212 -open in the core and visible in BIPS
KQ0047A03	(1.55-1.65)?	No fracture found at this location but a change in mineral content can be observed in the core
KQ0047B01	No	No obvious open fracture indication found in the BIPS image from the borehole.
KQ0047B02	No	No obvious open fracture indication found in the BIPS image from the borehole.
KQ0047G01	(0.15-0.4)?	Several fractures found in both the core and BIPS.
	0.4	0.394 –open in the core and in BIPS
	(2.05-2.15)?	No fracture found at this location, however a closed fracture network containing chlorite is observed in the core.
KQ0047H01	(0.1-0.2)?	0.199 – open fracture in the core but not in BIPS
	(170)?	No fracture found at this location but a change in mineral content can be observed in the core.
KQ0047I01	(0.85-0.9)?	No fracture found at this location but a change in rock type can be observed in the core.

In the crater structures in this study, the fracturing could be detected on outcrops of the crystalline rock in the target area. The impact crater structures were identified by abrupt variation of fracture frequency over a rather limited area. 'Normally' fractured rock in the region surrounding changes into extremely highly fractured rock in the central up-lift or rim area of the crater. The variation of the fracture frequency with respect to the location in the impact structure was mapped. The results of these investigations were compared to the result of measurements of the electric resistivity on the same outcrops. A negative correlation was found: the electric resistivity decreases for an increase in fracture frequency.

Electric resistivity

Electric currents are transmitted through the rocks mainly by means of two mechanisms: electric conductivity (charge transport) and dielectric polarization (charge separation) (Carmichael 1989). In geophysical applications, the reciprocal of the electric conductivity (*i.e.* electric resistivity) is the parameter traditionally used. This parameter is commonly measured in ohm-meters (Ωm). The electric conductivity depends on:

- the amount of electrically conductive minerals or elements in a rock type;
- the amount of water - as water is bipolar, it is also conductive, which results in the effect of the water content in the rock on the electric resistivity. In turn, the water content depends on the porosity and the amount of water conductive features in the rock such as fractures.
- the presence of several water-dissolved salts that also affect the electric resistivity.

The rock types commonly found in the investigation areas are granites and gneisses. The main components of granite are quartz and feldspars. Granite is a rather homogenous mixture of these two minerals, with different grain sizes. These minerals are quite non-conductive: they generally have a resistivity larger than 10 000 Ωm. This leaves the water and its content of dissolved compounds to be the conductive element in these rocks. As mentioned before, the water content of the rock depends on the porosity, which in the case of granites is generally low (lower than 1%). This leaves the fractures as the only water bearing features in this rock. The content of the water varies depending on the local hydrological systems encountered, but generally in the Baltic shield it has been found that at depth larger than 500 m the salinity of the water increases. This has been found at the ca 6 km deep drillhole in the Siljan impact structure in central Sweden, about 120 km inland from the Swedish coast, where the salinity of the water increases at about 4 km depth (Juhlin 1991). In the Laxemar area on the south-eastern coast of Sweden the increase in salinity has been found at about 1 km depth (Ekman 2001).

In these two studies, the electro-magnetic Very Low Frequency (VLF) method with a 10 m long antenna was used to measure the resistivity (Geonics EM16R, VLF-R; *e.g.* Geonics 1979, Müller and Eriksson 1981, Hjelt *et al.* 1985). The VLF-R is a "radio" receiver that measures the electro-magnetic waves transmitted on very low frequencies from transmitters located at different places in the world. Depending on the structure to measure, the transmitter located at the optimal position with respect to the structure is selected. This method is based on the fact that Earth is not a perfect conductor, and the angle between the two components in an electro-magnetic wave (electric and magnetic) will vary, as well as the strength of the signal, depending on what is found underneath the instrument. The antenna is aligned to the direction of the transmitter to measure the horizontal electric field. The electric component is compared to the magnetic field that is induced in the VLF-R reference coil (the phase angle). The measurement results in a resistivity value and a measure of the phase angle between the electric and magnetic components. From these data, a two layer model is created.

The penetration depth of this method depends on the frequency used and the resistivity of the examined medium. When using a frequency of 15 kHz, the penetration depth is:

- 60 m for a resistivity of about 200 Ωm
- 200 m for a resistivity of about 2000 Ωm
- 600 m for a resistivity of about 20 0000 Ωm

For this study the radio-transmitters GBR (16.0 kHz) located in Rugby, England and NAA (17.8 kHz) located in Maine, USA were used.

Fracture frequency calculations

As the goal of the investigation at the Björkö structure was to decide if this structure is suitable for geothermal energy retrieval by circulating water in the fractures, it was of interest to calculate the fracture area per unit of volume of rock mass. The fracture frequency was obtained for the Björkö structure. The results from the investigation at the Lockne meteorite impact structure (paper VI) were also obtained with the same method and supported by the results from the Björkö investigation.

The fracture frequency on rock outcrops was measured in a window from which the frac-

ture length on a rock surface is observed (Fig. 21). The calculation of the fracture frequency had the aim of identifying the potential fracture surface in a rock volume for heat exchange. For each fracture, the surface of both walls was considered. Granitic rocks often display an orthogonal fracture pattern where one fracture ends in another. Considered this, the fractures were assumed to be squares. The distribution function of the fracture length in the Björkö area was also used. The equation used to calculate the fracture frequency (F) in this investigation is:

$$F = \frac{2 \cdot 1.17 \cdot (1+y) \sum_{i=1}^{n} \lambda_i^2}{(1-e^{-8.8L}) \cdot s^3} \qquad (11)$$

where y is the difference between the function where spacing is the same as the trace length and the spacing function for the outcrops, λ is the trace length of the fractures, s is the side length of the sampling surface, and L is the mean trace length at the location. The factors 2 and 1.17 account for the two surfaces of the fracture and the undersampling of the horizontal fractures on a sub-horizontal outcrop, respectively. The fractures with a dip of less than 15° to the horizontal surface were assumed to be underrepresented and were accounted for by the factor 1.17, adding on about 17% of fractures to remove this bias. In the drillcore of the crystalline rock from the Björkö investigation, the sub-horizontal fractures were found to be about 15 % of the total amount of the fractures.

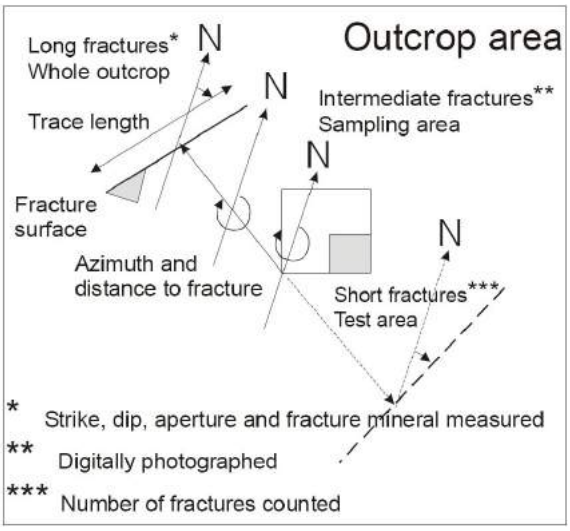

Fig. 21. Reference system for the fracture sampling on outcrops in the Björkö structure area.

The Lockne meteorite impact structure

The Lockne structure was caused by a meteorite impact that occurred about 455 Ma ago (Grahn and Nõlvak 1993). During that time, the impact area was covered by the Ordovician Sea in which limestone of the Dalby formation was being deposited. It is a 7 km wide structure in the crystalline basement (Lindström *et al.* 2005). The Lockne impact is one of few impacts of this size that has impacted the sea, which has been preserved. This structure is well preserved due to the Caledonian orogeny, which had already started further to the west when this event took place, moving large sedimentary deposits on top of the area, covering and preserving the structure (Lindström *et al.* 1996). This area is just at the present margin of the Caledonian mountain range (Fig. 22). The sedimentary deposit was about 80 m thick, consisting of Cambrian shale and Ordovician limestone (Lindström *et al.* 2005). Underlying these deposits is the crystalline basement in which the Revsund granite is the dominant rock type in this area. The crystalline basement had been eroded to a peneplain before the sedimentary sections were deposited.

The marine environment prevailing at the time of impact has caused superficial differences to the crater morphology, with a large amount of resurging material and a morphology generally not encountered in terrestrial crater structures. The impact was strong enough to penetrate the sedimentary rock and crush the crystalline basement underneath. The fragmentation of the crystalline rock was the main target of this fracture investigation partly because the less anisotropic nature of the granite compared to gneisses but also due to the high resistivity of the intact parts of the granitic rock, where the decrease of resistivity is due to the water conductive fractures.

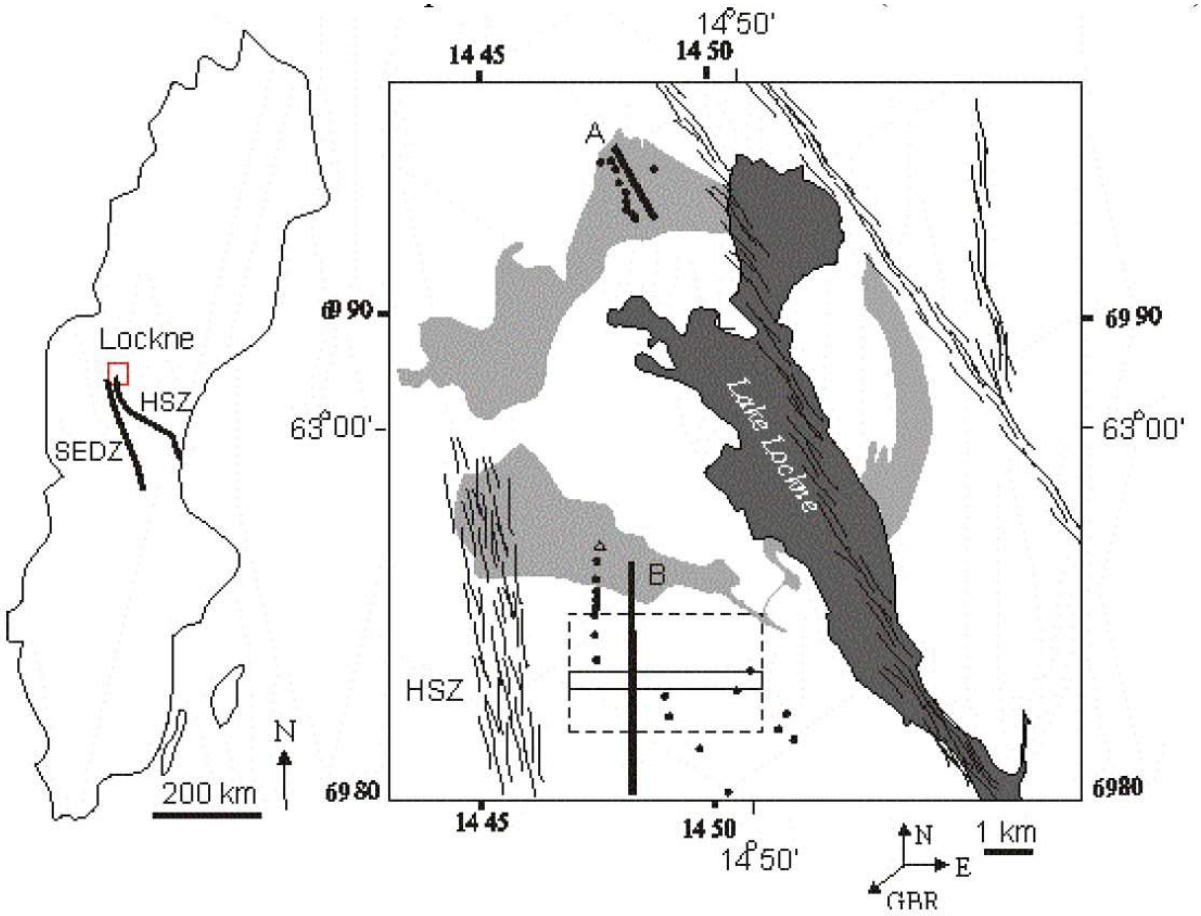

Fig. 22. Location of the study area in Sweden where two major deformation zones are seen, the Stora-Handsjön ductile zone (SEDZ) and the Hassela Shear Zone (HSZ). The HSZ can be seen as thin lines (after Högdahl, 2000). The light grey areas in the map are the extent of the Tandsby breccia (Lindström et al 1996). The sites for fracture frequency and electric resistivity measurements are marked with dots. The two thick lines indicate sections A and B on which the measurements are projected. The large box (broken line) at section B shows the transition zone. The step in fracture frequency/electric resistivity is marked by the narrow box. The direction to the GBR radio transmitter in southern England is to the SW. Coordinate numbers refer to the Swedish National Grid.

Only outcrops of crystalline rock were investigated which were assumed to be autochtonous with respect to the crater i.e. the fractured material has not been displaced in connection to the Caledonian orogeny. To investigate the change of fracture frequency and its effect on the electric resistivity, two sections of the crater where the crystalline rock was exposed were selected (Fig. 22).

At each site, the measurements were divided into two groups, one for large fractures (with a trace length between 0.25 and 5 m) and one for small fractures (with a trace length between 0.1 and 0.25 m). The large fractures were counted over the entire outcrop, whereas the small fractures were counted within 0.25 m^2, because of their large number on each outcrop. The maximum distance between large fractures was censored to 5 m because of the size of the outcrops, which had a width of about 5 to 10 m. The truncation for the small fractures was 2 cm. Fractures smaller than 2 cm were not possible to distinguish from the mineral structure of the rock type. For information on the calculation of the fracture frequency from these data the reader is referred to section 0 of the calculation of the fracture frequency.

From the results of the calculated fracture frequency of the crystalline outcrops in the Lockne area, it can be seen that the section cutting the northern limit of the Lockne crater (section A in Fig. 22 and Fig. 23) shows a

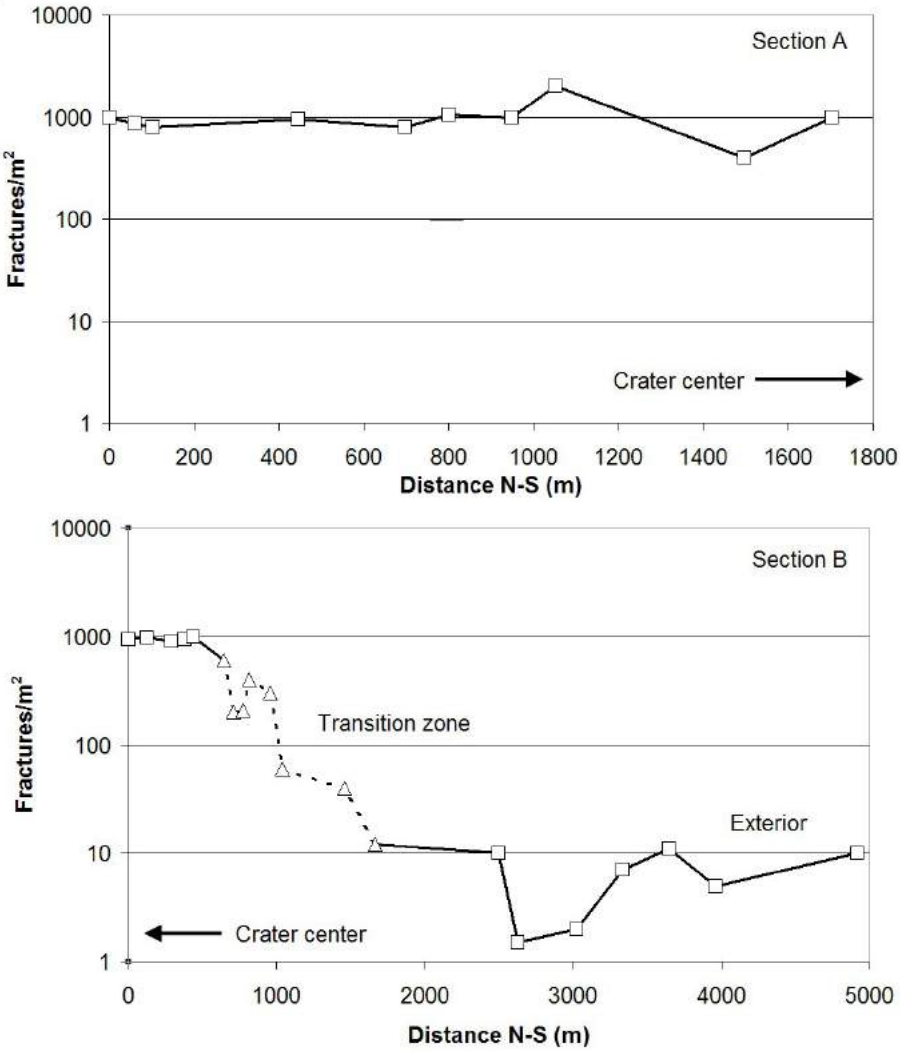

Fig. 23. Projection of the fracture frequency (number of fractures/-m²) to the northern, section A, and southern, section B, respectively. The transition zone between high and low fracture frequency is marked with triangles in section B. For the location of the sections and the individual measurements see Fig. 22.

high fracture frequency close to about 1000 fractures/m^2, over a distance of 1700 m, whereas the section in the south-western part (section B) varies from over 1000 fractures/m^2, to about 2 fractures/m^2. The transition from high to low fracture frequency can be seen on moving out from the crater. There is a transition from high fracture frequency to low fractures frequency from about 500 to 1600 m along this section (Fig. 23b). In the south-western section, the transition from high fracture frequency within the crater to low fracture frequency outside the crater can be clearly seen. In the northern section, such a transition cannot be found. This implies that the crater limit has not been encountered in the northern area and thus it is possible that the Lockne crater is larger than hitherto assumed. Unfortunately, the area north of the last crystalline outcrop is covered with sedimentary rocks. The only means of investigating the crystalline basement in this area is by geophysical investigations and drillings.

The correlation of fracture frequency and electric resistivity on these outcrops can be found together with the results from the similar investigation in the Björkö area (Fig. 24). A negative linear correlation between the logarithm of fracture frequency and the logarithm of electric resistivity was found.

The suggested Björkö meteorite impact structure

The Björkö structure has been suggested to be a crater mainly based on the results of geophysical and geological investigation methods. The Björkö crater is located in a post-glacial landscape, in crystalline rock overprinted by large fracture zones. The presence of the Jotnian Mälaren sandstone

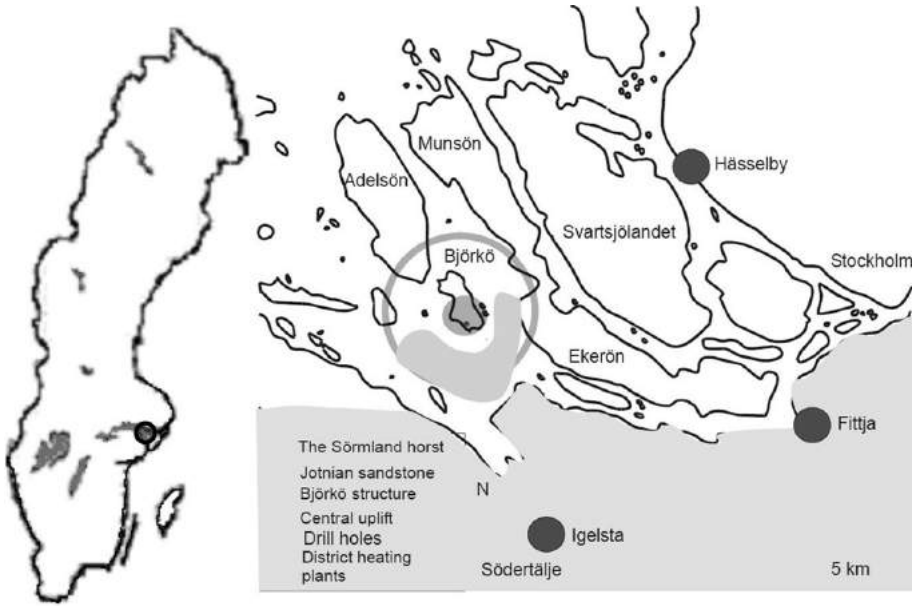

Fig. 24. The Björkö structure. Left: location of the study area in Sweden, Right: location of the Björkö structure west of Stockholm.

(1.2 Ga) on islands in Södra Björkfjärden, a bay in Lake Mälaren, indicated that there is a structural feature in which this sedimentary rock could be preserved (Wickman 1988). A marine geophysical investigation presented by Flodén *et al.* 1993, 2003 using seismic reflection and refraction sounding delimits the distribution of the Jotnian sandstone to a semicircle of about 170° to the southeast of the southern part of the island Björkö. As this structure is located in Lake Mälaren the onland investigations are restricted to islands, and the surroundings of the structure.

The structure is about 10 km in diameter with a central uplift in the southern part of the island Björkö, Ingaberg (Fig. 25). No unambiguous proof of the impact has been identified in the form of shatter cones, microscopic planar deformation features, solid-state and fusion glasses, high pressure polymorphs or whole rock melting and vaporization. The shock pressure necessary to induce these effects must be larger than 5 GPa and up to 100 GPa (Grieve & Pesonen 1992). Despite the lack of these proofs, the combination of several geophysical characteristics indicates that this should be an impact structure (Henkel 2002).

The investigation show that there is a gravity low point in this structure compared to the surrounding area, and the electro-magnetic response from the crystalline basement also indicates large volumes of low resistive rocks. The presence and the properties of the sandstone in the depression, which is suggested to be the ring formation surrounding the central crater up-lift, complicates the interpretation of the geophysical results. The erosion level of the structure is unknown and its age is estimated to about 1.2 Ga based on a K-Ar data from a claystone bed immediately above the granitic basement (Flodén *et al.* 1993). The Jotnian sandstone was deposited on top of palaeo-Proterozoic gneiss and younger Stockholm granite (1.8 Ga). The sandstone sequence starts with a thin layer of claystone followed by a breccia, containing crystalline clasts from the underlying granite and gneiss.

Terraces in the Stockholm granite at Ekerö limiting the eastern extent of the Mälaren sandstone indicate down faulting at the rim of the eastern part of the structure. Tension cracks filled with quartz are found extending in the east-west direction at this site (Gorbaschev and Kint 1961). In the western part of the structure, breccia is found again, this time on the island of Pingst, which has been strongly affected by the large Södertälje-Adelsö-Torsviken fault zone striking in the WNW direction.

Two drillings have been performed in the area: one at the island Midsommar, and one in the southern part of Björkö, to the depths of 950 and 912 m, respectively. These drillholes are a part of the investigation aiming to provide information on the hydraulic potential of the Björkö structure for the geothermal energy project. Heat should be retrieved

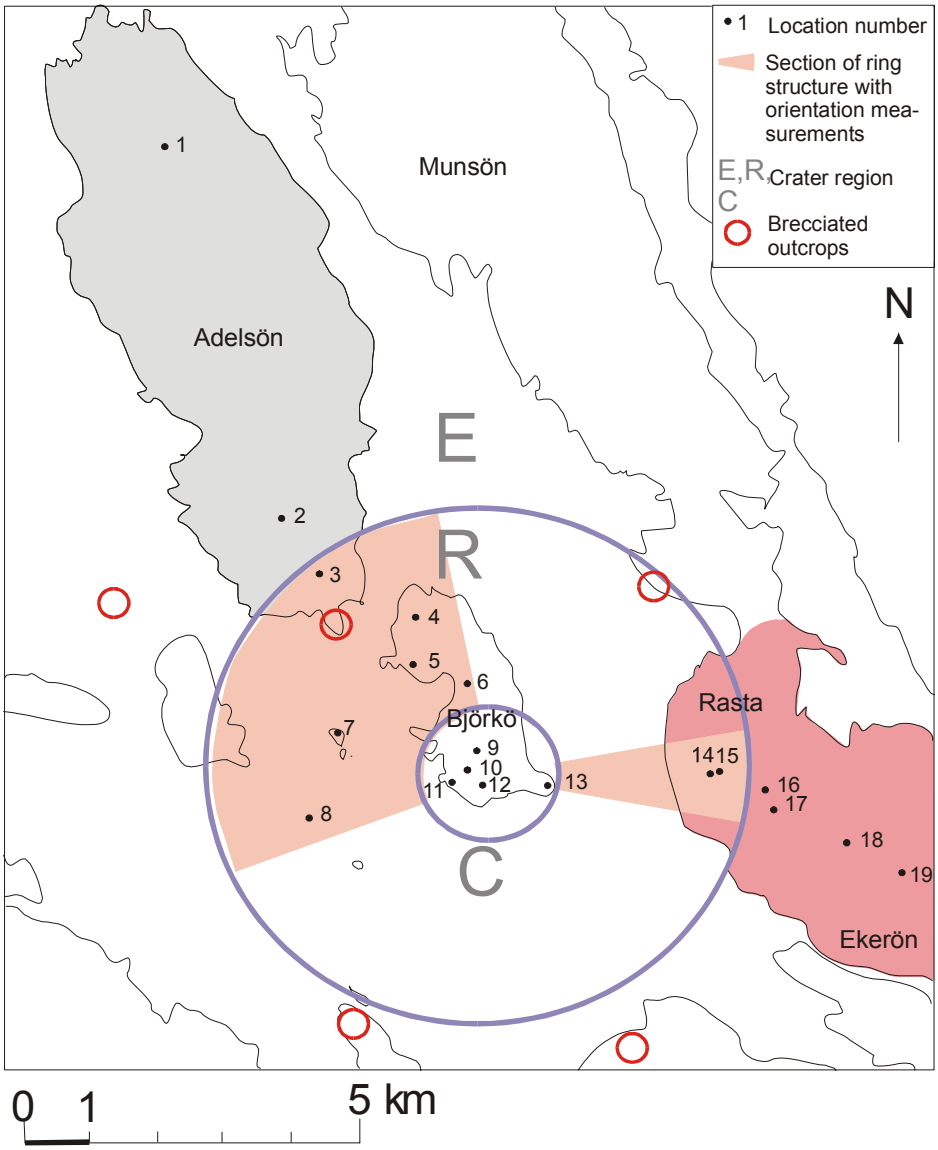

Fig. 25. Location of outcrops and long fractures that have been mapped (window sampling). The crater regions are: Exterior (E), Ring structure (R) and Central uplift region (C). The circles indicate the approximate boundaries of the regions. The coloured sections at Adelsö and Ekerö represent the northern and eastern tectonic blocks in the area, respectively. The numbers represent the locations.

from the large fractured rock mass associated with impact structures at depth. The drilling on the island Midsommar was performed to investigate the depth to the crystalline basement in the ring formation below the Mälaren sandstone. The sandstone continued down to the depth of about 950 m and the drilling was terminated without reaching the crystalline basement. The drilling in the southern part of the mountain Ingaberg on southern Björkö is performed in the fractured Stockholm granite.

An investigation of the fracturing in this area was carried out by Bäckström (2004). Beside the exploitation of the structure for energy production, the aim of the investigation was to improve the statistical basis for the correlation between the fracture frequency and the electric resistivity in crystalline rocks. Subsequent goals were also: i) the evaluation of the effect of water-filled fractures in crystalline rocks on the electric resistivity; ii) the description of the impact crater structures and the extent of the impact-generated brecciation by applying electric and electro-magnetic methods and; iii) the development of a tool for prospecting for geothermal energy in crystalline basement. The investigation was

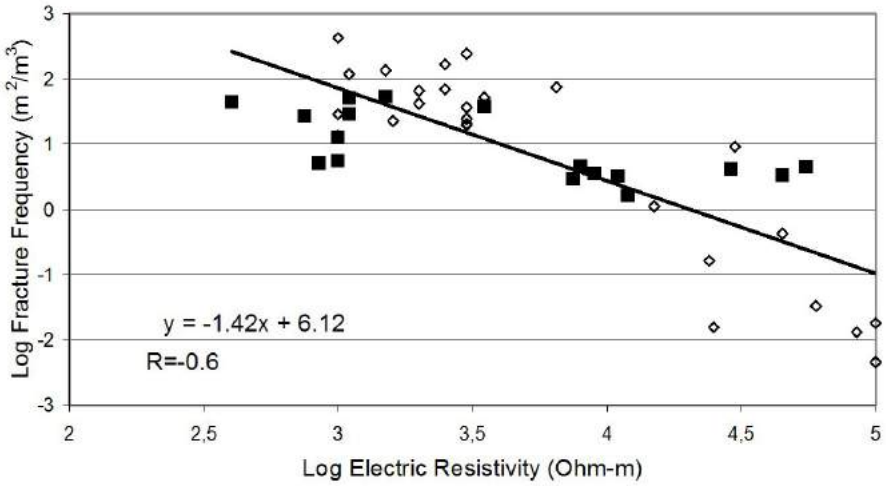

Fig. 26. The relation between the fracture frequency and the electric resistivity for Björkö (filled squares) combined with values for the Lockne structure (empty dia-

performed on outcrops spread in an area of about 20×20 km, i.e. twice the diameter of the suggested crater (Fig. 25).The main limitation of the investigation was the access to the outcrops due to the fact that the crater is located within Lake Mälaren and only a few islands are accessible. The outcrops with high fracture frequency are more prone to erosion thus making them less likely to be found.

The fracture mapping on eighteen outcrops was limited to the crystalline basement as that was the target rock for the geothermal project. The fracture mapping was performed on outcrops and the drillcore from Ingaberget (called: BJO-01). The electric resistivity was measured on the outcrops in the area and in the drillhole from the southern part of the mountain Ingaberg. In the central uplift area of the crater, five measurements were performed, eight in the ring formation measurements and six in the surroundings area. The size of the outcrop surface on which the fracture frequency was measured depended on the fracture frequency: either 1×1 m for outcrops with high fracture frequency or 3×3 m for outcrops with low fracture frequency. These measurements were then compared to the electric resistivity measurements from the same outcrop and the correlation between the two was determined (Fig. 26). As shown in the diagram, a negative correlation exists between the logarithm of the fracture frequency and the logarithm of the electric resistivity. Rock volumes with high fracture frequency produce low electric resistivity and *vice versa.*

NATURAL AND MAN-MADE DAMAGE OF ROCK

Microscale – Implementation of damage mechanism in numerical modelling

During mechanical testing in uniaxial conditions, Class I behaviour can be identified by a negative slope of the post-failure part of the axial stress-axial strain curve. This results in a stable fracture propagation of the damage fractures where work must be done on the specimen for the continuation of failure. In contrast, Class II behaviour is identified by an axial strain that does not monotonically increase after the peak stress (Wawersik and Fairhurst, 1970). A positive slope of the post-failure part of the axial stress-axial strain curve implies that failure is unstable or self-sustained and elastic energy must be extracted from the specimen to control the failure. In other words, the rock specimen has a capacity to store more strain energy than is required to continue the failure process, thus, the decrease of the elastic strain in the post-failure part of the curve is not matched by the increase of the non-elastic strain (He *et al.* 1990) with violent effects. It has been suggested that this behaviour is influenced by the non-uniform failure of the specimen (Hudson *et al.* 1972) remembering that what is measured is an 'engineering' stress strain curve determined by the overall stress and strain across and along the rock specimen. All the specimens of Ävrö granite displayed a Class II behaviour (Fig. 12).

For Class II behaviour, a method for regulating the compressive energy other than just controlling the axial strain rate has to be used, otherwise the specimen would collapse uncontrollably just after the peak stress. Using the lateral strain as an indicator and programming a linear increase of the lateral strain, this uncontrollable behaviour can be avoided because the axial strain is incrementally reduced as the radial strain increases, which allows the specimen to release the stored strain energy. When equilibrium is re-established, the specimen is reloaded until the failure locus is reached again and fracture propagation restarts, thus producing a controlled step-by-step stable behaviour of the specimen (Wawersik and Fairhurst, 1970). This might occur rapidly in a servo-controlled testing machine.

In the DECOVALEX THMC Project, two numerical modelling methods were able to reproduce Class II behaviour for rocks with different microstructures (Paper III): the Elasto-Plastic Cellular Automaton (EPCA) and the Displacement Discontinuity Method (DDM) implemented in FRACOD.

The Elasto-Plastic Cellular Automaton (EPCA) method combined with a homogeneity index was applied when modelling the uniaxial compressive tests of a rock type with Class II behaviour. The EPCA can be used to divide the rock specimen into a system of cell elements (Dems and Morz 1985; Zheng *et al.* 2005). The elastic parameters of each element, such as Poisson's ratio, Young's modulus, cohesive strength, *etc.*, are generated according to a Weibull probability density function. The homogeneity index, m, is used to describe the heterogeneity of the material. The deformational state of each cell is updated according to the cellular automaton updating and follows the elasto-plastic loading and unloading rule (Feng et al. 2006). At each step, the updated stresses within each element are substituted into the failure criterion, such as Mohr-Coulomb's or Drucker-Prager's criterion, to verify whether yielding of the cell element will occur or not. A function of the softening coefficient, α, decides whether the stress-strain curve will follow the strain case with negative post-peak slope (Class I) or the strain case with positive post-peak slope (Class II) (Pan et al. 2006)(Fig. 27).

The influence of pre-existing fractures on the propagation of the newly induced fractures highlights the importance of fracture mechanics modelling this behaviour. A method based on the propagation and interaction of fractures (fracture mechanics) combined with

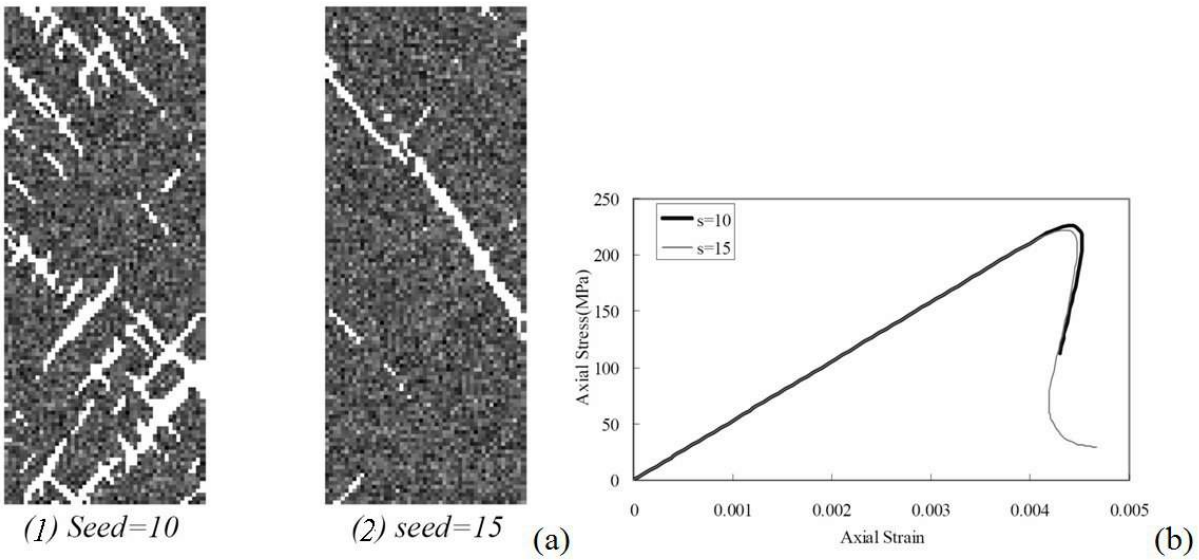

Fig. 27. (a) Illustration of the fracture development from the EPCA simulation of the saline experiment with two different elemental seeds: 1) seed =10 and 2) seed =15. (b) The resulting complete stress-strain curves for the simulation with different seeds of the uniaxial compression of samples subjected to a saline fluid.

the Displacement Discontinuity Method (DDM) is applied in the numerical code FRACOD (Shen *et al.* 2005, Paper III). This code requires information concerning the pre-existing flaws, their initial state and the properties of the newly induce fracture that can be handle during failure (Fig. 28). Models that consider the intact rock as a homogenous and flawless elastic body and where new cracks can be introduced at critical stress locations leading to macrocrack formation can be set up. Pre-existing cracks can also be included to consider the effect of their properties, orientation, length, density and the fracture toughness in different directions. This can improve the soundness of the simulations results.

These models could have benefited from explicitly taking into account the geometry of the pre-existing fractures in relation to the loading direction. The results from both kinds of models show a development of *en echelon* shear fractures rather than tensile fractures. This might also be due to the resolution of the models that oversee the development of the tensile micro crack in the early phases of the simulated tests.

Mesoscale – EDZ fracturing processes around a tunnel

Micro-fracturing, macro-fracturing, redistribution of *'in-situ'* stresses and rearrangement of rock structures will occur in the EDZ and result in drastic changes of mechanical stability and permeability to flow in the rock mass, mainly through the appearance of fractures and cracks induced by excavation. The combined disturbance from stress relief and blast-

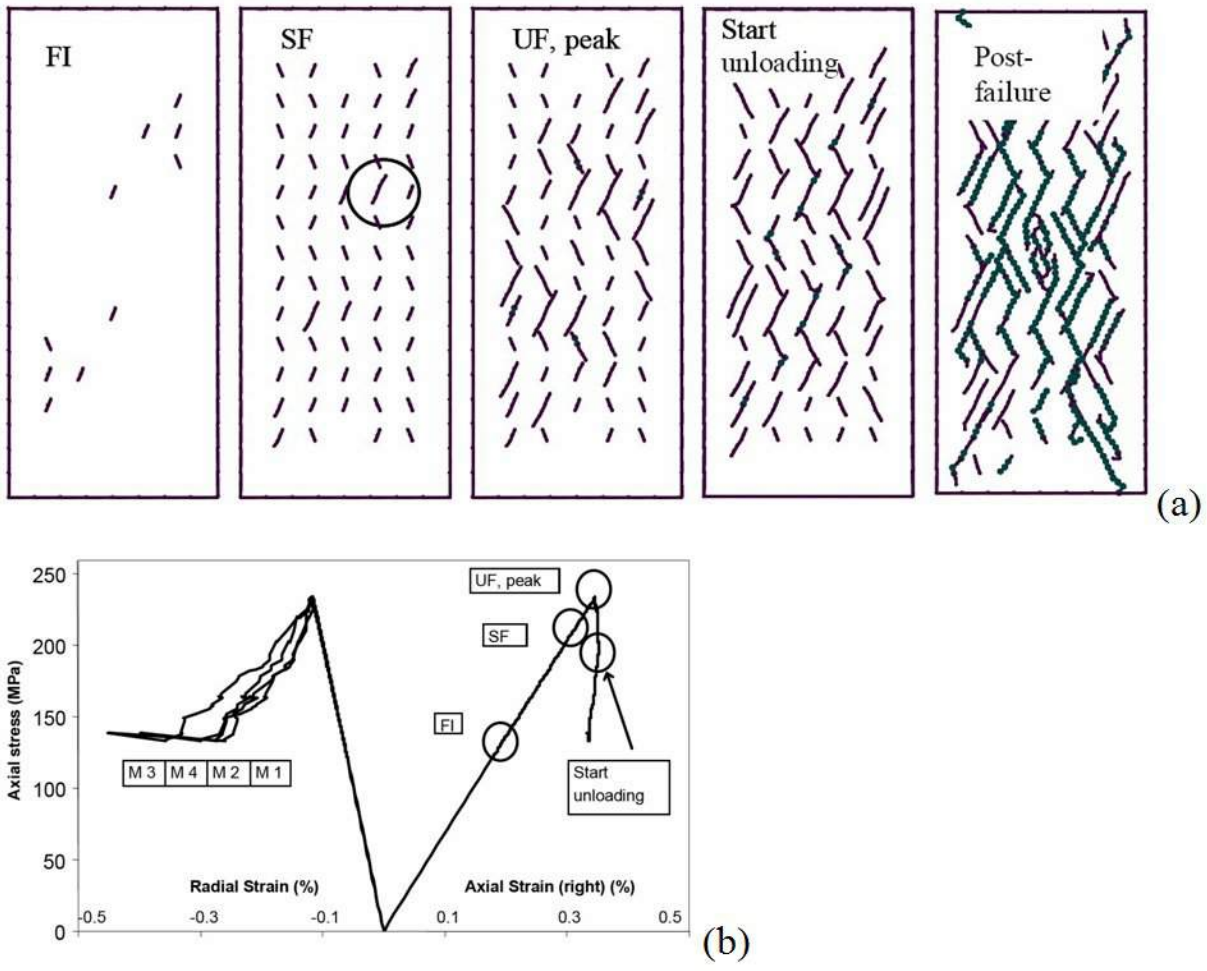

Fig. 28. (a) The simulated fracture pattern at; fracture initiation (FI), stable fracture propagation (SF), unstable fracture propagation (UF), unloading at the peak stress, and the continuation of cracking. (b) Simulated stress-strain curve illustrating the failure behaviour via both radial and axial strains. The situation represented by FI, SF, UF and start unload can be seen in (a).

ing can produce a dramatic increase in axial conductivity of a narrow volume of rock adjacent to the drift. The increase is estimated to be at 1000-10,000 times, which is from 10^{-10} to 10^{-6} m/sec in terms of hydraulic conductivity. This conclusion was achieved from the results of the BMT test at Stripa Mine where the increase of hydraulic conductivity in the EDZ was the result of the creation of a shallow network of fractures.

In the EDZ, different types of fractures are formed. The 'blast induced fractures' originate and extend from a blasting drillhole in or immediately adjacent to the tunnel walls. Tunnelling 'induced fractures' do not necessarily originate from the blasting drillhole itself but do not present infilling material and can be observed at the contour of the tunnel. These fractures are probably caused by the high stresses and release by the blasting process or by the redistribution of stresses due to the excavation of the tunnel. In several instances, onion-skin fractures forming which have a preferred orientation parallel to the periphery of the opening can be observed (Fig. 29). They are created from the combination of high gas pressure and high tangential stress. These were observed in earlier studies of the EDZ in the Blasting Damage Investigation at Äspö (HRL) (Pusch 1989, Pusch and Stanfors 1992) where the geological fracture characterization show that, due to undesired deviations of blasting drillholes, the blasting was frequently not effective. This conclusion lead to the development of the evaluation method presented in this study (Paper IV and Paper V).

For the DECOVALEX-THMC Project, Task B, phase 3, numerical modelling of the development of the EDZ including the model of the fracture network presented in Fig. 16c was carried out focusing on mechanical responses and long-term chemo-mechanical effects (Rutqvist *et al.* 2008). The time-dependent changes in mechanical and hydrological properties in the EDZ are processes such as creep, sub-critical crack growth and healing of fractures that might cause "weakening" or "hardening" of the rock over the long term. Five research teams were studying the development of the fracture

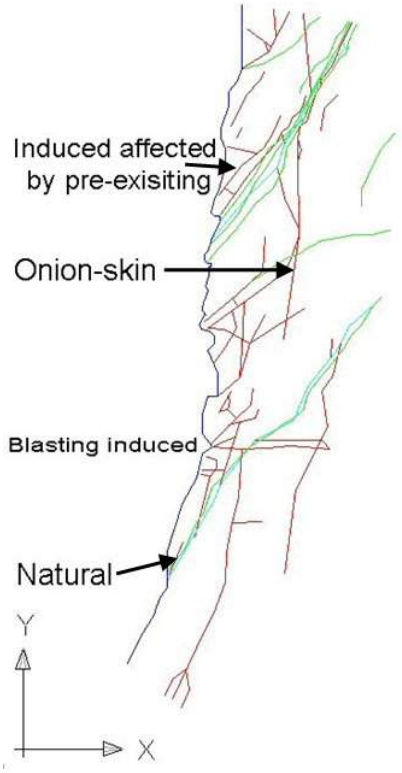

Fig. 29. The fractures produced in the EDZ from a mapping of a cut-out in the TASQ tunnel, where the red fractures are open fractures whereas the green are closed and the two light blue are natural fractures.

model with evolution of temperature, boundary stresses, and fluid pressure extracted from the full-scale simulation at the FEBEX Case, Äspö HRL. The teams used a wide range of modelling approaches including boundary element, finite element, finite difference, particle mechanics, and cellular automata methods.

For a circular opening with the stress situation at about 500 m depth in the Äspö HRL, the general situation is that the stress increases and becomes compressive at the crown and invert, whereas at the spring line (middle of the walls) the stress becomes tensile because the major principal *'in-situ'* stress is horizontal. In Fig. 30, the differential stress situation for the TBM tunnel of the ZEDEX Project at about 420 m depth in the Äspö HRL is presented (Emsley *et al.* 1997). The stress induced damage, can occur in regions of high differential stress (σ_1-σ_3) where the stress may be so concentrated that the crack initiation stress of the intact rock is reached. For the case of Ävrö granite, the crack initia-

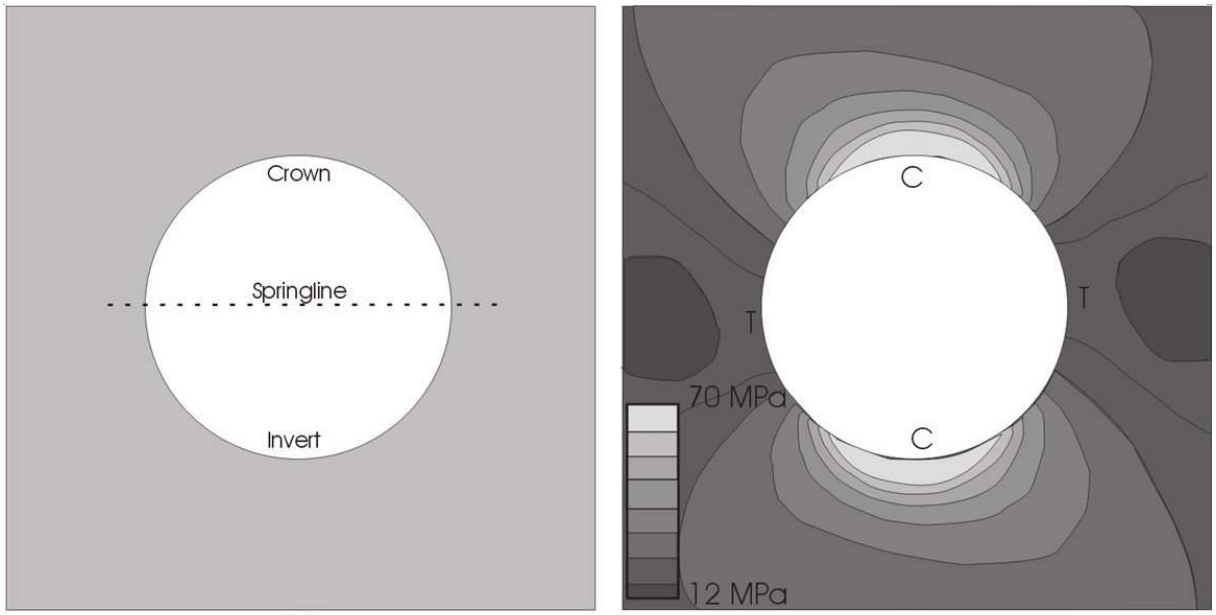

Fig. 30. (a) The definition of locations in the tunnel. (b) ZEDEX Project: differential stresses (σ_1-σ_3) around a TBM tunnel (Emsley et al. 1997).

tion stress is about 130 MPa (Table 1). Around the opening, there can be areas where the minor principal stress σ_3 is tensile, reaching the tensile strength of the rock and causing failure. For the case of Ävrö granite, the tensile strength is about 13 ± 1.5 MPa (SKB, 2006).

As presented in Fig. 30b, the stress does not exceed the crack initiation stress, thus, the tunnel mainly remains in elastic regime. This applies if there are no fractures in the rock mass. However, the stress relief from the excavation can cause the extension and dislocation of existing cracks as result of the change in shear and normal stresses adjacent to the fracture surface. This was examined by means of the numerical modelling in the DECOVALEX THMC Project where the mechanical properties and the fracture network from the TASQ tunnel were analysed. In this project, the combined effect of fractures and stress field is simulated with time. The redistribution of stresses around the opening causes tensile stress at the springline of the tunnel (Fig. 30) that results into opening up the fractures and increased permeability. At the crown, high differential stress can in turn induce shear strains. If the shear strain does not cause shear failure, the permeability of the rock should decrease. If the shear strain are sufficiently high, they can lead to shear failure of the already exist fractures or of the tunnelling induced fractures. Slip may cause the opening of flow paths (Rutqvist *et al.* 2008).

For the simulated first one hundred years, the increase of the deviatoric stress and strain causes the permeability to increase, whereas after this time the stress state will have stabilised, with reduced deviatoric stress. From modelling results using the FRACOD, the displacement of fractures and their intersections near the crown of the tunnel at the time of excavation as causes higher hydraulic conductivity. The stress state around the tunnel does not cause any new fractures according the models. This can be due to the fact that the models used the peak compressive strength of the Ävrö granite instead of the crack initiation stress. However, the highest compressive stress found in the models was about 100 MPa while the crack initiation stress is about 130 MPa. It is therefore unlikely that new fractures would be induced because of the stress state around the tunnel.

During the modelling using the elasto-plastic-cellular-automaton code (EPCA), a laboratory test using a strength of about 80 MPa for the rock matrix and a friction angle of 27° for the fractures, resulted in a large zone of

failure caused by deviatoric stress (Fig. 31). The failure area is mainly caused by shear failure due to a large deviatoric stress and may still be limited in the more constrained areas away from the tunnel wall. However, some tensile failure was observed close to the spring line.

Macroscale – Conceptual modelling of meteorite impact craters

The fracturing processes of associated with the formation of impact craters is the main target of this section on meteorite impact. Fortunately, it is not common that an impact of a meteorite the size of those that created Lockne or Björkö craters hits Earth. For this reason, the actual processes involved in meteorite impact are not available for direct study. Therefore, we must rely on observations of the resulting structures and simulation using numerical models. The impact process changes pressures and temperature far above what we can expect, even at large depths inside Earth. Even though the access to the resulting structures is easer than at depth, the complexity of the interaction with the free rock surface and the change of pressure and temperature near the surface cause large anomalies. The high energy involved in meteorite impacts causes phase changes to occur, from solid to fluid, gas and plasma. This complicates matters when trying to explain the stress propagation and resultant fracturing.

The process of formation of a crater is here called 'cratering' process. In general, this can be sub-divided into three stages: 1) contact and compression; 2) excavation and; 3) modification (Gault *et al.* 1968). As the cratering process is a continuous process where different stages occur and grade into each other, this sub-division of the cratering process is rather simplistic (Melosh 1989). Ultimately, the main parameters of an impact are the stress wave and its thermodynamic processes. These are events where an extreme amount of energy is released into a rather low energy environment during a very short time-span. This causes plastic yielding, thermodynamic irreversible stress waves and the effect of porosity on stress wave propagation to influ-

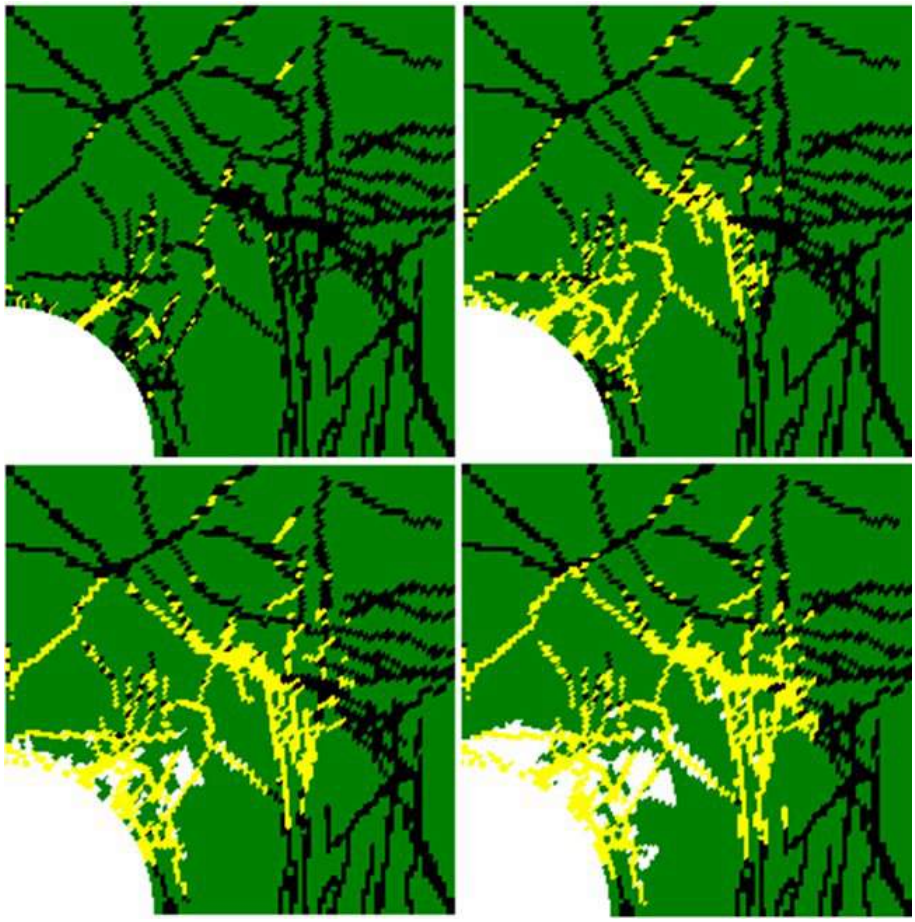

Fig. 31. Evaluation of failure with the Mohr-Columb's failure criterion for the rock matrix and fractures (yellow areas in the model) by means of modelling with the CAS2 code (Rutqvist et al. 2008) during excavation after the following removal of the internal pressure: a) 25%; b) 55%; c) 80% and; d) 100%.

ence the cratering process.

Stress wave propagation through solids is described by two components: the longitudinal or P-wave and the transverse or S-wave. The P-wave can travel through both solid and fluids, although fluids slow the wave down. The P-wave can also be called the primary wave as the wave speed for the longitudinal wave is larger than that for the transverse or S-wave. The S-wave cannot travel though fluids nor through gasses because fluids and gases cannot sustain a significant shear stress. The S-wave is also called the secondary wave, due to its secondary arrival at the seismograph in the case of earthquakes.

The interaction between the impactor (in this case the meteorite) and the target (in this case Earth) results in different morphologies of the crater. The diameter of the resulting crater mainly depends on the size of the impactor and its velocity, in other words on the energy released by the impact. The resulting craters are divided depending on their size:

- 'simple craters' with diameters up to 2 km in sedimentary rock, and 4 km in crystalline rock on Earth (Dence 1972). These craters are bowl-shaped with a raised rim. The crater walls are steepest close to the top and shallow towards the crater floor.
- 'complex craters' are larger than the simple craters and having experienced collapse (modification) after their formation. They have a less elevated rim, wall terraces and a central uplift. For large complex craters the central uplift can collapse into a peak-ring, thus, these structures are called peak-ring craters (Melosh & Ivanov, 1999).
- 'multi-ringed basins' are 'the whales' of craters. As the name implies these structures display several ring structures. These large scale structures are sometimes considered as the next stage in morphology change with size after large complex craters (peak-ring craters). However, several authors are hesitant to this simple explanation, as this assumption is contradicted by observations from the surfaces of several heavenly bodies. It seems probable that the formation of the ring structures requires a mechanism different from the complex crater formation. (Melosh 1989, Ivanov 2005).

Contact and compression stage

At the moment of the impact, the stress wave will act as an elastic wave only in parts of the process. The reflection of the elastic wave at free surfaces and density interfaces have to be taken into account, as well as the plastic yielding at the Hugoniot elastic limit of the involved rocks (Melosh 1989).

The cratering processes starts at the contact between the meteorite and Earth, as the effect of large meteorites on the atmosphere is relatively small and would perhaps only slightly slow down the meteorite. The meteorites travel at velocities between 11.2 km/s and 72.8 km/s. The velocities range from the Earth's escape velocity to the maximum velocity that can be attained when combining the Earth's escape velocity with the heliocentric orbital velocity (Melosh, 1989). When the meteorite strikes Earth, it causes material to move downwards and outwards, transmitting a large part of its energy to it in the form of compression and acceleration. This interaction results in a shock pressure where the peak pressure is a function of the impact velocity, the physical properties of the meteorite and the material it hits. This pressure creates shock waves between compressed and uncompressed material. For example, the impact of an iron body into silicate materials at 30 km/s results in a peak shock pressure of 1600 GPa (Ahrens & O'Keefe 1977).

The shock wave propagates into the meteorite and eventually engulfs and distorts it as the object slows down and compresses. The energy has now been transferred to the target and propagates out causing the material to flow completely hydrodynamically as the shock pressure reaches the material strength. The reflection of the shock wave at the rear end of the object causes a rarefaction (release) wave to follow the shock wave into the target where it travels with the speed of

sound in the compressed material, unloading it to near-zero pressure and further decelerating it (Fig. 32). The shock wave causes a stress difference between the longitudinal and the transverse stress component and, when the strength of the wave increases, this differential stress can overcome the yield stress of the material, *Y*, after which plastic flow begins.

At "low" pressures, rock materials follow Mohr-Coulomb's failure criterion whereas, at "high" pressures, the strength of the rock is nearly constant (purely cohesive). Failure is characterized by plastic distortion rather than brittle fracturing. The slope of the failure envelope of the rock during "low" pressures (the friction angle) rises more steeply than the stress in a longitudinal elastic wave. As the failure envelope eventually flattens out at "high" pressures, the elastic stress trajectory intersects it at *Y/2*. The longitudinal stress at this point is described by:

$$\sigma_L = -\sigma_{HEL} = -\left(\frac{1-\nu}{1-2\nu}\right)Y \qquad (12)$$

where σ_{HEL} is defined as the Hugoniot Elastic Limit (HEL).

The propagation speed for a strong compression wave depends on its strength. Beyond HEL, the bulk modulus, which increases with pressure, contributes to the speed (Fig. 32). Longitudinal elastic waves travel at the speed c_L whereas stronger waves break into an elastic precursor and a slower-moving plastic wave that may travel at the speed of a longitudinal pressure wave, c_B, also called the bulk sound speed.

$$c_B = \sqrt{\frac{K_0}{\rho_0}} \qquad (13)$$

Still stronger waves travel faster than the elastic sound speed (supersonic shock pulse) and thus have no precursor (Melosh 1989).

The high pressure in a shock wave is relieved

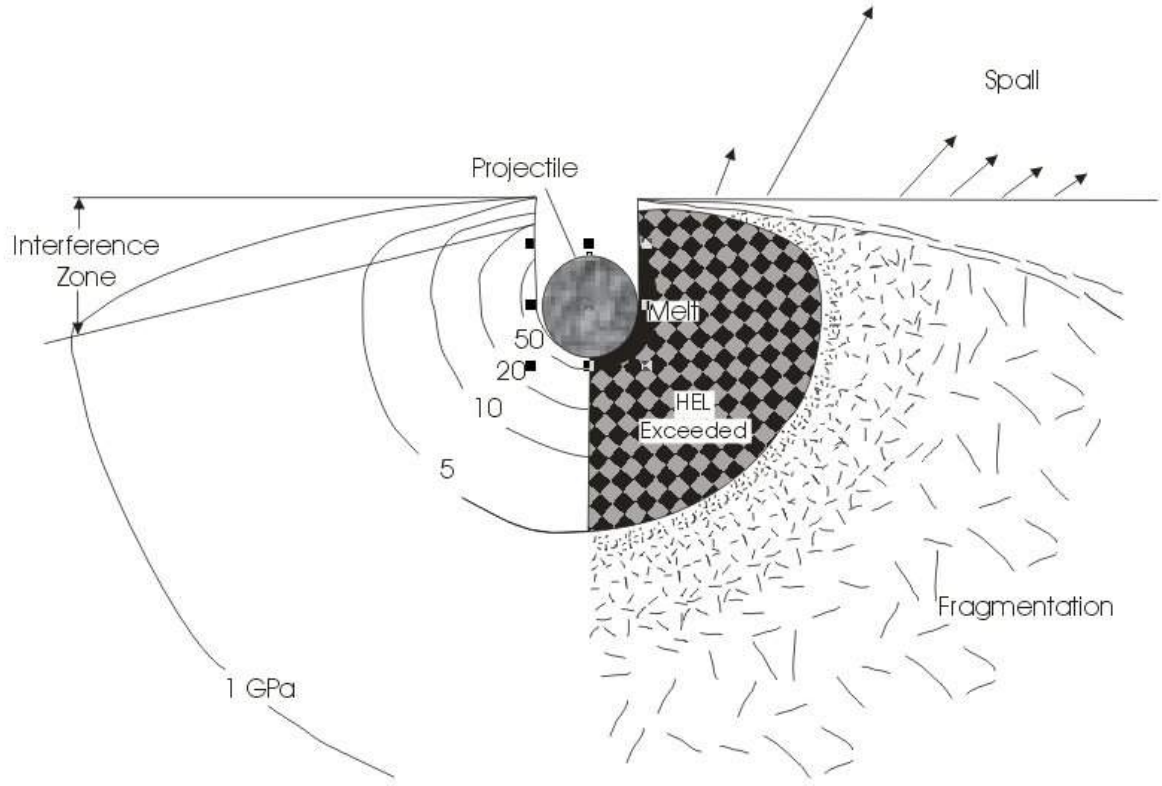

Fig. 32. Schematic image of the pressure situation at the site of a meteorite impact (after Melosh 1989).

by the propagation of a rarefaction wave from the free surfaces into the shocked material. Unlike elastic wave reflection, where the tensional relief wave propagates away from the free surface at the same speed c_L as the incident compression wave, the rarefaction wave generally moves faster than the shock wave. The rarefaction wave will be elongated as the wave front will travel through a high-pressure region, whereas the later part will travel through a low-pressure region. Even though the wave front of the rarefaction wave moves faster than the shock wave, the low-pressure wave will move with the speed c_B if the material that it moves through is still solid. The material will still have a residual velocity behind the rarefaction wave, and this is crucial for the excavation of the crater.

Melting and vaporisation occur in connection with an impact, which generally is calculated based on knowledge of the melting point of the different materials and an integration of the volume enclosed within the limiting pressure contours in the crater model (Fig. 32). Near Earth's surface, the situation of a free-surface as boundary condition causes the pressure to be near-zero, which moves the melting further down into Earth. The later modification of the formed crater will rearrange the position of the melt.

The free-surface, by definition a surface of zero pressure, causes several specific interactions during the cratering processes such as reflection of rarefaction waves (when the shock wave interacts with the free surface) and sharp pressure gradients. The pressure in the rarefaction wave is the equivalent to the pressure in the shock wave but with opposite sign. The tensional phase of the rarefaction is not limited to the near-surface area but propagates downwards to great depth and fractures the rock. This is the origin of the brecciation beneath craters, also called the breccia lens (Melosh, 1989).

Excavation stage

The motion that the passage of the shock wave has left in the material is directed radially away from the impact site. The rarefaction wave from the free-surface is directed down into the rock creating a pressure gradient directed upwards behind the shock. This adds an upward component to the radial velocity. The excavation flow field is illustrated in Fig. 33.

The material follows the paths parallel to the velocity vectors at each point. Material near the free-surface is ejected out of the crater and material inside the crater is displaced down and out into the rock where space for this excess material is created by plastic deformation of the surrounding rock. The material inserted into the surrounding rock causes a rise of the surface.

This flow opens a hemispherical cavity, and the excavation grows with a decreasing rate until it has reached its maximum depth determined by the lithostatic stress and the strength of the material. As there is less resistance to growth laterally near the free surface, the crater continues to grow near the surface giving it a more bowl shaped appearance than a perfect hemisphere. This cavity is called the transient crater. The formation of a simple crater does not continue much further from this situation.

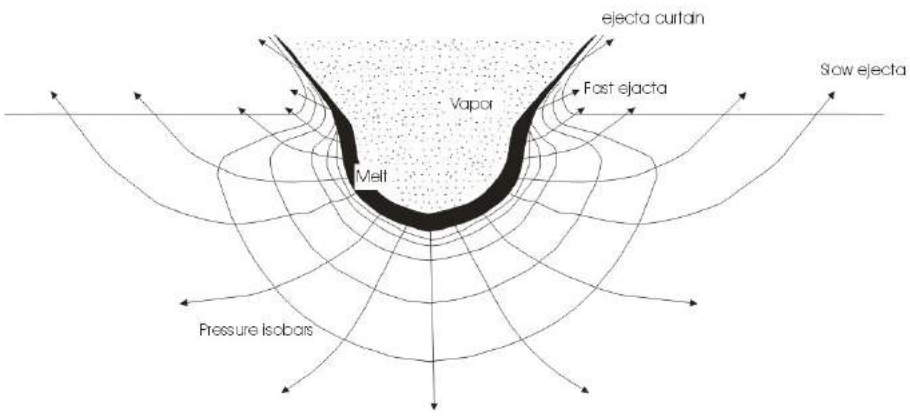

Fig. 33. Geometry of the excavation flow field (after Melosh 1989).

The depth of excavation is not the same as the depth of the final crater when the cratering processe is concluded. For complex caters the depth to diameter ratio depends on the target material. For sedimentary layers, the ratio is much smaller, *i.e.,* the craters are shallower than for crystalline materials. This difference depends on the strength of the material. The apparent depth to diameter ratio for complex craters on Earth is calculated by (Grieve and Pesonen 1992):

$$d_a = 0.12D^{0.30} \quad (14a)$$

$$d_a = 0.15D^{0.43} \quad (14b)$$

where d_a is the apparent depth measured from the original ground surface to the top of the breccia lens. These ratios are for sedimentary (a) and crystalline (b) targets, respectively. As the complex craters on Earth are of rather old age, they have all been eroded, which affects the validity of these equations.

Impact craters can form in more than one target material. The interactions in connection with the cratering processes are strongly depending on the thickness of the overlying layer and the size of the resulting crater. Studies of the Moon, with its thick weaker layer of regolith on top of strong consolidated lava, have been used by Oberbeck & Quaide (1968) to determine the effect of layering of the target material. They found that four distinct morphologies could be identified with transitions between them. The ratio between the diameter of the crater and the layer thickness could be used to describe these morphological changes (Table 3).

During the excavation phase in the cratering process, large amounts of material are ejected from the crater. This material is strongly shocked and contains lithic material, minerals and melt fragments. The size of the fragments determines if they can escape the Earth's gravitational field. Generally the escaped part constitutes a small fraction of the ejected material. The ejected material deposited on Earth generally follows ballistic trajectories. The material with the steepest ballistic trajectory is ejected from the centre of the crater.

The material that does not escape the crater is incorporated into the walls of the crater, creating an uplifted rim. This uplift and the added ejected material result in a considerable rise above the surrounding landscape. The rim of craters often instils the observer with the impression that there is a mountain ahead, where in fact there is a large hole in the ground.

Modification stage

The modification stage can be said to start when the outward movement of the material flow halts and then begins to move back towards the centre of the crater. This depends on gravity and the elastic rebound of the underlying compressed rock. In small craters this is generally only identified as debris sliding back, whereas in large craters the floor rises, central peaks appear and the rim sinks down into wide zones of stepped terraces

Table 3. Proportion between diameter of crater and the thickness of layers of different materials (Oberbeck and Quade 1968).

Ratio crater diameter / layer thickness (D/ t_L)	Morphology
$D/ t_L < 4$	The energy from the impact is not large enough to affect the lower layer and a bowl shaped crater forms solely in the upper layer
$4 < D/ t_L < 7.5$	A low central mound forms in the bottom of the crater, on top of the strong layer
$7.5 < D/ t_L < 10$	The stronger layer experiences fracturing but the floor of the crater is flat as the energy is not large enough to excavate it
$D/ t_L > 10$	The energy at the intersection between layers is large enough to excavate a crater in the lower layer, although a larger carter is formed in the weaker layer

(Melosh and Ivanov 1999).

The larger an impact crater is, the further the initial transient crater is from gravitational stability. Both the Björkö and Lockne craters are smaller than about 10 km, in diameter, but should be ascribed to the class of the "complex craters". Therefore, this section will concentrate on the processes in craters of this size.

Even though the formation stages of impact craters are intertwined, the transition between simple and complex crater formation is abrupt. The morphology change from simple to complex craters depends on the collapse under gravity when the strength threshold is exceeded. This depends on the magnitude of the gravity field of the target on which the craters are formed. Impact craters of the Björkö or Lockne size have probably experienced modification in shape after the excavation phase by wall collapse and central uplift driven by gravitation. The elastic rebound will be largest where the flow path of excavated material is horizontal, *i.e.,* close to the centre. The stresses associated with the collapse of craters are far lower than the measured strength of intact rock, but it is highly likely that the material involved in the collapse is not intact any more.

As mentioned earlier, the strength of the target material will affect the newly formed structure. For the two impact structures studied here, the depth to diameter ratio depends on the target material. For sedimentary layers, the craters are shallower than for crystalline materials because the failure strength of the material is lower for the sedimentary rocks. In the case of the Lockne crater the marine environment and a sedimentary layer on top of the crystalline basement certainly modified the appearance of the crater. It is believed, however, that at depth the effect on the fragmentation of the basement is present.

The Björkö structure is believed to be a terrestrial impact due to the sandstone infill found in the ring structure (Gorbatchev and Kint 1961). However, regarding the processes of fracturing of the deep crystalline basement, the two impact craters are quite similar. The Björkö crater is deeply eroded since its formation about 1.2 Ga ago. The Lockne crater is less eroded due to overthrusting by the Caledonian mountains soon after its formation. Perhaps the northern limit of the structure is still covered by sedimentary rocks.

Fracture patterns

The fracturing of the target at depth is already finished after the excavation stage. The target is crushed in a half-sphere emanating from the impact site. The half-sphere is found from geophysical mapping and drillings in the volume beneath the crater (Stöffler and Ostertag, 1983) (Fig. 34a). The fracturing occurs in tension from the rarefaction wave. For large craters (larger than 10-20 km) the lithostatic stress may serve as a factor preventing rock fracturing at depth. The attenuation of the fracturing around the Dellen crater in Sweden has been measured by Henkel (1992). He found that for a crater with a diameter of 19 km, the increased fracturing due to the impact can be found until 1 km outside the crater rim. The fracture network seen close to the planet surface around complex craters are to a large part an effect of the modification stage. This is a chaotic event, which will modify large parts of the surface around the crater. The crater rim, which has been elevated by the material being projected into the walls of the transient crater, will become unstable and collapse, for complex crates. This will form terraces along the crater rim (Fig. 34b). Besides these terrace structures, there are radial fractures formed oriented approximately perpendicular to the crater rim (Gurov *et al.* 2007). In Fig. 35, the modification of the crater and the resulting final crater can be seen. The rebounding of the lithosphere will cause the central up-lift to form. During this formation, faults will form surrounding it, as seen in Fig. 35b.

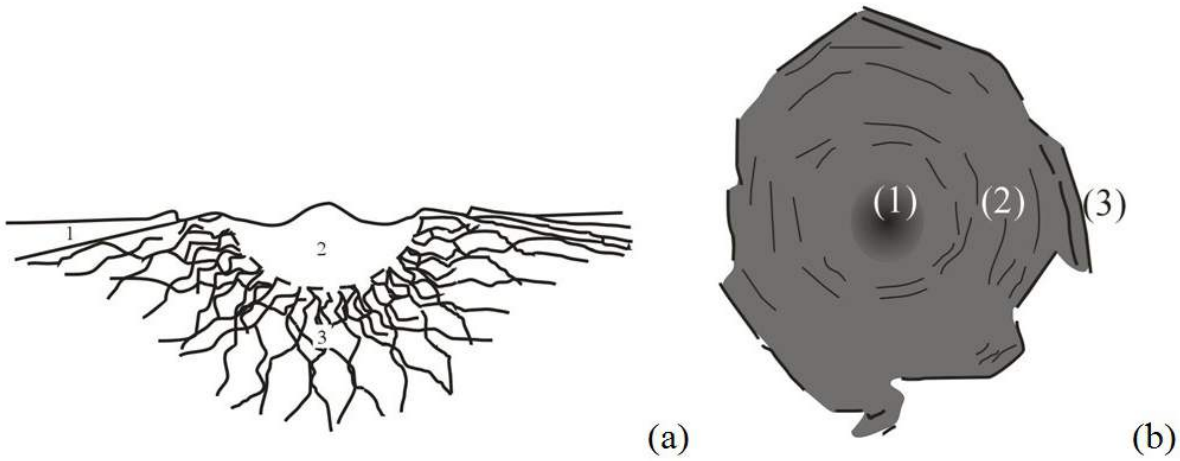

Fig. 34. (a) Resulting fracturing of a crater from experiment by Zenchenko and Tsvetkov (1999): where (1) is the zone of surface spalling; (2) sand-like material; (3) fractured half-sphere under the crater floor. (b) Sketch from results of seismic reflection profiles of the Mjölnir impact structure, outside the coast of Norway. The structural elements are: (1) the central uplift, (2) annular basing and the outer zone with faults, and (3) marginal faults (Tsikalas et al. 1998).

During the impact several new rock types, sk impactites are formed. The impact melt rock is composed predominantly of the target rocks, but can contain a small but measurable amount of the impactor.

DISCUSSION

This thesis started with the statement that this subject was immense. That has not been changed during the presentation and discussion that followed. Hopefully the pressing matter that fractures play a key role in the behaviour of crystalline rock on all scales has been conveyed. I would like to take the opportunity to discuss the differences and similarities of the fracture patterns observed at different scales and the different methods used for their characterisation.

When investigating the failure process of rock at a microscopic scale, microfracturing appears to highly dependent on the mineralogy, fabric and microstructures of a given rock type. Microfractures preferably begin to grow from initial flaws in the rock that have a favourable angle to the stress state. These initial flaws can be weaknesses in the matrix due to thermal contraction during cooling, cleavage planes in minerals (*e.g.,* feldspars and mica) and mineral boundaries (*e.g.,* between quartz grains). In the first part of the thesis, the effect of a pre-existing set of microfractures on the propagation of a fracture set, induced under a controlled stress conditions at a laboratory scale, was shown. The effect of the pre-existing microfracture set on the propagation of a new microfracture was shown in paper I and II. When there is a large angle between the two sets of microfractures, the early set impede the propagation of the later set compared to when the angle between the two sets is small. In conclusion, the pre-existing fractures modify the rock properties, imparting anisotropy to the fracture toughness.

The test results reported in paper I all show a strong Class II behaviour which has been suggested to be due to non-uniform failure or localisation of failure during testing (Hudson *et al.* 1972, He *et al.* 1990). During the numerical simulation of the Class II behaviour in the DECOVALEX-THMC Project presented in paper III, it was found that different elemental spatial distributions will lead to different failure modes in the elasto-plastic cellular automaton (EPCA) simulations of the laboratory tests (Pan *et al.* 2006). The Class II behaviour has been found by several authors to be influenced by the non-uniform failure or localisation of failure. It is thus proposed that the pre-existing fracture patterns perhaps contribute

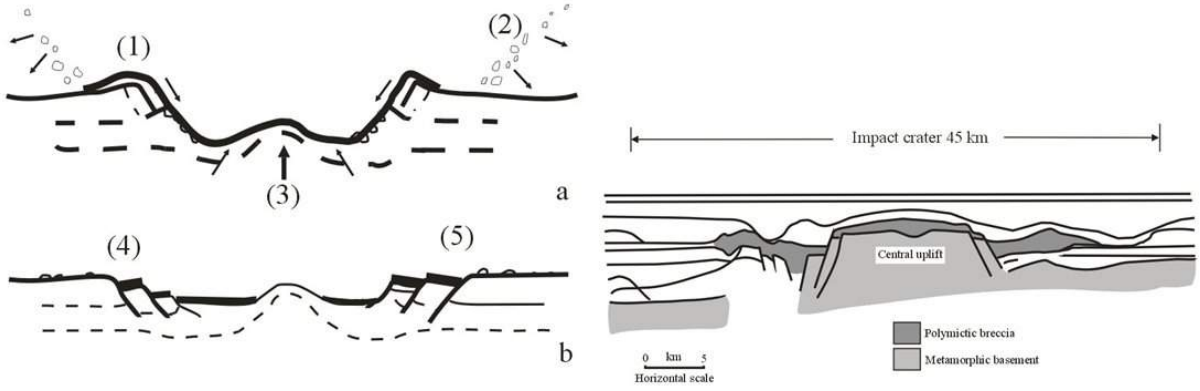

Fig. 35. The modification of a complex crater:(a) the rebounding and formation of the central up-lift and the rim collapse, where (1) is the faulting of the rim, (2) is the displaced blocks and (3) is the rebound causing the central up-lift; (b) the final crater, where (4) is the terraced wall. (c) The Montagnais structure. Interpretation of reflective seismic sections of the off coast structure in Nova Scotia (modified after Jansa et al. 1989).

to the Class II behaviour found in the specimens used in the study.

The laboratory experiments in paper II were performed to investigate the effect of the hydrological environment on the Ävrö granite. Water saturation and salinity were found to have an effect on the mechanical properties of the granite. The specimens saturated with saline water exhibit a larger decrease in elastic properties than the specimens saturated with distilled water for longer immersion time (Fig. 12b). An effect of salinity on the post-failure behaviour of brittle rocks was also found. With high saline water, the specimens act in a more ductile manner than those with low salinity water. The data are unfortunately rather limited and no definite conclusions on the distinction between chemical effects and heterogeneity of the rock material could be made. In several studies, the decrease in strength of rock specimens due to the presence of liquids during uniaxial compressive strength (UCS) testing is suggested to be either the results of the influence of the liquid on the crack tips, or the result of the influence of the liquid on the surface energy of the fracture (Vutukuri *et al.* 1974). Mechanical tests on the strengths of different rock types with specimens saturated in different chemical environments, prior and sometimes during testing, have revealed a complex mechanical behaviour (*e.g.,* Feucht and Logan 1990, Karfakis and Akram 1993, Seto *et al.* 1998, Feng *et al.* 2001).

The UCS tests by Feng *et al.* (2001) were conducted on crystalline rock specimens with an environment where the joint effect of the pH and the salinity was investigated. It was found that a high salinity together with extreme pH determined a decrease in strength. Another study of the sub-critical fracture growth parameters and fracture toughness of rocks under laboratory conditions was conducted for the DECOVALEX-THMC Project by Backers *et al.* (2006) and Rinne *et al.* (2008). Here the fracture toughness in Mode I fracturing was found to decrease for specimens saturated with deionised water as well as specimens saturated with 10 % NaCl compared to dry samples. The sub-critical crack growth parameters identified in these studies rather suggest that the crack velocity is slightly higher for specimens saturated with saline water at low stress intensities then for the other conditions. This indicates that the *'in-situ'* tensile strength of the Ävrö granite will decrease with time due to salinity of the pore water (Rinne *et al.* 2008). All these results suggest that an effect of salinity on the mechanical properties of the Ävrö granite exists, and further studies should be made to identify the importance of this effect and its long-term implications for the stability of excavations.

The propagation of microfractures has been found to be affected by pre-existing microfractures and the measurable mechanical properties of the specimen show an effect of the salinity of the pore water (paper I and II). In several studies, it has been shown that a pre-existing fracture set has a stronger influence on fracture propagation in the sound rock than the mineral shape and distribution. Furthermore, in several studies the effect of salinity on crystalline rock has been identified and the influence of the liquid on the crack tips, or the influence of the liquid on the surface energy of the fracture, has been identified as likely causes for the reduction of the strength of the rock material. The existence of fractures in the specimen increases the likelihood of the chemical components to find a surface on which chemical reactions and exchange of ions can occur and thus increase the effect of the chemical component. This is perhaps why there is such a large effect of the chemical environment on the mechanical properties measured in these specimens.

The rock fails under uniaxial loading by developing numerous Mode I microfractures. Several examples of such microfractures linking together to form embryonic macroscopic shear failure planes have been identified in the specimens from this study (Paper I). These coalescent fractures are also found on the mesoscopic scale investigated in the EDZ surrounding a tunnel (Paper IV and V). As stated above, the removal of rock will inevitably change the stress situation in the rock mass surrounding the underground opening, allowing the introduction of slip along existing fractures and the production of new fractures. Also as stated above, the main influences on the development of the EDZ around tunnels are the geological conditions, the stress state and the excavation method. The excavation method for the Swedish underground repository is the drill-and-blast method (SKB 2004). This method has been chosen because of its flexibility with respect to complicated geometries and its cost-efficiency for excavations in hard rocks compared to the tunnel boring machine (TBM). On the other hand, drill-and-blast creates a larger EDZ around the excavation than does the TBM which is detrimental to the safety and hydrological isolation of the tunnel (Emsley *et al.* 1997). Many hazards connected to tunnelling are related to the tunnel sections near the excavation front just after blasting. The workers installing the support and geologists are often exposed to this environment. The hazards are strongly related to the constant risk of rock fall and to the time spent at the front. The amount of data directly retrieved by the geologists depends on the span of this time. Thus, a characterisation method has to fulfil the following requirements (Maerz *et al.* 1996, Warneke *et al.* 2007):

Speed: measurements should not interfere with operations and results must be available before drilling of the next blasting round begins.

Accuracy and precision: measurements must be of sufficient accuracy and reproducible.

Simplicity: measurement method must be easy to implement by available personnel.

Cost: purchase, operation and maintenance of the equipment must be within a specific budget.

Reliability: equipment must function under a large range of conditions, including high/low temperature, humid and/or dusty environments.

Versatility: methods must be operational for different shapes and sizes of tunnels, shafts and inclined ramps.

Clarity of results: output data must be immediately usable and the time for producing graphical and numerical outputs must be limited.

In short, a method that is compatible with the blasting process is required. The 3D laser scanning method has here presented and been applied in the studies covered by this thesis (Paper IV and V). Detailed geometric data obtained with a 3D laser scanner were used to provide basic audit data for comparing the "as-designed" tunnel with the "as-built" tunnel at the TASQ Tunnel of the Äspö HRL. This produces a measure of the accuracy of the blasting process and a measure of excess damage to the walls.

In the earlier studies of the EDZ at the Äspö HRL (Pusch and Stanfors 1992, Emsley *et al.* 1997, Olsson *et al.* 2004), it was concluded that the orientation of the contour drillholes for the blasting was crucial for the development of damage at the tunnel walls. Thus, a fast and reliable method of measuring, presenting and evaluating the position and orientation of the resulting contour drillholes is needed. The 3D drillhole model produced in this study (Paper V) can identify the three-dimensional orientation of the contour drillholes and thereby identify errors in the drilling of these holes. This information can be used for better contour drilling in the next drilling campaign. The strength of this method is the quantity and quality of retrieved information. From the geometric data, the comparison between "as-built" and "as-designed" tunnel, the 3D model of the fractures in the tunnel and the 3D drillhole-model, the position of areas with large rock damage and its cause can be identified. In turn, this can be used in the planning of further drill-and-blast campaigns as it gives a controlling method of the blasting performance.

The fracture mapping of a cut-out of the tunnel wall in the TASQ tunnel was used in the modelling of the time-dependent behaviour of the EDZ of a circular tunnel. The modelling was performed with the mechanical properties available from the rock mass around the TASQ tunnel. It was shown that the main damage produced in the tunnel periphery was in connection to the pre-existing fractures, whereas the use of the peak strength from the laboratory experiments kept the rock mass within the elastic regime and no new fractures were initiated. If the uniaxial compressive strength of the material was lowered to about 80 MPa (compared to the peak strength of about 250 MPa), the damage development was quite extensive. This modelling campaign showed that the knowledge of the fracture network in the tunnel periphery is crucial to be able to predict the behaviour of the rock mass.

When building repository tunnels, the possibility of using *'in-situ'* damaging testing methods will be limited, as the goal is to keep the rock mass system as intact as possible. Thus, remote, non-destructive methods for detecting damage in the rock mass should be used. Geophysical methods that measure the physical properties of the rock mass remotely are useful but must be calibrated to the particular situation at site. Often, several methods need to be combined to produce a clear enough image of the situation. In this study, the ultrasonic wave velocity was measured in the rock mass along eight boreholes drilled in the periphery of the tunnel to identify the extent of the EDZ. The ultrasonic wave velocity detected the microscale damage in the rock mass closest to the tunnel periphery, but the larger open fractures along the boreholes were also identified. This method characterises a small rock volume along the borehole and has a high enough resolution to identify the microscale and macroscale mechanical variations in the rock mass close to the tunnel profile.

The seismic method is useful when identifying the structure of impact craters and has extensively been used for that purpose (*e.g.,* Juhlin & Pedersen 1987, Milkereit *et al.* 1992, Keiswetter *et al.* 1996, Poag 1996, Lindström *et al.* 1999, Scholz *et al.* 2002, Tsikalas *et al.* 2002). In the studies of the two large scale structures presented in this thesis, the main objective was the characterisation of the fractured rock mass produced by a meteorite impact. The degree of fracturing does gradually change into intact rock. This gradual change does not produce any abrupt change between fractured rock and non-fractured rock, thus the seismic method will not detect this variation well. In these two studies the geophysical method sensitive to the amount of water in the rock mass such as the electric resistivity was used. The variation of electric resistivity between the different rock types in the Lockne crater structure was identified and found to be distinct enough to differentiate the rock types from each other based on the electric resistivity. In the Lockne area the sedimentary rocks could be differentiated from the crystalline rocks as well as the brecciated crystalline rock from the intact. The electric resistivity and fracture frequency measured at outcrops in the Lockne structure

has shown that in the southwestern section, the fracture frequency varied from high within the crater, to low values in the area uninfluenced by the impact with more intact rock. In contrast, the northern limit of the crater does not show this decrease in fracture frequency (paper VI). This implies that the Lockne crater can be larger than previously assumed, or that the outcrops found in the northern area are on top of a so called "ejecta flap" where the brecciated crystalline rock from inside the crater has been deposited on top of the surrounding intact rock (Lindström *et al.* 2005).

The correlation between fracture frequency and the electric resistivity in crystalline rock was initiated during this investigation and continued during the investigation of the Björkö structure. The electric resistivity is sensitive to the water content in the rock mass, and so it was also used in the investigation of the volume of fractured rock mass in the Björkö geothermal energy project. The highly brecciated rock on the outcrops in this area as well as in the Lockne area gave the opportunity to strengthen the correlation between the electric resistivity and fracture frequency of crystalline rock by providing extremely fractured situations (Paper VI).

The Lockne crater was formed in a marine environment with a sedimentary layer on top of the crystalline basement, whereas the Björkö crater was probably formed in an arid terrestrial environment. These different formation environments will affect the formation process of the crater, mainly close to the surface. The layered target which Lockne constitutes will cause the explosion to have a higher position, than if the target was crystalline rock (Ormö 1998). The shape of the volume of rock that has been fragmented is likely to be a half-sphere emanating from the impact site in both cases as the craters are not large enough for the lithostatic stress to influence the fragmentation. The correlation between fracture frequency and electric resistivity in crystalline rock derived from these two investigations spans from low fractured crystalline rock to extremely highly fractured rock. This correlation should be useful in remote investigations of fracture frequency in similar situations as the ones it has been developed from, *i.e.* large structures, such as fracture zones and impact craters in crystalline rock masses at the Baltic shield, except in areas with larger quantities of conductive minerals.

CONCLUSIONS

In this study, rock fracture characterisation was carried out from field scale to laboratory scale. Development of fracturing during uniaxial compressive tests, tunnel blasting and meteorite impacts has been investigated by means of different geological and geophysical tools. Fracture density and patterns were characterized in terms of spatial variation and orientation. The investigations were performed on crystalline rock, specifically several types of granite. These granites are not characterised by any strong foliation and the matrix in the rock masses is essentially homogenous. Therefore, only the anisotropy of the rock mass due to fracturing was considered in this study. Rock masses displaying foliation or, in the case of the laboratory specimens, large feldspar crystals have been avoided. The main conclusions of the research work are listed below.

1. The 'intact' specimens used for the laboratory experiments were found to include pre-existing microcracks. However, the effect of the mineral matrix does not seem to govern the orientation of the micro-cracks. The spatial orientation of the pre-existing micro-cracks is sub-vertical and their strike is about 10° from the direction of the maximum *in-situ* horizontal stress. This suggests that the microcracks have been formed as a result of tensile conditions, as their orientation is close to perpendicular to the *in-situ* minor principal stress.
2. Observation on the rock specimens indicates that the pre-existing fractures inhibit the propagation of the test-induced fractures. This modifies the rock properties, imparting an anisotropy to the fracture toughness. As the Class II behaviour has been found to be related to heterogeneities in the rock mass, the pre-existing

fractures are likely to contribute to the behaviour.

3. The influence of pre-existing fractures on the propagation of the experimentally induced fractures highlights the role of fracture mechanics in accounting for the deformational behaviour of the samples. It is therefore advisable to consider the pre-existing fractures when attempting to numerically model this behaviour. There are several modelling tools based on the displacement discontinuity method (DDM) that describe the propagation and interaction of fractures (fracture mechanics). These models should therefore benefit from information concerning the pre-existing fractures in their initial state.

4. In this study, an effect of saline water on Young's modulus and the compressive strength has been found. Stiffness and strength decrease with increasing salinity of the porewater. With longer immersion time, the effect is greater. The post-failure behaviour of brittle rocks also shows an effect of the salinity. The specimens with high salinity in the porewater act in a more ductile manner than those with low salinity porewater. This is an indication from a small set of samples and no final conclusions on the effect of the chemical influence on the rock material could be made.

5. During numerical simulations of a fracture network obtained from geometric data from a cut-out in the TASQ tunnel wall, it was found that the pre-existing fractures are reactivated by tunnel excavation. The excavation affects the rock mass in two ways: it changes and causes fractures due to the energy release of the used explosive, and it changes the local stress around the pre-existing fractures near the opening, causes new fractures to form. These results also show the importance of the pre-existing fractures. To model the EDZ without considering pre-existing fractures results in the rock mass around the opening staying within the elastic regime and new fractures might not being produced. The EDZ deterioration is of course strongly dependent on the mechanical properties of the rock mass, and by using the peak strength from the laboratory experiments, no new fractures are formed in the rock matrix around the TASQ tunnel.

6. Investigations of the tunnel as-built compared to the tunnel as-designed have shown that, by analysing geometrical data obtained by 3D laser scanning of a tunnel, several locations of extreme overbreak could be identified. With further analysis of the drillholes visible in the contour of the tunnel, together with a model of the fractures derived from the geometric information, the most probable cause for these overbreaks has been identified as pre-existing fractures in one case and deviation of drilling in the other.

7. The method of performing fracture mapping from the 3D model of the geometric data, together with the images of the tunnel wall from orthogonal laser intensity, has been shown to identify the same fracture sets as manual mapping of the tunnel wall. The orientation of the main fracture sets obtained by the two techniques coincides. This shows that fracture mapping from laser scanning can be used as a complementary method to manual geological mapping.

8. From geophysical investigations, the EDZ of the tunnel was found to be about 0.3 m for the walls, whereas the damage in the roof and the floor was variable. The results show that the ultrasonic method can detect the location of open fractures crossing the borehole in crystalline rocks. Fractures are distinguished as more abrupt changes in several of the properties derived from the ultrasonic wave propagation. The changes in rock type have been identified as less distinct changes. This validates this method in the situation investigated here. The validation of the geophysical investigation methods to each case is crucial to retrieve useful information; otherwise the full potential of a geophysical investigation will not be achieved.

9. From another geophysical investigation at a much larger scale, the relation between fracture frequency and electric resistivity measured on outcrops shows a difference between the exterior areas in fracture frequency between the sites of Lockne and Björkö. The exterior region of the Lockne structure is less fractured than the exterior of the Björkö structure. This strengthens the correlation as it positions the Björkö data in the gap between the high fracture frequency and low fracture frequency clusters found in the Lockne data.
10. An improvement of the correlation of fracture frequency and electric resistivity from the investigations of the two impact structures was produced. The resistivity can be used as a tool to detect fractures at large depth and as a means to identify the extent of fractured structures. In this way, structures suitable for geothermal energy retrieval can be prospected.
11. On different scales, different methods of rock fracture characterisation are useful, as shown in the study presented here. On a small scale – although the mineral matrix has an influence – the fractures have a strong effect on further fracture development, and thus the mechanical properties of the rock mass.
12. Simulations at the tunnel scale show that the knowledge of pre-existing fractures is a key issue for understanding the damage development in the rock mass surrounding underground excavations in crystalline rocks. Methods to characterise these fractures should be used to control the outcome of the blasting operation.
13. Investigations on the macroscale demonstrate that the knowledge of the correlation between the electric properties of water filled fractures in a rock mass can be used during preliminary estimations of the extent of fracturing in a large volume of rock to be exploited as a resource.
14. The identification of fractures has been made on several scales, with both direct measurements in laboratory and *in-situ*. Two different geophysical methods have been used in the identification of fractures on different scales. The first is the ultra-sonic seismic methods used to identify the EDZ around tunnels. The second is the electric resistivity method, and was used to remotely measure the features of impact structures. The ultra-sonic method identifies individual fractures on the meter scale whereas smaller fractures manifests as a general decrease of seismic wave velocity. The electric resistivity method identifies even larger fractures as a general decrease of electric resistivity of a large volume of rock. The use of the most advantageous method to identify fractures on the different scales must be sought. Remote methods to identify fracture in the rock mass and their further development and validation are crucial in most non-destructive site investigations.

REFERENCES

Ahrens, T. J., O'Keefe, J. D., (1977) *Equations of state and impact-induced shock-wave attenuation on the moon.* In Impact and explosion cratering. Eds. D. J. Roddy, R. O. Pepin, R. B. Merrill. Pergamon Press, New York, 639-656.

Al-Shayea, N. A., (2005) *Crack propagation trajectories for rocks under mixed mode I–II fracture.* Engineering Geology 81. 84-97.

Ask, D., (2004) *New developments of the Integrated Stress Determination Method and application to the Äspö Hard Rock Laboratory, Sweden.* Doctoral thesis at The Royal Institute of Technology, Stockholm (KTH). Trita-LWR. PHD 1010. 66 p.

Autio, J., (1997) *Characterization of the excavation disturbance caused by boring of the experimental full scale deposition holes in the Research Tunnel at Olkiluoto.* Swedish Nuclear Fuel and Waste Management Company (SKB), Stockholm, Sweden.. Technical report. 97-24. 118.

Backers, T., Antikainen, J., Rinne, M., (2006) *Time dependent fracture growth in intact crystalline rock: laboratory procedures and reults.* Proceedings of the 2nd International Conference on Coupled T-H-M-C Processes in Geo-Systems: Fundamentals, Modeling, Experiments and Applications, GeoProc 2006, 437-443.

Borm, G., Giese, R., Otto, P., Amberg, F., Dickmann, Th., (2003) *Intergrated Seismic Imaging System for Geological Prediction during Tunnel construction.* ISRM 2003 - Technology roadmap for rock mechanics, South African Institute of Mining and Metallugy. 5 p.

Bossart, P., Meier, P. M., Moeri, A., Trick, T., Mayor, J.-C., (2002) *Geological and hydraulic characterisation of the excavation disturbed zone in the Opalinus Clay of the Mont Terri Rock Laboratory.* Engineering Geology 66. 19–38.

Boulon, M., Armand, G., Hoteit, N., Divoux, P., (2002) *Experimental investigations and modelling of shearing of calcite healed discontinuities of granodiorite under typical stresses.* Engineering Geology 64. 117– 133.

Bäckblom, G., Martin, C. D:, (1999) *Recent Experiments in Hard Rocks to Study the Excavation Response: Implications for the Performance of a Nuclear Waste Geological Repository.* Tunnelling and Underground Space Technology 14(3). 377-394.

Bäckblom, G., Stanfors, R., Gustafson, G., Rhen, I, Wikberg, P., Olsson, O. & Thegerström, C., (1997) *Äspö Hard Rock Laboratory - Research, Development and Demonstration for Deep Disposal of Spent Nuclear Fuel.* Tunneling and underground space technology 12(3). 385-406.

Bäckström, A., (2008) *Äspö Hard Rock Laboratory - DECOVALEX - Validation of the ultrasonic borehole investigation in the TASQ tunnel.* International Progress Report. Swedish Nuclear Fuel and Waste Management Company (SKB). 84 p.

Bäckström, A., (2004) *Investigation of the correlation of fracture frequency and electric resistivity in impact craters in crystalline rocks.* Licentiate thesis at The Royal Intitute of Technology, Stockholm (KTH). TRITA-LWR.LIC 2019. 99 p.

Bäckström, A., Henkel, H., (2003) *Geology and rock physical properties in the Björkö (Mälaren) area.* Dep. of Land and Water Resources Engineering, Royal Institute of Technology. Report to Swedish Energy Agency.

Börgesson, G., Pusch, L., Fredriksson, A., Hökmark, H., Kaenland, O., Sanden, T., (1992) *Final report of the rock sealing project –Identification of zones disturbed by blasting and stress release. Stripa Project 92-08*. Swedish Nuclear Fuel and Waste Management Company (SKB), Stockholm, Sweden.

Cai, M., Kaisera, P.K., Martin, C.D., (2001) *Quantification of rock mass damage in underground excavations from microseismic event monitoring.* International Journal of Rock Mechanics & Mining Sciences 38. 1135–1145.

Cardarelli, E., Marrone, C., Orlando, L., (2003) *Evaluation of tunnel stability using integrated geophysical methods*. Journal of Applied Geophysics. 52. 93-102.

Carlson, S. R., Young, R. P., (1993) *Acoustic Emission and Ultrasonic Velocity Study of Excavation-Induced Microcrack Damage at the Underground Research Laboratory*. International Journal of Rock Mechanics & Mining Sciences. 30. 901-907.

Carmichael, R. S., (1989) *Practical Handbook of Physical properties of Rocks and Minerals*. CRC Press Inc. Florida, USA. 741 p.

Chandler, N., (2004). *Developing tools for excavation design at Canada's Underground Research Laboratory*.International Journal of Rock Mechanics & Mining Sciences 41. 1229–1249.

Christiansson, R. Hamberg, U., (1991) *Blasting danage investigation in access ramp section 0/526-0/565 m – tunnel excavation and geological documentatoion*. Swedish Nuclear Fuel and Waste Management Company (SKB), Stockholm, Sweden. PR-25-91-12. 39 p.

Dence, M. R., (1972) *The nature and significance of terrestrial impact structures*. International Geological congress 24th (Montreal, Canada) Harpell's, Quebec. 77-89.

Ekman, L., (2001) *Project deep drilling KLX02-phase 2- Methods, scope of activities and results summary report SKB*. Swedish Nuclear Fuel and Waste Management Co (SKB). Technical report Tr-01-11. 188 p.

Eloranta, P., Hakala, M., (1999) *Laboratory testing of Hästholmen equigranular rapakivi granite in borehole HH-KR6*. Report Posiva Oy, Working Report 99-47. 154 p.

Emsley, S., Olsson, O., Stenberg, L., Alheid, H.-J., Falls, S. (1997) *ZEDEX-A study of damage and disturbance from tunnel excavation by blasting and tunnel boring*. Swedish Nuclear Fuel and Waste Management Co (SKB). Technical Report 97-30. 198 p.

Eriksson, L., (1980) *Elektriska och magnetiska metoder för påvisande av svaghetszoner i berg.*(in Swedish) Geol. Surv. Sweden, Geofysiska byrån rep. 8012. 64-80.

Eriksson, L., Johansson, R., Thunehed, H., Triumf, C.-A., (1997) *Metodtester ytgeofysik 1996. Bestämning av berggrundens bulkresistivitet och djupet till salint grundvatten med halvregional resistivitetsmätning, elektrisk sondering samt transient elektromagnetisk sondering*. Svensk Kärnbränslehantering AB (SKB) PR D-98-01.

Fairhurst, C. E. & Hudson, J. A., (1999) *Draft ISRM suggested method for the complete stress-strain curve for intact rock in uniaxial compression*. International Journal of Rock Mechanics and Mining Sciences 36. 279-289.

Fardin, N., (2003) *The effect of scale on the morphology, mechanics and transmissivity of single rock fractures*. Doctoral thesis at The Royal Intitute of Technology, Stockholm (KTH). TRITA-LWR.PHD 1008. 172 p.

Feng, X.-T., Pan, P.-Z., Zhou, H., (2006*) Simulation of the rock microfracturing process under uniaxial compression using an elasto-plastic cellular automaton*. International Journal of Rock Mechanics and Mining Sciences 43(7), 1091-1108.

Feng, X-T., Chen, S. and Li, S., (2001) *Effects of water chemistry on microcracking and compressive strength of granite*. International Journal of Rock Mechanics and Mining Sciences 38. 557-568.

Feucht, L. J. and Logan, J., (1990) *Effects of chemically active solutions on shearing behaviour of a sandstone*. Tectonophysics 175. 159-176.

Flodén, T., Söderberg, P. and Wickman, F.-E., (1993) *Björkö-a possible Middel Proterozoic impact structure west of Stockholm*. Geologiska Föreningen i Stockholms Förhandlingar 115(1). 25-38.

French, B. M., (1998) *Traces of Catastrophe: A Handbook of Shock-Metamorphic Effects in Terrestrial Meteorite Impact Structures*. LPI Contribution No. 954, Lunar and Planetary Institute, Houston. 120 p.

Fujii, Y., Takemura, T., Takahashi, M., Lin, W. (2007) *Surface features of uniaxial tensile fractures and their relation to rock anisotropy in Inada granite*. International Journal of Rock Mechanics and Mining Sciences 44. 98–107.

Gault D.E., Quaide, W. L., Oberbeck, V. R., (1968) *Impact cratering mechanisms and structures*. In: B. M. French and N. M. Short (Eds.) Shock Metamorphism of Natural Materials. Mono Book Co., Baltimore, Md. 87-99.

Gorbaschev, R. & Kint, O., (1961) T*he Jotnian Mälar Sandstone of the Stockholm Region, Sweden*. Bulletin of the Geological Institutions of the Univeristy of Uppsala 40. 51-68.

Grahn, Y. & Nõlvak, J., (1993) *Chitinozoan dating of Ordovician impact event in Sweden and Estonia. A preliminary note*. Geologiska Föreningen i Stockholms Förhandlingar 115. 263-264.

Grieve, R. A. F. & Pesonen, L. J., (1992) *The terrestrial impact cratering record*. Tectonophyiscs 216. 1-30.

Gurov, E. P., Koeberl, C., Yamnichenko, A., (2007) *El'gygytgyn impact crater, Russia: Structure, tectonics, and morphology*. Meteoritics & Planetary Science 42(3). 307-319.

Hagerman, T. H., (1943) *Om Svenska bergarter och deras provning för konstruktionsändamål*. (In Swedish) Statens provningsanstalt, Stockholm. Meddelande 85. 179 p.

Harrison, J. P., Hudson, J. A., (2000) *Engineering Rock Mechanics – part 2: Illustrative worked examples*. Pergamon. Oxford. 506 p.

He, C., Okubo, S., Nishimatsu, Y., (1990) *A study on the class II behaviour of Rock*. Rock Mechanics and Rock Engineering 23. 261-273.

Henkel, H., (2002) *The Björkö geothermal project*. Norges geologiske undersökelse Bulletin. 439. 45-50.

Henkel, H., (1992) *Geophysical aspects of meteorite impact craters in eroded shield environments, with special emphasis on electric resistivity*. Tectonophysics 216. 63-89.

Henkel, H., (1988) *Tectonic studies in the Lansjärv region*. Swedish Nuclear Fuel and Waste Management Co. Technical Report 88-07. 66 p.

Hirahara, N., Ishihara, T., Maeda, N., Sugihara, K., Sato, T., (1999) *In-situ experiment on effect of excavation method on excavation disturbance at the Tono mine in Japan*. Radioactive Waste Management and Environmental Remediation – ASME. 8 p.

Hjelt, S. E., Kaikkonen, P., Pietilä, R., (1985) *On the interpretation of VLF resistivity measurements*. Geoexploration 23. 171-181.

Hoek, E. (2007) *Rock engineering – course notes by Evert Hoek*. http://www.rocscience.com/hoek/pdf/Practical_Rock_Engineering.pdf. 312 p.

Hudson, J. A., Harrison, J. P. (1997) *Engineering Rock Mechanics – an introduction to the principles*. Pergamon. Oxford. 444 p.

Hudson, J. A., Jing L. (2007). *DECOVALEX-THMC, Task B – Understanding and characterizing the Excavation Disturbed Zone (EDZ)-Phase 2 report*. SKI Report 2007:08. 107 p.

Hudson, J.A., Crouch, S.L., Fairhurst, C., (1972) *Soft, Stiff and Servo-controlled Testing Machines: A Review with Reference to Rock Failure*. Engineering Geology 6, 155-189.

Hudson , J. A., Bäckström A, Rutqvist J., Jing L., Backers T., Chijimatsu M., Feng X.-T., Kobayashi A., Koyama T., Lee H.-S., Pan P.-Z., Rinne M., Shen B., (2008) *Final Report of DECOVALEX-THMC Task B. EDZ Guidance Document - Characterising and Modelling the Excavation Damaged Zone (EDZ) in Crystalline Rock in the Context of Radioactive Waste Disposal*. SKI report. 68 p.

Högdahl, K., (2000) *Late-orogenic, ductile shear zones and protolithic ages in the Svecofennian Domain, central Sweden*. Meddelanden från Stockholms Universitet institution för Geologi och Geokemi. Ph.D. Thesis no. 309. 85 p.

Ivanov, B. A., (2005) *Numerical Modeling of the Largest Terrestrial Meteorite Craters*. Solar System Research. 39(5). 381–409.

Jaeger, J. C., Cook, N. G. W., Zimmerman, R. W. (2007) *Fundamentals of Rock Mechanics*. Fourth edition. Blackwell publishing. Oxford. 475 p.

Jansa, L. F., Pe-Piper, G., Robertson, P. B., Friedenreich, O., (1989) *Montaignais: A submarine impact strucutre on the Scotian Shelf, eastern Canada.* Geological Society of America Bulletin 101. 450-463.

Janson T, Ljunggren B, Bergman T. (2007) *Modal analyses on rock mechanical specimens, Specimens from borehole KLX03, KLX04, KQ0064G, KQ0065G, KF0066A and KF0069A.* Swedish Nuclear Fuel and Waste Management Co (SKB). Progress Report 07-03. 24 p.

Jing, L., (2003). *A review of techniques, advances and outstanding issues in numerical modelling for rock mechanics and rock engineering.* International Journal of Rock Mechanics and Mining Sciences 40(3). 283-353.

Juhlin, C., (1991) *Scientific summary report of the Deep Gas Drilling Project in the Siljan ring Impact Structure.* Vattenfall Utvecklings AB, Report u(G) 1991/14. 257 p.

Juhlin, C., Pedersen, L. B., (1987*) Reflection seismic investigations of the Siljan impact structure, Sweden.* Journal of Geophysical Research 92(B13). 14,113-14,122.

Karfakis, M. G., and Akram, M., (1993) *Effecs of chemical solutions on rock fracturing.* International Journal of Rock Mechanics and Mining Sciences and Geomechanics Abstract 30(7). 1253-1259.

Keiswetter, D., Black, R., Steeples, D., (1996) *Seismic reflection analysis of the Manson impact structure.* Journal of Geophysical Research 101(B3). 5823-5834.

King, M. S., Angloti, J. M., Bernabini, M., Johnson, B. T., Bollo, M. F., Gendzwill, D. J., Herget, G., Meneley, W., Drozd, K., Lukes, J., Daw, G. P., Kennett, P., Muir Wood, A. M., Trenter, N. A., (2006) *Suggested methods for geophysical logging of boreholes.* In: R. Ulusay & J.A. Hudson (Eds.). The complete ISRM suggested methods for rock characterization, testing and monitoring: 1974-2006. Ankara. Turkey. 59-74.

Klose, C. D., Loew, S., Giese, R., Borm, G., (2007) *Spatial predictions of geological rock mass properties based on in-situ interpretations of multi-dimensional seismic data.* Engineering Geology. 93. 99-116.

Kornfält, K.-A., Wikman, H., Nordlund, E., Chunlin, L., (1991) *Blasting damage investigation on access ramp section 0/526-0/565 m - optical examination of microcracks in thin sections of core samples and acoustic emission pf core samples.* Swedish Nuclear Fuel and Waste Management Co (SKB). Progress Report 25-91-15. 30 p.

Kowallis, B.J., Wang, H.F., (1983) *Microcrack study of granite cores from Illinois deep borehole PH-3*. Journal of Geophysical Research 88. 7373–80.

Koyama, T., (2007) *Stress, flow and particle transport in rock fractures.* Doctoral thesis at The Royal Institute of Technology, Stockholm (KTH). Trita-LWR. PHD 4498. 210 p.

Kranz, R. (1983) Microcracks in rocks: a review. Tectonophysics, 100. 449-480.

Lanaro, F., (2001) *Geometry, mechanics and transmissivity of rock fractures.* Doctoral thesis at The Royal Institute of Technology, Stockholm (KTH). Trita-AMI. PHD 1043. 144 p.

Lanaro, F., Matsui, H., (2008) *BEM-DDM modelling of rock damage and its implications on rock laboratory strength and in-situ stresses.* Japan Atomic Energy Agency (JAEA) Research 2007-093. 237 p.

Lindström, M., & Sturkell, E. F. F., (1992) *Geology of the Early Palaeozoic Lockne Impact structure, Central Sweden*. Techtonophysics 216. 169-185.

Lindström, M., Flodén, T., Grahn, Y., Hagenfeldt, S., Ormö, J., Sturkell, E. F. F., Törnberg, R., (1999) *The lower palaeozoic of the probable impact crater of hummeln, Sweden*. Geologiska Föreningen i Stockholms Förhandlingar 121. 243-252.

Lindström M., Ormö, J., Sturkell, E., von Dalwigk, I., (2005) *The Lockne crater: revision and reassessment of structure and impact stratigraphy*. Impact Tectonics. Christian Koeberl and Herbert Henkel (eds). 357-388.

Lindström M., Sturkell, E. F. F. Törnberg, R., Ormö, J., (1996) *The marine impact crater at Lockne, central Sweden*. Geologiska Föreningen i Stockholms Förhandlingar 118. 193-206.

Liu, S., Anwar, A. H. M. F., Kim, B. C., Ichikawa, Y., (2006) *Observation of microcracks in granite using a confocal laser scanning microscope*. International Journal of Rock Mechanics and Mining Sciences 43. 1293–1305.

Lowrie, W., (1997) *Fundamentals of Geophysics*. Cambridge University Press, Cambridge. 354 p.

Maerz, N. H., Ibarra, J. A., Franklin, J.A., (1996) *Overbreak and underbreak in underground openings Part 1: measurement using the light sectioning method and digital image processing*. Geothechnical and Geological Engineering. 14. 307-323.

Martin, C. D., Chandler, N. A., (1994). *The progressive fracture of Lac du Bonnet granite*. International Journal of Rock Mechanics and Mining Sciences & Geomechanical Abstracts 31(6). 643-659.

Mattsson, H., Thunehed, H., Triumf, C.-A., (2005) *Compilation of petrophysical data from rock samples and in situ gamma-ray spectrometry measurements, Stage 2 – 2004 (including 2002)*. Swedish Nuclear Fuel and Waste Management Co (SKB). P-04-294. 69 p.

Melosh, H. J., (1989) *Impact cratering – A geological process*. Oxford monographs on geology and geophysics No 11. 245 p.

Melosh, H. J., Ivanov, B. A., (1999) *Impact crater collapse*. Ann. Rev. Earth Planet. Sci. 27. 385-415.

Milkereit, B., Green, A., Sudbury working Group, (1992) *Deep geometry of the Sudbury structure from seismic reflection profiling*. Geology 20. 807-811.

Murrell, S. A. F., (1958). *The strength of Coal under triaxial compression*. In Mechanical Properties of Non-metallic Brittle Materials. Butterworths Scientific publications, London. 123-153.

Nara, Y., Kaneko, K. (2006). *Subcritical crack growth in anisotropic rock*. International Jounrnal of Rock Mechanics and Mining Sciences 43. 437-453.

Nara, Y., Koike, K., Yoneda, T., Kaneko, K. (2006) *Relation between subcritical crack growth behavior and crack path in granite*. International Journal of Rock Mechanics and Mining Sciences 43. 1256-1261.

Nasseri, M. H. B., Mohanty, B. (2008) *Fracture toughness anisotropy in granitic rocks*. International Journal of Rock Mechanics & Mining Sciences 45. 167–193.

Nilsson, L., (1991) *Blasting damage investigation on access ramp section 0/526-0/565 m – hudraulic tests*. Swedish Nuclear Fuel and Waste Management Co (SKB). Progress Report 25-91-16. 21 p.

Oberbeck, V. R., Quaide, W. L., (1968) *Genetic implications of lunar regolith thickness variations*. Icarus 9. 446-465.

Olsson, O., (1992). *Site characterization and validation - final report. Stripa Project 92-22*. Swedish Nuclear Fuel and Waste Management Company (SKB), Stockholm, Sweden.

Olsson, O., (1991) *Blasting damage investigation on access ramp section 0/526-0/565 m – geophysical investigations in boreholes*. Swedish Nuclear Fuel and Waste Management Co (SKB). Progress Report 25-91-13. 99 p.

Olsson, M., Niklasson, B., Wilson, L., Andersson, C., (2004) *Äspö HRL – Experience of blasting of the TASQ tunnel*. Swedish Nuclear Fuel and Waste Management Co. Research report (R-04-73). 75 p.

Ormö, J., (1998). *Impact cratering at sea*. Meddelanden från Stockholms Universitet institution för Geologi och Geokemi. Ph.D. Thesis no. 300. 166 p.

Ouchtelony, F., Sjöberg, C., Johansson, S.-E., Nyberg, U., (1991) *Blasting damage investigation on access ramp section 0/526-0/565 m – damage zone assessment by vibration measurements*. Swedish Nuclear Fuel and Waste Management Co (SKB). Progress Report 25-91-14. 52 p.

Pan, P.-Z., Feng, X.-T., Hudson, J. A., (2006) Simulations on Class I and Class II curves by using the linear combination of stress and strain control method and elasto-plastic cellular automata. International Journal of Rock Mechanics and Mining Sciences 43(7).1109–1117.

Park, R. G., (1997) *Foundations of Structural Geology*. (Third Edition). Chapman & Hall, London. 202 p.

Poag, C. W., (1996) *Structural outer rim of Chesapeak Bay impact crater: Seismic and borehole evidence*. Meteoritics & Planetary Science 31. 218-226.

Price, N. J., Cosgrove, J. W. (1990) *Analysis of geological structures*. Cambridge University Press. Cambridge. 502 p.

Priest, S. D., (1993) *Discontinuity analysis for rock engineering*. Chapman & Hall. London. 473 p.

Push, R., (1989) *Influence of various excavation techniques on the structure and physical properties of "near-field" rock around large boreholes*. Swedish nuclear fuel and waste management co (SKB) TR-89-02.

Push, R., & Stanfors, R., (1992) *Zone of disturbance around blasted tunnels at depth*. International Journal of Rock Mechanics and Mining Sciences 29 (1992) (5). 447-456.

Renshaw, C. E., (1995) *On the relationship between mechanical and hydraulic apertures in rough-walled fractures* .Journal of Geophysical research – Solid Earth 100(B12). 24629-24636.

Rinne, M., Shen, B., Backers, T. (2008) *Time and chemical effects on rock sample failure - results from laboratory tests and numerical modelling*. Proc. of the 3rd International Conference on Coupled T-H-M-C Processes in Geo-Systems: Fundamentals, Modeling, Experiments and Applications, GeoProc 2008, in press.

Roberts, J. L., (1989) The Macmillan Field guide to Geological Structures. Macmillan Press, Cambridge. 250 p.

Rutqvist J., Bäckström A., Jing L., Hudson J., Feng X.-T., Pan P.-Z., Rinne M., Shen B., Lee H.-S., Backers T., Koyama T., Kobayashi A., Chijimatsu M., (2008) *DECOVALEX-THMC Task B, Phase 3: A BenchMark Simulation Study oF Coupled THMC Processes in the Excavation Disturbed Zone associated with Geological Nuclear Waste Repositories*. Swedish nuclear inspectorate (SKI) report. 51 p.

Scholz, C. A., Karp, T., Brooks, K. M., Milkereit, B., Amoako, P. Y. O., Arko, J. A., (2002) *Pronounced central uplift identified in the Bosomtwi impact structure, Ghana, multichannel seimic reflection data*. Geology 30(10). 939-942.

Schuster, K., (2007) *Äspö Hard Rock Laboratory-DECOVALEX-Ultrasonic borehole measurements in the TASQ tunnel (450 m level) at Äspö HRL performed by BGR in November 2006*. Swedish Nuclear Fuel and Waste Management Co (SKB). Internal Progress Report 07-08. 120.

Seto, M., Vutukuri, V. S., Nag, D. K., Katsuyama, K., (1998) *The effect of chemical additives on the strength of rock*. Journal of the Japan Society for Civil Engineering. No.603/III-44. 157-166.

Shen, B., Rinne, M., Stephansson, O., (2005) *FRACOD^{2D} User's manual version 2.1*, 2005, 82 p.

Singh, S. P., Xavier, P., (2005) *Causes, impact and control of overbreak in underground excavations.* Tunnelling and Underground Spacer Technology 20. 63-71.

SKB, (2006). *Preliminary site description- Subarea Laxemar – version 1.2.* Swedish Nuclear Fuel and Water Management Co (SKB) Research report (R-06-10). 643 p.

SKB, (2004) *Deep repository - Underground design premises: Edition D1/1.* Swedish Nuclear Fuel and Waste Management Co (SKB). Research report (R-04-60). 111 p.

Starzec, P., (2001) *Characterization and modelling of discontinous rock mass: Geostatistical interpretation of seismic response to fracture occurrence, discrete fracture network modelling and stability predicitions for inderground excavation.* Doctoral thesis Department of Geology Chalmers University of technology, Göteborg, Sweden. 125 p.

Steele, A., Reynolds, D. A., Kueper, B. H. & Lerner, D. N. (2006) *Field determination of mechanical aperture, entry pressure and relative permeability of fractures using NAPL injection.* Géotechnique 56(1). 27–38.

Stöffler, D., Ostertag, R., (1983) *The Ries Impact crater.* Fortschr. Miner. Bd. 61(2). 71-116.

Therriault, A., & Lindström, M., (1995) *Planar deformation features in quartz grains from the resurge deposits of the Lockne structure, Sweden.* Meteoritics 30. 700-703.

Thunehed, H., Triumf, C.-A., Pitkänen, T., (2004) *Oskarshamn site investigation. Geophysical profile measurements over interpreted lineaments in the Laxemar area.* Swedish Nuclear Fuel and Waste Management Co (SKB). P-04-211. 33 p.

Thunehed, H., Triumf, C.-A., (2006) *Detailed ground geophysics at Laxemar, autumn/winter 2005/2006 Magnetic total field and resistivity.* Svensk Kärnbränslehantering AB (SKB) P-06-137. 53.

Thunehed, H., Triumf, C.-A., (2005) *Oskarshamn site investigation. Detailed ground geophysical survey at Laxemar. Magnetic total field and resistivity.* Svensk Kärnbränslehantering AB (SKB) P-05-188. 37 p.

Tsang, C.-F., Bernier, F., Davies, C., (2005) *Geohydromechanical processes in the Excavation Damaged Zone in crystalline rock, rock salt, and indurated and plastic clays—in the context of radioactive waste disposal.* International Journal of Rock Mechanics and Mining Sciences 42. 109–125.

Tsikalas, F., Gudlaugsson, S. T., Faleide, J. I., (1998) *The anatomy of a buried complex impact structure: The Mjölnir Strucutre, Barents Sea.* Journal of Geophysical research 103 (B12). 30,469-30,483.

Tsikalas, F., Faleide, J. I., Eldholm, O., Dypvik, H., (2002) *Sesmic correlation of the Mjølnir marine impact crater to shallow boreholes.* In : Plado J, Pesonen LJ (Eds) Impact studies (Impacts in Precambrian Shileds). Springer-Verlag, Berlin, Heidelberg. 307-321.

Twiss, R. J., Moores, E. M., (1992) *Structural Geology.* W. H. Freeman and company, New York. 531 p.

Ulusay, R., Hudson, J. A., (2007) *The complete ISRM suggested methods for rock characterization, testing and monitoring: 1974-2006.* ISRM Turish National Group. Ankara. Turkey. 628 p.

Vutukuri, V. S., Lama, R. D., Saluja, S. S., (1974) *Handbook on Mechanical properties of rocks. Vol 1.*Trans tech publications, Clausthal, Germany. 280 p.

Walton, W. H., (1958) *Mechanical Properties of Non-metallic Brittle Materials.* Butterworths Scientific publications, London. 492.

Warneke, J., Dwyer, J. G., Orr, T., (2007) *Use of a 3-D scanning laser to quantify drift geometry and overbreak due to blast damage in underground manned entries.* Rock Mechanics: Meeting Society's challenges and Demands – Eberhart E., Stead D. & Morrison T. (eds). Taylor and Francis Group, London. 93-100.

Wawersik, W. R. (2000) *The value of laboratory experiments for code validations.* International Journal of Rock Mechanics & Mining Sciences 37. 307–316.

Wawersik, W.R., Fairhurst, C., (1970) *A study of brittle rock failure in laboratory compression experiments.* International journal of Rock Mechanics and mining Sciences 7. 561-575.

Wickman, F.E., (1988). *Possible impact structures in Sweden.* In: A. Boden and K.G. Eriksson (Editors), Deep Drilling in Crystalline Bedrock. I. The Deep Gas Drilling in Siljan Impact Structure, Sweden and Astroblemes. Springer, Berlin. 298-327.

Zenchenko, Y., Tsvetkov, V., (1999) *Formation of a flattened subsurface fracture zone around meteorite craters.* Geological Society of America, Special paper 339. 223-227.

Zheng, H., Liu, D. F., Lee, C.F., Ge, X. R., (2005) *Principle of analysis of brittleplastic rock mass*. Int J Solids Struct 42.139–58.

Zimmerman, R. W. Bodvarsson, G. S., (1996) *Hydraulic Conductivity of Rock Fractures*. Transport in Porous Media 23. 1-30,

Zimmerman, R. W., King, M. S., (1985) *Propagation of acoustic waves through cracked rock.* 26th US Symposium on Rock Mechanics. 739-745.

Zuidema, P., (2003) *The importance of the excavation damage zone for post-closure safety of deep geological repositories: some introductory remarks.* In: Impact of the excavation disturbed or damaged zone (EDZ) on the performance of radioactive waste geological repositories, Proceeding of a European commission CLUSTER conference held in Luxembourg on 3-5 November 2003. 3-6.

Åkesson, U., Hansson, J., Stigh, J. (2004) *Characterisation of microcracks in the Bohus granite, western Sweden, caused by uniaxial cyclic loading.* Engineering Geology 72. 131–142.